Aus dem Berlin-Brandenburg Zentrum für Regenerative Therapien
der Medizinischen Fakultät Charité – Universitätsmedizin Berlin

DISSERTATION

Characterisation of the immune response after yellow fever vaccination

zur Erlangung des akademischen Grades
Doctor medicinae (Dr. med.)

vorgelegt der Medizinischen Fakultät
Charité – Universitätsmedizin Berlin

von

Nicole Bethke

aus Berlin

Gutachter/in: 1. Prof. Dr. A. Thiel

2. Prof. Dr.med. P. Reinke

3. Priv.-Doz. Dr. A. Scheffold

Datum der Promotion: 08.04.2011

CONTENTS

1 Abbreviations

α	anti
APC	antigen-presenting cell
APC	allophycocyanine
BCR	B cell receptor
BSA	bovine serum albumin
CD	cluster of differentiation
CMV	cytomegalovirus
Cy5	indopentamethyncyanine
DAMP	damage associated molecular pattern
DAPI	4',6'-diamino-2-phenyl-indol, dihydrochloride
DC	dendritic cell
EBV	Epstein-Barr virus
EDTA	ethylenediaminetetraacetic acid
E-protein	envelope protein
FACS	fluorescence activated cell sorting
FITC	fluoresceine isothiocyanate
FSC	forward scatter
g	centrifugal force: g = 9.81 m/s^2
HLA	human leucocyte antigen
HIV	human immunodeficiency virus
IFN	interferon
Ig	immunoglobulin
IL	interleukin
KIR	killer cell immunoglobulin-like receptor
LF	lethal factor
mDC	myeloid dendritic cells
MFI	mean fluorescence intensity
MHC	major histocompatibility complex
moDC	monocyte derived dendritic cell
NK	natural killer
NS protein	non-structural protein
PAMP	pathogen associated molecular pattern

PBMC	peripheral blood mononuclear cells
PBS	phosphate-buffered-saline
pDC	plasmacytoid dendritic cell
PE	phycoerythrine
PerCP	peridinin-chlorophyll-protein complex
RNA	ribonucleic acid
RT	room temperature
SSC	side scatter
TCR	T cell receptor
T_{CM}	central memory T cell
T_{EM}	effector memory T cell
TLR	Toll like receptor
TNF	tumor necrosis factor
YFV	yellow fever virus
YFV-AND	yellow fever vaccine-associated neurotropic disease
YFV-AVD	yellow fever vaccine-associated viscerotropic disease

2 Introduction

2.1 The Immune System

To protect the mammalian organism, complex mechanisms of pathogen encounter and for the maintenance of self-tolerance are established by the immune system. The immune system is characterized by two fundamental arms, namely the innate (unspecific) and the adoptive (specific) immunity. Both acquire the activation of leucocytes, which develop and maturate from precursor cells (progenitors) in the bone marrow. From there they start to migrate through peripheral tissue, circulate in the blood and in the lymphatic system.

2.1.1 The Innate Immune System

Seeking the definition of innate immunity, one has to consider the fact that it is a form of a first line defence against pathogens without the generation of an immunological memory. Therefore evolutionary highly conserved and fast mechanisms, which are already used by vertebrates, are applied. Supporting the given physical and chemical barriers, like epithelial borders or the tissue pH-value, mainly cellular mediated mechanisms are involved. Important components are, besides phagocytosis by macrophages and granulocytes, the secretion of cytotoxic substrates and the subsequent lysis of pathogens by natural killer cells (NK cells). Nevertheless, not only defensive strategies are used but also mediating tasks are performed by dendritic cells (DCs). These cells reside in most tissues of our body and migrate to the regional lymph node after activation where they gain contact with circulating naïve T cells. Dendritic cells produce cytokines like interleukin 12 (IL-12) and interleukin 18 (IL-18) or type I IFN (IFNα) and are specialized for the acquisition, processing and presentation of antigens to cells of the adoptive immune system, thereby connecting the two fundamental parts. The recognition of conserved molecular patterns shared by bacteria, viruses and parasites occurs through different Pattern-Recognition Receptors (PRR), which are already encoded in the germ line. Main microbial mediators like pathogen-associated molecular pattern molecules (PAMP e.g. like peptidoglycans, LPS, lipoteichoic acid) or endogenous damage-associated molecular pattern molecules (DAMP) are recognized by these receptors and thereby alter the effector function of dendritic cells (Kapsenberg 2003). The classification of PRR can be performed according to their cytosolic molecules including Nod-like receptors (NLR) or their trans-membrane molecules like

Toll-like receptors (TLR) (Janeway Charles A. 2004). Only some of the TLRs are able to induce type I IFN production by DCs, which is essential in antiviral defence (Liu 2005). For example, the single-stranded RNA is recognized via the TLR 7/8 preferentially expressed on plasmacytoid DCs (Diebold, Kaisho et al. 2004; Heil, Hemmi et al. 2004). Myeloid DCs, preferentially expressing the TLR 2, 3, 4 and 8, are the main producer of cytokines such as interleukin 12 (IL-12) and interleukin 18 (IL-18), which can bias the $CD4^+$ T cell differentiation towards a pro-inflammatory Th_1 subset (Macatonia, Hosken et al. 1995; Brightbill, Libraty et al. 1999; Kapsenberg 2003).

After an immature dendritic cell residing in the periphery has been activated due to pathogen recognition, it undergoes multiple maturation processes. At first, maturation leads to an initial up-regulation of antigen sampling and increases the number of surface peptide:major histocompatibility complexes (MHC) to enhance the capacity of antigen presentation. Antigen presentation is based on different classes of major histocompatibility complex (MHC) molecules. Genes necessary for the MHC are localised on chromosome 6 and contain two classes: MHC class I (HLA-A, HLA-B, HLA-C), which is located on every nucleated cell and class II (HLA-DR, HLA-DP, HLA-DQ), which is present on APCs and B cells. Both classes are able to display peptide fragments derived from the pathogen's proteins.

Further maturational steps up-regulate the expression of CD80 (B cell activation antigen B7.1) and CD86 (B cell activation antigen B7.2) on the surface of these antigen-presenting cells (APCs). These are co-stimulatory molecules interacting with their ligand CD28 (Tp44) on T cells. Once a dendritic cell is matured, it can induce helper $CD4^+$ T cell type 1 (Th_1) differentiation, helper $CD4^+$ T cell type 2 (Th_2) differentiation and due to helper-dependent licensing prime cytotoxic $CD8^+$ T cells (CTLs).

Taken together, high levels of MHC, adhesion and co-stimulatory molecules are widely considered to be maturation markers for immunogenicity of DCs (Reis e Sousa 2006).

Natural killer cells are one of the three major lymphocyte subsets comprising approximately 10-15% of the circulating lymphocytes. NK cells are one of the key players of a cytotoxicity based cellular immune response in the defence against intracellular pathogens and malignant transformed cells.

Two distinct populations of NK cells can be found in humans. These are subdivided according to the cell-surface density of their lineage-specific marker CD56 (Neural Cell Adhesion Molecule, NCAM) and the expression profile of the killer cell immunoglobulin - like NK receptors (KIRs) and CD16, an FCγ receptor type III. The majority of $CD56^+$ NK

cells, namely $CD56^{dim}$, express the CD56 surface molecule in a minor-density fashion, whereas the expression of KIRs and CD16 is high. The $CD56^{dim}$ subset promotes a natural cytotoxicity that is characterized by the release of perforin and granzyme and the cell mediated cytotoxicity of an antibody-coated target via their FCγ receptor type III. Nevertheless a small subset of approximately 10% has a high-density of CD56 expression called $CD56^{bright}$, but low or no expression of KIR receptors and CD16. This subset accounts for a high cytokine production capacity being rather immunoregulatory than natural cytotoxic, as they are the first interferon-γ (IFNγ) producers during an immune response (Cooper, Fehniger et al. 2001). A further feature of the $CD56^{bright}$ subset regards their homing capacity to secondary lymphoid organs by highly expressing the adhesion molecule CD62L (L-selectin) and the chemokine receptor CCR7 (Frey, Packianathan et al. 1998; Campbell, Qin et al. 2001).

One important mechanism NK cells use for the discrimination between diseased and healthy cells and the maintenance of self-tolerance is the expression of specific natural killer cell receptors (NKRs). One can subdivide these NKRs according to their inhibitory (e.g. subsets of killer cell immunoglobulin-like receptors (KIR) or NKG2A receptor) or activatory (e.g. subsets of KIR and C-type lectin receptors like NKG2D) potential (Raulet and Vance 2006). As inhibitory and activatory NKRs are expressed on the same NK cell the transmitted signals have to be balanced tightly. To maintain self-tolerance the contact between an autologous cell expressing the MHC class I complex and a NK cell expressing an inhibitory NKRs results in a transmission of an inhibitory signal overcoming the stimulatory signals from the activatory NKRs. This in turn prevents cytotoxic activity and cell lysis by the NK cell. Once the cell down-regulates MHC class I either due to infection or tumorous transformation this so called “missing self recognition” leads to the attack by NK cells (Gasser and Raulet 2006; Raulet and Vance 2006; Yokoyama and Kim 2006).

2.1.2 The Adaptive Immune System

Central mediators of an adoptive immune response are T- and B cells, which regulate the elimination of pathogens through activation of their specific T- and B cell receptor thereby allowing them to react with a broad spectrum of effector mechanisms. Therefore in the draining lymph node a specific selection of a lymphocyte population and their subsequent turnover into effector cells with clonal expansion, which takes several days, is necessary. Those effector cells however do not have a long life-time and undergo

apoptosis. Nevertheless, a significant number of cells persists and become memory cells after antigen elimination.

A hallmark of protective immunity is determined by the clonally selection of antigen-specific B cells that generate neutralizing antibodies (Pulendran and Ahmed 2006). B lymphocytes, marked with the lineage surface marker CD19, are the main modulators of a humoral immunity. Their activation and differentiation into antibody secreting plasma cells and thus developing a humoral memory is triggered by the antigen itself and in most cases require the help of T cells. B cell activation is performed by the B cell antigen receptor (BCR) that at first transmits signals directly from the membrane into the cytosol and secondly delivers the antigen into the intracellular space where it is degraded and returned to the B cell surface as peptides bound to the MHC class II complex. This peptide:MHC class II complex can be recognized by antigen specific helper T cells that respond to the same antigen. This is called linked recognition (Janeway Charles A. 2004). However therefore it is not crucial that T and B cells recognize identical epitopes or the same protein but the physical association between them is necessary. After recognition the antigen specific helper T cell is able to secrete effector molecules that synergize in B cell activation. One important mechanism is the interaction of the membrane-bound CD40L (CD154) with its receptor CD40 on the B cell surface (Bishop and Hostager 2003). By that, other co-stimulatory processes like B7 and CD28 interaction and CD30 ligation are started. All in all B cell antigen receptor activation, CD40 ligation and IL-4 cytokine secretion (and in later stages as well IL-5 and IL-6) by $CD4^+$ helper T cells lead to B cell proliferation and finally into differentiation into antibody secreting short-lived plasma cells (Janeway Charles A. 2004).

For the development of an unique antigen-specific B cell receptor, composing the humoral memory, immature B cells exhibit a large number of gene segments encoding the variable (V), diversifying (D) and the joining (J) region of the antibody molecule. These gene segments are assembled by somatic recombination to a variety of V(D)J arrangements ensuring an unique B cell receptor (membrane-bound antibody) for each B cell. As B cells are able to clonally expand, this BCR also represents a clonal marker. At first, all B cells express the membrane-bound antibody IgM. Later on, during their further maturation they acquire a second cell-surface antibody IgD. Once the naïve B cells get activated by an antigen and responding T cell help at the T-cell zone of lymphoid organs, they migrate into B cell follicles to form so called germinal centers becoming a germinal center B cell. These steps are mandatory for a somatic

hypermutation, which generates mutations at a high rate in the V region of the antibody-encoding genes necessary for affinity selection. Furthermore the antibody encoding genes are also remodelled by class-switch recombination thereby replacing the originally expressed immunoglobulin heavy-chain constant region genes by those of another class (Kuppers 2003; Charles A. Janeway 2004; Janeway Charles A. 2004; Radbruch, Muehlinghaus et al. 2006). Finally the selection of affinity matured germinal center B cells results in either short-lived plasma cells or memory B cells as indicated in Figure 1.

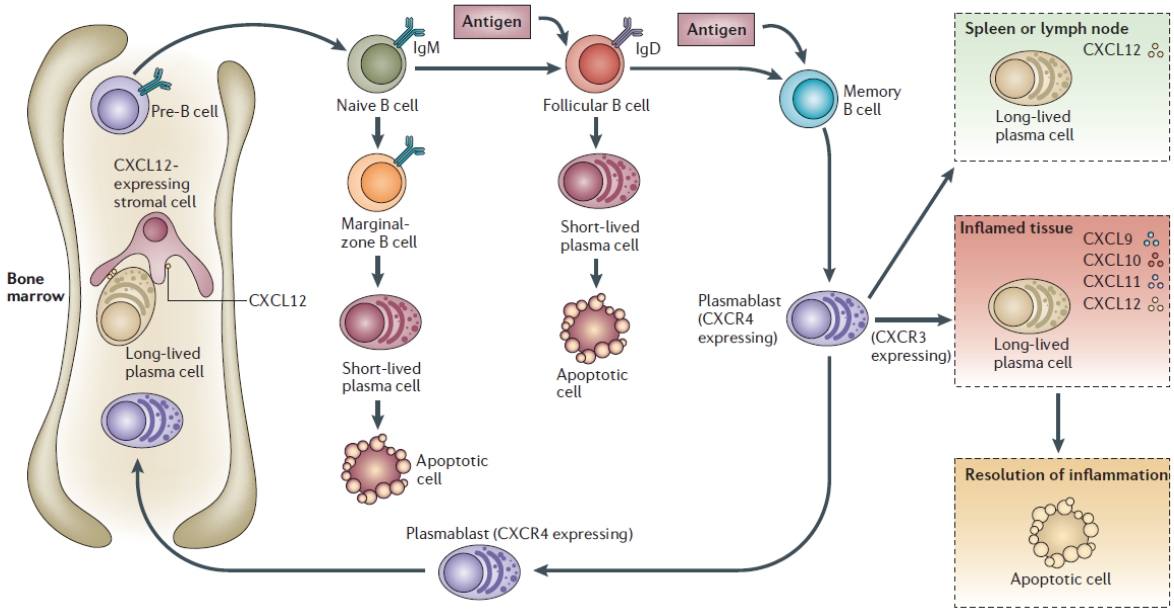

Figure 1: The fate of B cell life in a humoral immune response
B cells exiting the bone marrow as immature precursor B cells expressing IgM further mature into antigen-naïve B cells and then into either marginal-zone B cells or follicular B cells. After antigen engagement these B cells start to secrete antibodies being referred to plasmablasts and short-lived plasma cells. Memory B cells are long-lived developing from follicular B cells and carry their class switched membrane-bound high affinity selected antibody. After a second antigenic encounter these memory B cells can differentiate into plasmablasts, which are then competent to become long-lived plasma cells. These long-lived plasma cells either stay in secondary lymphoid organs (spleen or lymph node) or migrate to inflamed tissue or to the bone marrow. Reproduced from Radbruch, Muehlinghaus et al. (Radbruch, Muehlinghaus et al. 2006)

Nevertheless also specific T lymphocyte responses are believed to have a critical role for the optimal protection. In the case of an acute infection with the human immune deficiency virus (HIV) the development/ initiation of virus –specific $CD8^+$ T cells correlated with the initial control of primary viremia (Koup, Safrit et al. 1994; Musey, Hughes et al. 1997). Also in long-term non-progressors potent cellular immune

responses were positively correlated with the control of viral replication in HIV-1 infected individuals (Kiepiela, Ngumbela et al. 2007).

The cellular based protection of the adoptive immune response depends on T lymphocytes, which are required for the defence of intracellular spaces, e.g. in the case of virus infections, parasites and some bacterial infections. In general one can distinguish two major T cell classes defined by their expression of cluster of differentiation (CD) marker CD4 and CD8 as well as their morphology and functional properties. These two T cell types differ in the class of MHC molecule that their T cell receptor (TCR) recognizes. Whereas CD8-positive T cells bind to peptides bound on a MHC class I molecule CD4-positive T cells only interact with MHC class II molecules (Janeway Charles A. 2004). One important property of the adoptive immune response is the antigen driven clonally restricted differentiation of naïve lymphocytes into protection providing effector T cells. For the activation and differentiation into an effector T cell, a naïve T cell must recognize at least two distinct sequential signals as indicated in Figure 2. Activation of naïve T cells is organized via the immunological synapse where the intense contact between the T cell receptor (TCR) and the MHC molecule on a professional antigen-presenting cell is realized. The first mandatory signal is the contact between the TCR and the peptide:MHC complex. After that, the further amplification of T cell activation is dependent on the level of co-stimulatory molecules. For this purpose the ligation between the surface molecule CD28 with its co-stimulatory membrane-bound B7 molecules on the corresponding APC is essential. As long as both of the necessary signals are achieved, naïve $CD4^+$ T cells starts to secrete exclusively the cytokine interleukin 2 (IL-2). In the case of only TCR stimulation and pending co-stimulatory signals the naïve $CD4^+$ T cell gets functionally inactive (no IL-2 secretion) and remains in an anergic state. As described $CD4^+$ T cells need both signals to become active whereas in the case of $CD8^+$ T cells an insufficient co-stimulation (e.g. the APC is not infected itself and therefore is not able to provide sufficient co-stimulatory molecules) can be overcome by the professional assistance of helper $CD4^+$ T cells. They either secrete cytokines like IL-2 to activate $CD8^+$ T cells by themselves or due to their surface molecule CD40L they are able to maturate APC by ligation to the responsive receptor CD40, a process called licensing. A mature APC in turn is able to properly activate $CD8^+$ T cells. Therefore this helper-dependent $CD8^+$ T cell priming does not require simultaneous recognition of antigen by the $CD4^+$ and $CD8^+$ T cells, but rather can occur as two sequential interactions (Clarke 2000).

The further destiny of an activated $CD4^+$ T cell is determined by the polarizing cytokines that drive the T cells to a helper $CD4^+$ T cell type 1 (Th_1) or a type 2 (Th_2) manner. Upon the further influence of interleukin 12 (IL-12) and interferon gamma (IFNγ) these $CD4^+$ T cells can differentiate to Th_1 cells. Those produce more pro-inflammatory cytokines like interleukin 2 (IL-2), IFNγ and tumor necrosis factor alpha and beta (TNFα and -β), which then lead to a MHC up-regulation and an activation of macrophages and cytotoxic $CD8^+$ T cells (CTL) thereby supporting the cellular immunity driven by cytotoxic T cells against intracellular pathogens (Macatonia, Hosken et al. 1995; Kapsenberg 2003). IL-4 induces the development of Th_2 cells that secrete IL-4, IL-5 and IL-10 and thereby are able to promote B cell differentiation and antibody class switch supporting a humoral immune response against extracellular pathogens (Sallusto and Lanzavecchia 2002; Wan and Flavell 2009).

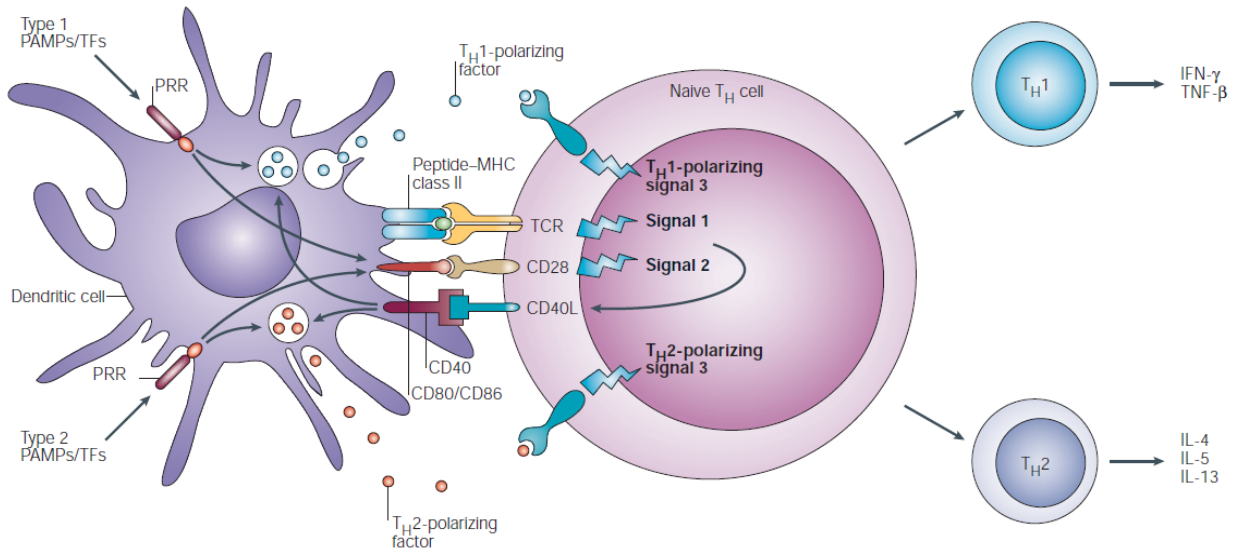

Figure 2: T-cell stimulation and further polarization into T helper cell 1/2 (Th_1/Th_2) requires specific signals. *Signal 1* is mediated by interaction of the T cell receptor (TCR) with the presented peptide:MHC complex. *Signal 2* is referred to the co-stimulatory signal, mainly mediated by the ligation of CD28 with maturation markers CD80 and CD86 that are expressed by dendritic cells. The further polarizing cytokine secretion of e.g. interleukin-12 (IL-12) or interleukin-4 (IL-4) results in the development of Th_1 or Th_2 cells, respectively. Reproduced from (Kapsenberg 2003)

The effector mechanisms used by $CD8^+$ T cells include cytokine production, e.g. IFNγ or TNFα thus leading to a triggered apoptosis of the affected cell. Apoptosis can be as well facilitated by the binding of cell surface molecules like Fas-ligand (FasL, CD95) or TRAIL leading to the induction of the caspase 3 and 8 pathway and cell death (Duiker, Mom et al. 2006; Krammer, Arnold et al. 2007). Furthermore $CD8^+$ T cells are well equipped with intracellular vesicles containing perforin and granzyme B, which when

exocytized initially perforate the cell membrane and proteolyze amino acids thereby inducing apoptosis of the infected cell. To phenotypically describe cytotoxic $CD8^+$ T cells during an acute phase of an infection the surface expression level of CD38 and HLA-DR are widely used (Lechner, Wong et al. 2000; Sauce, Almeida et al. 2007).

A central feature of the adoptive immune system and a further hallmark of protection is the establishment of an immunological memory that is achieved during the primary antigen contact. This makes it so special and capable of reacting against pathogens during a secondary antigen contact with a fast recall response, a great magnitude and high efficiency.

Before a special antigenic exposure naïve T cells are detectable at very low frequencies. After antigen contact the ligation of co-stimulatory molecules with the CD28 molecule on naïve T cells and the IL-2 cytokine production results in the expansion of naïve T cells for the following 4-5 days to markedly higher frequencies (*"clonal expansion" phase*). Here the further phenotypical and functional fate of these T cells can be divided into non-effector T cells and effector T cells (Sallusto, Geginat et al. 2004). As the non-effector T cells represent a precursor cell population with the ability of becoming long-lived central memory T cells (T_{CM}) they are not directly involved in the pathogen defence. In contrast, the effector T cell population is characterized by providing efficient effector functions like cytokine production or a cytotoxicity based immunity. After a successful immune response and pathogen removal the *"clonal contraction" phase* starts with the numeric reduction of effector T cells due to apoptosis. Only a small subset of approximately 5% of the effector T cells do not die after infection and persist as end-stage effector-memory T cells (T_{EM}) that decline over time. These cells together with the already established memory precursor cells feed the pool of memory cells in a third so called *"memory" phase*. Important phenotypical features of these cell types are the differential expression of splice variants of the surface-membrane protein CD45. In human the isoform CD45RA is exclusively expressed on naïve $CD4^+$ T cells whereas upon antigen contact these naïve T cells subsequently replace this isoform by another CD45RO variant. Furthermore T_{CM} cells exclusively express the chemokine receptor CCR7 and/ or other homing receptors like e.g. CD62L (L-selectin) allowing them to enter secondary lymphoid organs. T_{EM} cells are CCR7 negative and can only be found in spleen, blood and other non-lymphatic tissues (Sallusto, Lenig et al. 1999; Badovinac and Harty 2003; Sallusto, Geginat et al. 2004). The T_{CM} as well as T_{EM} cells are able to respond to an antigen during a secondary

immune response (the so called *"recall phase"*). By that T_{CM} cells count for a reactive memory as they have an enhanced proliferative capacity following a secondary stimulation with a possible differentiation into secondary effector T cells. During that process T_{CM} cells loose their homing receptor CCR7 and their co-stimulatory receptors CD28 and CD27 (Appay, Dunbar et al. 2002; Romero, Zippelius et al. 2007). T_{EM} cells belong to a protective memory with immediate effector function following a secondary pathogen contact.

Nowadays there is considerable interest in developing vaccines capable of inducing a robust immune reaction thereby initiating a competent life-long immunological memory providing host protection against a re-challenge with the real antigen. Thereby a long-term protective immunity depends on the quality and quantity of the memory T cell population that develops. To increase the number of memory T cells several regulatory mechanisms might be used for vaccine development like (1) enhancing the expansion phase, (2) reducing the contraction phase or (3) stabilizing the memory phase (Kaech, Tan et al. 2003; Pulendran and Ahmed 2006).

To recruit higher numbers of naïve T cells in the expansion phase the abundance and duration of an antigen exposure are important parameters that are responsible for the efficiency of the T cell response. Not only the number of naïve T cells that are recruited is essential but also their proliferative capacity with the number of cell divisions they undergo (Homann, Teyton et al. 2001; Appay, Dunbar et al. 2002). Nevertheless besides the proliferative properties of T cells the amount of an antigen is important. Titration of different antigenic stimuli in mice with equal numbers of transferred TCR-transgenic T cells have revealed that the higher the antigen concentration the larger the effector T cell population that develops (Mercado, Vijh et al. 2000; Kaech and Ahmed 2001). This further gets accelerated by the strength and duration of TCR signaling, which can be influenced by the players of the innate immune system. As the cells of the innate immunity link the innate and adoptive immune systems a pathogen that preferentially senses directly via PRR is essential. Moreover also the definitive maturation status of a responding dendritic cell is a crucial step characterized by the up-regulation of MHC- and co-stimulatory molecules and enhanced production of pro-inflammatory cytokines and chemokines. These co-stimulatory molecules within the inflammatory environment might also act as an early augmentation of TCR-mediated signals. Furthermore due to the long extended dendrites these mature antigen-presenting cells display an enlarged contact area between MHC molecules on DCs and

the TCR. Additionally the T cell expansion phase can be enhanced by the recruitment of NK cells driving T cells towards a robust Th_1 manner by their IFNγ production (Martin-Fontecha, Thomsen et al. 2004). One important parameter to reduce the contraction phase can be addressed by the signal that directs an effector T cell towards a memory status or towards cell death due to apoptosis. Cytokines like IFNα as well as members of the IL-2 family (e.g. IL-2, IL-4, IL-7 and IL-15) can enhance T cell survival. In human and non-human primates infected with HIV respectively SIV exogenous administration of IL-2 was able to increase the total number of CD4+ T cells and reduce viral load (Barouch, Craiu et al. 2000; Lalezari, Beal et al. 2000). Also for the stabilization of the memory phase a homeostatic turnover with a slow decrease of antigen specific memory T cells over time is achieved by cytokines like IL-7 and IL-15 (Surh and Sprent 2008).

2.2 The Yellow Fever Virus

The yellow fever virus (YFV) belongs to the family of flaviviridae, a type of RNA-viruses that vary in size between 40-60 nm. The virus has three structural proteins: core (C), membrane (M), and envelope (E), and seven nonstructural proteins (NS1, NS2A, NS2B, NS3, NS4A, NS4B, and NS5) necessary for a viral replication. Within the virus envelope, made of membrane lipids originating from the endoplasmic reticulum of the host, the viral proteins (M-protein and E-protein) are imbedded. The envelope encloses the virus capside and the single stranded virus RNA. Carriers of flaviviruses are anthropodes that are mosquitoes and ticks. Derived from this was the denotation of arboviruses („arthropod-borne viruses"). This insect associated transmission pathway was first described by Nott, Beauperthuy and Finlay (Finlay 2001). The yellow fever virus is transmitted by mosquitoes in YFV - endemic areas in the world like the tropical African and South American territories. Other important human pathogen flaviviruses are e.g. the West Nile virus or the tick-borne encephalitis virus (David M. Knipe 2007).

2.2.1 Pathogenesis

The yellow fever infection is transmitted by a mosquito belonging to the genus *Aedes* causing a form of a hemorrhagic fever. There are three different ways of viral circulation. Besides the so called sylvanic and intermediate cycles, the most important is the urban cycle. Within the sylvanic and intermediate cycles, the yellow fever virus circulates between mosquitoes and monkeys with only few spontaneous human infections, whereas within the urban cycle the virus circulates between mosquitoes and humans involving great areas with a high population density thereby also causing epidemics.

The disease occurs in different stages. Following an incubation time of approximately 3-6 days, flew-like symptoms including headaches, fever and nausea might appear. This mild infection phase usually ends after 3-4days. About 24 hours later, 15 % of the cases enter the second, so called toxic, phase of the disease with recurring fever accompanied by jaundice and hemorrhagic diathesis due to liver failure. Taken together usually 50% of the patients die 6-11 days after infection, mostly due to cardiovascular shock and multi organ failure with measurable highly elevated cytokine levels (cytokine storm) (Robertson, Hull et al. 1996; Monath 2001; Barrett and Monath 2003; WHO 2008).

The over-all lethality rate is about 10%, within epidemic situations this figure might even rise to 50% due to insufficient logistic structures (WHO 2008). Every year the incidence of new yellow fever infections was estimated to be around 200,000 with a lethality rate of 30,000 per year (Vaini, Cutts et al., 1998)

2.2.2 The Vaccine

Nowadays the treatment of a yellow fever infection is symptomatically restricted because a causal therapy until now is not available. Therefore, attention has shifted to the prevention of new infections with the flavivirus. Since 1937, a vaccine developed by Max Theiler (1899–1972) is available (Theiler and Smith 2000). For this vaccine, the 17D YF virus strain was generated using the wild-type strain Asibi from which it differs by only 32 amino acids especially within the envelope protein. The vaccine is a live, attenuated virus preparation made from the 17D YF virus strain, which was seeded and grown in embryonic chicken. There are two lineages (17DD and 17D204) of the yellow fever vaccine 17D available, sharing about 99.9% sequence homology. Since its introduction in 1945, over 400 million doses have been administered. All in all, until now the vaccination is considered a very safe and effective protection from the yellow fever infection (Monath 2001). A protective immune response is established approximately 10 days following vaccination. According to the guidelines and recommendations of the STIKO (Ständige Impfkommission) of the Robert-Koch Institute, a booster vaccination is required after 10 years (Koch-Institut 2008). Interestingly, even after 30 years neutralizing antibodies could be detected in the sera of some vaccinees (Niedrig, Lademann et al. 1999). Nonetheless, severe side effects, besides a hypersensibilisation due to embryonic chicken proteins, included the yellow fever vaccine-associated viscerotropic disease (YEL-AVD) and the yellow fever vaccine-associated neurotropic disease (YEL-AND). The first reports about severe adverse events following vaccination were published in 2001. About seven severe infections due to vaccination were reported between 1996-2001 resulting in a lethality rate of about 85%. In four of those cases, RNA of the vaccine 17D could be isolated. But interestingly, although initially proposed, none of the isolated viruses showed a re-mutation into the wild-type. Until now, worldwide about 43 cases of YFV-AVD have been described, with an incidence of about 0.5-1 cases per 100,000 doses distributed and a mortality rate of about 60% (Barrett and Teuwen 2009). Risk factors for the development of a YFV-AVD have been related to the vaccinees age and to a history of thymic disease irrespective of the origin

(Barwick 2004). Taken together, these factors point to the involvement of an inadequate immune response following vaccination leading to the development of severe side effects.

2.2.3 Yellow Fever Vaccination and Innate Immunity

To determine immunological responses following yellow fever vaccination with YFV 17D, a gene array analysis was established. By analyzing extracted whole-blood RNA, it could be shown that the expression profile of about 594 genes significantly changed with peak of modulation at day 3 and day 7 post vaccination. At these time points, three major key players for transcriptional regulation of downstream target genes, namely IRF7 (interferon regulatory factor 7) and STAT1 (Signal Transducers and Activators of Transcription 1) at day 3 and ETS2 (ETS transcription factor family) at day7 were found (Gaucher, Therrien et al. 2008). Further analysis of the expression profile of whole blood revealed that the YFV 17D vaccination induces numerous genes involved in innate immunity. These responses mainly affected Toll-like receptor associated genes (e.g. TLR 7), IFN-related genes, macrophage/ DC – related genes (e.g. CD86) as well as NK-associated genes (e.g. KIR2DL3, KIR2DL4) (Gaucher, Therrien et al. 2008).

The gene array data is supported by the fact that the YFV wild-type and vaccine viruses efficiently infect and replicate in human monocytes and macrophages (Marianneau, Georges-Courbot et al. 2001; Barros, Thomazini et al. 2004). Furthermore different authors described an efficient induction of dendritic cell maturation observed by up-regulating CD86, CD80, MHC class II and CD40. In contrast, Barba-Spaeth et al. found YFV-17D-dependent infection of human DCs irrespective of their maturation state but no infection of monocytes. Moreover, the maturation status of DCs was not affected by YFV 17D, only a small increase in CD86 and MHC class II but no expression of CD83 could be detected (Barba-Spaeth, Longman et al. 2005). All studies seem to agree that although YFV 17D infection of DCs is calcium-dependent, the plasma-membrane C type lectin DC-SIGN (Dendritic Cell-Specific Intercellular adhesion molecule-3-Grabbing Non-integrin) is not involved (Barba-Spaeth, Longman et al. 2005; Palmer, Fernandez et al. 2007). Rather than using the DC-SIGN receptor, the viral vaccine activates dendritic cell subsets via TLR 2, 7, 8 and 9, localized within the membrane (Querec, Bennouna et al. 2006; Palmer, Fernandez et al. 2007).

Taken together, the infection and viral replication within DCs lead to a dose-dependent response of pro-inflammatory cytokine production in human monocyte-derived and

plasmacytoid dendritic cells, namely an IL-6, TNFα, MCP-1, IP-10 and INF-α secretion. Additionally, consistent with the microarray expression profile, the IL-1β production of *in vitro* infected monocyte-derived DCs showed an up to nine-fold increase in a measurement, using the ELISA technique (Gaucher, Therrien et al. 2008). Nevertheless the level of IFNα/β secretion by dendritic cells was only detectable after 48h. This correlated well with a limited replication of YFV-17D in DCs and detection of RNA only until two days post infectionem. Subsequent degradation due to co-localization of the internalized YFV-17D with the lysosomal membrane protein LAMP-2 presumably serves as an explanation for the low virus production (Palmer, Fernandez et al. 2007). As another possible explanation might be the inhibitory mechanism that pDCs use under *in vitro* conditions. These high levels of IFNα, produced by pDCs, were detectable in the supernatant thereby preventing the spread of infection to other DCs with a subsequent decline in virus replication (Barba-Spaeth, Longman et al. 2005).

2.2.4 Yellow Fever Vaccination and Adoptive Immunity

Despite the fragmentary knowledge about the mechanisms of the interaction of the YFV 17D with the innate immune system, the overall protective immunity by neutralizing antibodies against yellow fever virus is generated in >95% of the vaccinees (Niedrig, Lademann et al. 1999; Monath 2001). This notwithstanding, it was shown that a protective effect of YFV 17D vaccination in a murine encephalitis model is dependent on helper $CD4^+$ T cells and B cells, indicating a fundamental role for their interaction in protection mediated by YFV immunization (Chambers and Nickells 2001). A neutralizing antibody response is generated about 7 days after vaccination and can be detectable for more than 30 years (Poland, Calisher et al. 1981; Niedrig, Lademann et al. 1999). Primary antibody targets for IgG are the E-Protein and NS1. Binding of antibodies to E-Protein limits a binding of the virus to the cell and binding of antibodies to NS1 promotes an antibody-dependent cytotoxic cell-mediated lysis by complement activation (Schlesinger, Brandriss et al. 1990; Reinhardt, Jaspert et al. 1998; Daffis, Kontermann et al. 2005). Regarding the characteristic features of antibody producing B cells, the analysis of the B cell activation using markers like CD69 and interleukin-10 receptor (IL-10R) revealed a significant increase in the frequency of CD69 and mean fluorescent intensity (MFI) of IL-10R at day 15 after vaccination (Martins, Silva et al. 2007). This data is supported by Gaucher et al. who verified an up-regulation of B cell activation genes using microarray analysis of whole blood. Signatures that predict a high antibody

response were described by Querec et al. by identifying TNFRSF17, a receptor for the B cell growth factor BLyS-BAFF (Querec, Akondy et al. 2009). Other markers used for the phenotypic characterization of B cells like e.g. CD23 (transiently immature B cells) and the low affinity IgG receptor Fc gamma RII (CD32) showed a rise in MFI of CD32 expression indicating a maturation of B cells at day 15, whereas CD23 frequency was decreasing at that time-point. Nevertheless, a reduced frequency of circulating $CD19^+$ B cells at day 7 could be also shown (Martins, Silva et al. 2007).

Already the measurement of the cellular based adaptive immunity revealed an increase in total $CD8^+$ T cells of about 10% at day 4 after vaccination (22.7% to 32.9% $CD8^+$ T cells of total lymphocytes) whereas for total $CD4^+$, no significant changes were found (Reinhardt, Jaspert et al. 1998). The molecular expression of T cells for adhesion and transmigration through vascular endothelium during the infection was assessed using adhesion molecules like CD62L, CD54 (ICAM-I) or CD18. Here, the frequency of $CD62L^+$ $CD8^+$ T cells was reduced on day 7 after vaccination, whereas no changes were detected for $CD54^+$ or $CD18^+$ $CD8^+$ T cells, nor wre any changes found in the $CD4^+$ compartment (Martins, Silva et al. 2007). Furthermore the authors could show a significant up-regulation in the MFI of CXCR3 on CD4+ and CD8+ T cells at day 15 indicating a chemotactic migration (Martins, Silva et al. 2007). As cytotoxic T cells also play an important role in an antiviral defence, they were of special interest for the clearance of YF 17D virus. First approaches on YFV 17D antigen specificities were addressed by Co et al. who found HLA-B35 restricted $CD8^+$ epitopes. Those $CD8^+$ T cell epitopes recognize the E, NS1, NS2b and NS3 proteins of the YFV 17D (Co, Terajima et al. 2002). Another HLA-$A2^+$ restricted epitope was recently mapped in $CD8^+$ T cells by Querec et al (Querec, Akondy et al. 2009).

Addressing the activation status of $CD4^+$ and $CD8^+$ T cells, Martins et al. could detect an up-regulation of HLA-DR on $CD4^+$ T cells as well as an increase of the activation marker CD69 on $CD8^+$ T cells at day 7 post vaccination. Moreover on day 15 after vaccination, both T cell subsets exhibited a significant increase in the MFI of IL-10R expression (Martins, Silva et al. 2007). In addition Miller et al. specified the antigen specific $CD8^+$ T cells with respect to their activation behavior and memory response. Following a transient viremia detected at day 3 and day 7 after vaccination, the peak of a $CD8^+$ T cell response appeared at day 15. On that day 4–13% of peripheral $CD8^+$ T cells expressed CD38 and HLA-DR (baseline expression of $CD38^+$ HLA-DR^+ $CD8^+$ T cells prior to vaccination about 0,5-2%). These $CD38^+$ HLA-DR^+ $CD8^+$ T cells already

started to secrete IFNγ at day 7 with a peak rising at day 14 (0,5 – 3% of all $CD8^+$ T cells) (Miller, van der Most et al. 2008). To further characterize the activation behavior of this $CD8^+$ T cell population the measurement of Ki-67^+ and Bcl-2^{low} was included. These markers, too, sharply increased from pre-existing level of 0,5% up to 3–11% at day 15 indicating a proliferating, activated phenotype (Ki-67^+) (Gerdes, Lemke et al. 1984) with susceptibility to apoptosis (Bcl-2^{low}) (Appay, Dunbar et al. 2002). While this Ki-67^+ Bcl-2^{low} $CD8^+$ T cell proportion displayed also other effector cell markers like granzymeB^{high}, $CCR5^{high}$, $CCR7^{low}$, $CD45RA^{low}$ and $CD62L^{int}$, Miller et al. used these surrogate markers to determine the population as antigen specific effector $CD8^+$ T cells (Miller, van der Most et al. 2008). Using this phenotype, the maximal expansion of these $CD8^+$ T cells could be detected at d30 with 0.5 to 17% of the cells recognized by tetramer-staining being specific for the NS4B protein (Akondy, Monson et al. 2009).

Regarding the further developing subsets of memory T cells (naïve, effector, central and effector memory T cells), already a population defined by their surface molecules CD45RO revealed an up-regulation, with 70% and 43% of these cells being positive for $CD8^+$ $CD45RO^+$ and $CD4^+$ $CD45RO^+$, respectively, at day 30 after vaccination (Santos, Bertho et al. 2005). Recently, Co et al. could reveal more details regarding that issue by studying the $CD8^+$ T cell responses against four defined HLA-B35 restricted epitopes. They could show that early after vaccination (day 7-28), a very heterogeneous phenotype with naïve, effector and effector memory T cells was expressed by YFV 17D-specific $CD8^+$ T cells. At later time-points, the pre-dominant phenotype found was $CCR7^-$ $CD45RA^+$ $CD27^+$ $CD28^+$ (Co, Kilpatrick et al. 2009). The data could be supported by the work of Akondy et al, who also described memory $CD8^+$ T cells that down-regulate the expression of CD127, Bcl-2, CCR7 and CD45RA within the effector phase. The gradual down-regulation of these markers was then followed by a contraction phase resulting in a pool of memory T cells that re-expressed CD127, Bcl-2 and CD45RA but not CCR7 (Akondy, Monson et al. 2009).

3 Aim

The yellow fever vaccine has been administered to over 400 million people globally; it induces a long-lasting immunity with neutralizing antibody responses for over 30 years. It is considered to be one of the most effective vaccines developed, as it provides a high immunogenicity as a live-attenuated vaccine. An important feature of the live-attenuated vaccine YFV-17D is its ability of cell infection and ongoing viral replication, thereby ensuring a widespread distribution of the antigen and a robust activation of the immune system. Moreover, because of the extensive experience, gathered over a long period of time, and the high efficiency with a responder rate > 99%, the yellow fever vaccine seems to be a good model for assessing the overall footprint of a protective primary vaccination on the immune system. As the yellow fever infection in Europe is not endemic, the yellow fever vaccine can also serve as a model of an acute viral infection in humans, as the virus is a “neo-antigen” and there is no known chronic stage of the yellow fever disease.

Taking into account that until now singular cellular mechanisms of protection have been described, the aim of this study was to provide a comprehensive picture of the cellular signatures resulting after yellow fever vaccination. Moreover this study was designed to help understand the complex immunological interplay especially within the early phase of an immune response, as recent studies tended to focus on one cell type with emphasis on later time points after vaccination. Furthermore, the aim of this study was to define protective hallmarks of the immune response by correlating different immune parameters with viral appearance or the generation of neutralizing antibodies.

4 Materials and Methods

4.1 Technical Equipment and Consumables

Table 1: Technical Equipment and Consumables

Equipment and Consumables	Company
17 IU/ml lithium heparin tube	Becton Dickinson (Heidelberg, Germany)
24-well plates	Nunc GmbH (Roskilde Denmark)
Blood Drawing cannula	BD Vacutainer® Safety-Lok™ Becton Dickinson (Heidelberg, Germany)
Multifuge 3SR Plus	Heraeus-Christ (Hanau, Germany)
FACS tubes	Falcon 5ml, round bottom Becton Dickinson (Heidelberg, Germany)
Begasungs-Brutschrank Function Line	Heraeus-Christ (Hanau, Germany)
Laser flow cytometer LSR II	Becton Dickinson (Heidelberg, Germany)
MX3000P QPCR Cycler	StratageneEurope(Amsterdam,Netherlands)
Pipette Eppendorf	0.5-10µl, 10-100µl, 50-200µl, 100-1000µl Eppendorf (Eppendorf, Germany)
Pipetting device	Pipetus akku (ICN Flow, Meckenheim, Germany)
Reaction tubes	Safe-Lock-Tubes 0,5ml; 1,5ml, 2ml Eppendorf (Eppendorf, Germany)
Serum tube	Becton Dickinson (Heidelberg, Germany)
Sterile bench	HERA safe (Heraeus, Germany)
Stimulation tubes	TC-Tube 12ml Cellstar Greiner Bio-One GmbH (Frickenhausen, Germany)
Thermoblock	Biometra (Göttingen, Germany)
TruCOUNT tubes	Becton Dickinson (Heidelberg, Germany)
Vortex Genie 2 Mixer	Bender & Hobein (Zürich, Swizerland)
Water Bath	IKA Labortechnik (Berlin, Germany)

4.2 Chemicals and General Reagents

All chemicals used were of purity grade p.A: (*pro analysi*, for analytical purpose) or of the highest purity standard available. All buffers and solutions listed were compounded by using bidistillated water.

Table 2: Chemicals and general reagents

Chemicals and General Reagents	Company
Beriglobin	Aventis, Germany (2mg/ml in PBS-buffer)
Brefeldin A	Sigma, Germany (5mg/ml in 70% Ethanol)
Carboxymethylcellulose	BDH Chemicals Ltd (Poole, UK)
CMV pp65	Jerini AG, Germany (10µg/ml)
DAPI	Roche, Germany (1µg/ml in PBS-buffer)
Dithiothreitol (DTT)	Invitrogen (Karlsruhe, Germany)
dNTP	Eppendorf (Hamburg, Germany)
Erythrocyte Lysing buffer	Becton Dickinson (Heidelberg, Germany)
Ethylendinitrilotetraessigsäure	Merck KgaA (Darmstadt, Germany)
EUROIMMUN-IIFA YFV	EUROIMMUN (Lübeck, Germany)
FACS Lysing solution	Becton Dickinson (San Jose, CA)
FACS Permeabilizing Solution	Becton Dickinson (Heidelberg, Germany)
FACSFlow	Becton Dickinson (Heidelberg, Germany)
FACSRinse	Becton Dickson (Heidelberg, Germany)
Fetal Bovine Serum	PAA Laboratories, Linz, Austria
Formaldehyde	Roth (Karlsruhe, Germany)
L-15 Medium (Leibovitz)	Gibco BRL, Invitrogen (Germany)
L-Glutamine	PAA Laboratories, Linz, Austria
PS cells (renal swine cells)	Robert-Koch-Institut (Berlin, Germany)
Purified Mouse α-Human CD28	Becton Dickinson (Heidelberg, Germany)
pYFV-NS3amp plasmid	Robert-Koch-Institut (Berlin, Germany)
QIAamp Viral RNA Mini Kit	Qiagen (Hilden, Germany)
Random hexamer primer	Invitrogen (Karlsruhe, Germany)
Reference virus strain 17D (lot number: 354/1)	Robert-Koch-Institut (Berlin, Germany)
Reverse Transcriptase	Invitrogen (Karlsruhe, Germany)

RNase-Inhibitor	Invitrogen (Karlsruhe, Germany)
Staphylococcal enterotoxin B	Sigma (Munich, Germany)
Tetanus toxoid	Chiron Behring (20LP/ml), Germany
Tween 20 2 % (v/v)	EUROIMMUN (Lübeck, Germany)
YFV 17D (Stamaril®)	Sanofi Pasteur MSD GmbH Germany

4.3 Buffers

Table 3: Buffers and Solutions

Buffer	Company
Naphthalene-Black	1 g Amido black
	13,6 g Sodium acetate
	Sigma-Aldrich (Munich, Germany)
	60 mL acetic acid
	ad 1.000 mL aqua
PBS-buffer	2,7 mM KCL
	1,5 mM KH_2PO_4
	137 mM NaCl
	8,1 mM Na_2HPO_4
PBS/BSA-buffer (pH 7,2 - 7,4)	PBS-buffer with
	5 g/l bovine serum albumin
	RocheDiagnostics(Mannheim, Germany)
PBS/BSA/EDTA-buffer (pH 7,2 - 7,4)	PBS/BSA-buffer with
	2 mM EDTA (Merck, Germany)

4.4 Vaccination

Approval for the study design was obtained from the local ethical committee at the Charité - Universitätsmedizin: After obtaining informed consent and signing an informant agreement, 18 healthy participants aged 22-53 years without previous yellow fever vaccination or known exposure were immunized once with YFV 17D. The vaccination was administered intramuscularly by a physician specialized in tropical medicine. The participants reported no adverse events except short term slight pain at the injection site and minor flu-like symptoms. Immediately before (day 0) and at 8 time points, (day 1,

day 2, day 3, day 4, day 7, day 10, day 14 and day 28) after vaccination, 20ml of heparinised whole blood and 10ml serum were drawn and analyzed. Blood was analyzed directly; sera were stored at -70 °C until use.

4.5 Immunofluorescence Staining

Using the flow cytometry technique, a cell staining with fluorochrome labeled antibodies is necessary. To prevent an unspecific binding of the antibodies to Fc-receptors, all staining was performed in the presence of the antibody Beriglobin (2mg/ml). The optimal antibody concentrations had already been titrated in pre-experimental studies.

4.5.1 Monoclonal Antibodies

Table 4: Used monoclonal antibodies

Antibody	Clone	Isotype	Coupling	Source
αBCDA-2 (CD303)	AC144	Mouse IgG1, κ	APC	Miltenyi Biotech
αCD3	UCHT1	Mouse IgG1, κ	Alexa 405	DRFZ
αCD4	SK3	Mouse IgG1, κ	AmCyan	BD Pharmingen
αCD4	TT1	Mouse IgG1, κ	PacOrange	DRFZ
αCD4	TT1	Mouse IgG1, κ	PE	DRFZ
αCD4	SK3	Mouse IgG1, κ	PerCP	BD Pharmingen
αCD8	SK1	Mouse IgG1, κ	APC-Cy7	BD Pharmingen
αCD8	SK1	Mouse IgG1, κ	PerCP	BD Pharmingen
αCD11c	MJ4-27G12	Mouse IgG2b	PE	Miltenyi Biotech
αCD14	TM1	Mouse IgG1, κ	Cy5	DRFZ
αCD14	TM1	Mouse IgG1, κ	PE	DRFZ
αCD14	M P9	Mouse IgG2b,κ	PerCP	BD Pharmingen
αCD16	3G8	Mouse IgG1, κ	APC-Cy7	BD Pharmingen
αCD19	SJ25C1	Mouse IgG1, κ	PerCP-Cy5.5	BD Pharmingen
αCD19	HIB19	Mouse IgG1, κ	PE	BD Pharmingen
αCD27	O323	Mouse IgG1, κ	APC-Cy7	eBioscience

αCD28	CD28.2	Mouse IgG1, κ	No labeling	BD Pharmingen
αCD31	WM59	Mouse IgG1, κ	PE	BD Pharmingen
αCD38	HIT2	Mouse IgG1, κ	FITC	BD Pharmingen
αCD45	HI30	Mouse IgG1, κ	FITC	BD Pharmingen
αCD45	2D1	Mouse IgG1, κ	APC-Cy7	BD Pharmingen
αCD45RA	L48	Mouse IgG1, κ	PeCy7	BD Pharmingen
αCD45RO	UCHL-1	Mouse IgG2a,κ	FITC	DRFZ
αCD56	B159	Mouse IgG1, κ	PE-Cy7	BD Pharmingen
αCD62L	Dreg 56	Mouse IgG1, κ	FITC	BD Pharmingen
αCD62L	Dreg 56	Mouse IgG1, κ	APC	BD Pharmingen
αCD127 (IL-7Rα)	eBioRDR5	Mouse IgG1, κ	PE	eBioscience
αCD154 (CD40L)	TRAP1	Mouse IgG1, κ	PE-Cy5	BD Pharmingen
αHLA-DR	L243	Mouse IgG2a	FITC	BD Pharmingen
αIgD	IA6-2	Mouse IgG2a,κ	FITC	BD Pharmingen
αIL-2	MQ1-17H12	Rat IgG2a	APC	BD Pharmingen
αIL-2	MQ1-17H12	Rat IgG2a	FITC	BD Pharmingen
αIL-4	MP4-25D2	Rat IgG1	APC	BD Pharmingen
αIFNγ	4S.B3	Mouse IgG1, κ	PacBlue	eBioscience
αKi67	B56	Mouse IgG1, κ	FITC	BD Pharmingen
αKIR2DL1/S1	EB6	Mouse IgG1, κ	Cy5	DRFZ
αKIR2DL2/L3/S2	GL183	Mouse IgG1, κ	Cy5	DRFZ
αKIR3DL1/L2/S1	AZZ158	Mouse IgG1, κ	Cy5	DRFZ
αNKG2A	131411	Mouse IgG2a,κ	PE	R&D Systems
αTNFα	MAb11	Mouse IgG1, κ	Alexa-700	BD Pharmingen
Isotype control	MOPC-21	Mouse IgG1, κ	PE	BD Pharmingen

4.5.2 Vital Cell Staining

Due to surface antigen modifications and inefficient antibody binding the NK cell panel and the DC panel were stained using a protocol for live cell treatment. 100µl heparinised whole blood was lysed with 2ml of BD Lysing buffer according to the manufactures instructions. After lysing and washing, the cell pellet was resuspended in 100µl PBS-buffer containing fluorescent labeled antibodies that were incubated for 10min at 4°C in the dark. After incubation, cells were washed with PBS+BSA+EDTA buffer and centrifuged at 300xg for 10min. The cell pellet was resuspended in 250µl PBS+BSA+EDTA buffer and analyzed immediately. Shortly before measurement, DAPI (end concentration 400 nM) that intercalates into the DNA of dead cells was added.
The subset panels used included:
CD4 cell-panel: αCD4, αCD31, αCD27, αCD62L, αCD45RA, αCD45RO
CD19 cell-panel: αCD19, αCD27, αIgD
CD8 cell-panel: αCD8, αCD3, αCD38, αCD45RA, αCD127
NK cell-panel: αCD3 Alexa 405, αCD56 PE-Cy7, αCD16 APC-Cy7, αCD62L FITC, αKIR2DL1/S1 Cy5, αKIR2DL2/L3/S2 Cy5, αKIR3DL1/L2/S1 Cy5, αNKG2A PE
DC-panel: DAPI, αCD45, αCD14, αCD56, αCD19, αCD11c, αCDBDCA-2, αHLA-DR

4.5.3 Analysis of Absolute Numbers of Cell Subsets in Whole Blood

To determine the absolute numbers of different leucocyte subsets, TruCount tubes containing a known number of fluorescent quantification beads were used. 50µl of heparinised whole blood was incubated in the dark at room temperature (RT) with 20µl of fluorescent antibodies directed against CD4, CD45, CD19, CD8, CD56 and CD14. After an incubation time of 15min, 450µl of 1x diluted FACS lysing solution was added for fixation of PBMCs and lysis of erythrocytes for another 15min at RT. Cells then were immediately analysed and absolute cell numbers were determined by calculating the ratio of fluorescent beads to cells acquired following the equation:

$$\frac{\frac{\#\ of\ events\ in\ region\ containing\ cell}{\#\ of\ events\ in\ absolute\ count\ bead\ region}}{} X \frac{\#\ of\ beads\ per\ test}{test\ volume} = absolute\ count\ of\ cell$$

The TruCount staining protocol was used for all other antibody staining panels determining the frequency of CD4 T-, CD8 T- and CD19 B cells despite the fact that no quantification tubes were used during these procedures.

4.6 Whole Blood Antigen Stimulation (Fast Immune Assay)

Whole blood antigen stimulation was performed essentially as previously described (Frentsch, Arbach et al. 2005; Meier, Stark et al. 2008).

In brief, 2 ml of whole blood was stimulated in 12ml round bottom stimulation tubes with αCD28 (1µg/ml) and specified antigen. CMV pp65 (10µl/ml), TT (20LF/ml) and YFV 17D (10.000 infectious particles/ml) were used as antigen. Stimulation with αCD28 alone served as a negative control, whereas the addition of SEB (1.5µg/ml) served as a positive control. SEB stimulation results in a specific cross-linking of MHC class II with the TCR consisting of defined Vβ family chains. After gently mixing the reagents, stimulation tubes were kept at an angle of 45° to enlarge the stimulation surface in the incubator at 37° for 6h. After 2h Brefeldin A (10 µg/ml) was added to the stimulation tube. Brefeldin A serves as an inhibitor of the Golgi-apparatus to enhance protein accumulation within the endoplasmic reticulum and to prevent secretion of cytokines. After further 4h, cells were removed from the incubator, mixed thoroughly and then divided in 2 x 1ml. After that 500µl of cold EDTA (20mMolar) was added to each stimulation tube and incubated for 10min at RT to stop the stimulation phase. The cells were washed with 5ml of cold PBS/BSA and pelleted by centrifugation at 300xg for 10min at 4°C. To stain for intracellular antigens like e.g. cytokines, cells have to be fixed and permeabilized. For erythrocyte lysis and fixation, the cell pellet was dissolved in 9ml 1x FACS lysing solution and incubated for 10min at RT. After washing with PBS/BSA and another step of centrifugation, the cell pellet was then resuspended in 500µl 1x permeabilization solution and incubated for 10min at RT. Following a next washing/ centrifugation step the cells were stained for extra- and intracellular antigens using fluorochrome-coupled antibodies. The cell pellet was dissolved in 100µl PBS/BSA/EDTA containing antibodies and then incubated for 30min at RT in the dark. As two different panels had been used, the initially stimulated 2ml of whole blood was split into two parts of 1ml each to stain for both. Antibodies used for staining after whole blood stimulation included:

First panel: αCD4 AmCyan, αCD4 Pacific orange, αCD14 PE, αCD40L PE-Cy5, αIFNγ Pacific Blue, αTNFα Alexa700, αIL-2 FITC and αIL-4 APC.

Second panel: αCD4 AmCyan, αCD4 Pacific orange, αCD14 PE, αCD40L PE-Cy5, αIFNγ Pacific Blue, αTNFα Alexa700, α-IL-2 APC and αKi-67 FITC.

After staining, the cells were again washed with PBS/BSA and spun down at 300xg for 10min at 4°C. Again the pellet was resuspended using 250µl of PBS/BSA and analysed with the flow cytometer. The data analysis was performed using FlowJo, gates were set according to control samples consisting of only αCD28 and no antigen (negative control) and αCD28 plus SEB (positive control). Figure 3 shows an example of the analysis of YFV-specific T cells in one representative of the vaccinees.

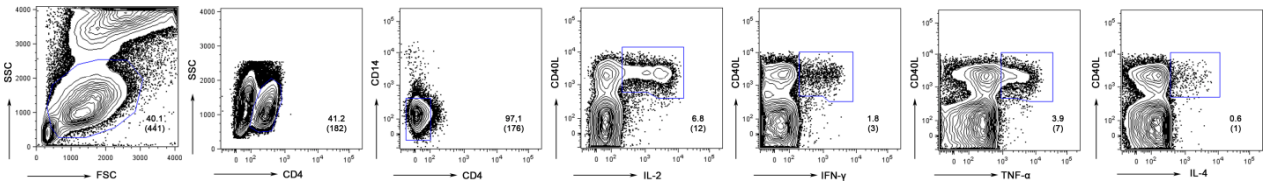

Figure 3: Gating strategy for SEB whole blood stimulation in one representative donor
After gating on lymphocytes (a), $CD4^+$ T cells (b) were excluded from $CD14^+$ monocytes (c) and further subdivided into $CD40L^+$ $IL\text{-}2^+$ (d), respectively $CD40L^+$ $IFN\gamma^+$ (e), $CD40L^+$ $TNF\alpha^+$ (f) and $CD40L^+$ $IL\text{-}4^+$ (g) cytokine producers. All gates for the negative control (anti-CD28) and specific antigen stimulation (CMV, TT, YFV 17D) were set according to the SEB positive control

4.7 Multiparameter Cell Analysis by Flow Cytometry

The flow cytometry technique makes it possible to get a better insight into the phenotypical characteristics on a single cell basis. It can be defined as a system for measuring and analyzing the signals that result as particles flow in a liquid stream through a beam of light (Givan 2001). Flow cytometry involves the illumination of particles by a light source and the subsequent analysis of the light emitted by these particles after this illumination. The illumination is realized by fluorescent labeled antibodies staining their specific antigen on cell surfaces or even the cytosol.

Nowadays, the laser technique consists usually of an argon laser delivering monochromatic coherent light. One problem of the laser light is the intensity decrease of the beam following a Gaussian profile, with the intensity being at its highest in the middle and decreasing towards the edges. The cells have to be focused to pass right through the middle of the laser beam to ensure maximum illumination of the fluorochromes. For this purpose, the sample needs to be organized into a stream of single cells by means of the fluidics of the flow cytometer. The sheath fluid provides a supporting system to direct the cells through the laser beam by creating a massive drag effect. Using the principle of hydrodynamic focusing the cells are able singly to pass through the different laser beams. The information about the properties and signatures of the analyzed cells are obtained by the light scattering and the fluorochrome emission.

The light that is scattered in the forward direction (usually at a small offset angle of about 3-10° from the laser beams axis) is called forward scatter (FSC) and roughly equals the cell size. Light that is scattered at an angle of about 90° offset from the laser beam is called sideward scatter (SSC), is collected by a lens and correlates with the granularity of the measured particle. Both FSC and SSC are unique for every particle.

Furthermore the properties of the cell can be described by using fluorochromes that emit light in a characteristic wavelength upon laser excitation. Flow cytometers are equipped with different fluorescence (FL-) channels that detect the emitted light using sensitive instruments like the photomultiplier tubes (PMTs). To control the specificity of detection, so called optical filters are used. These filters can block light by absorption or transmit light of a specific wavelength. Three major filters are used for detecting light, always starting with the long-wavelength and going towards the short-wavelength. The “long pass” filter only permits the transmission of light above a cut-off wavelength thereby also serving as a dichroitic mirror, while the “short pass” filter only allows light

below a cut-off wavelength and the “band pass” filter defines light in a narrow range of wavelengths. When light hits a photodetector a small current is generated resulting in an associated voltage that is proportional to the number of light photons detected. This voltage is then linearly or logarithmically amplified to be plotted graphically.

Taken together the emitted fluorescent light of different wavelengths, which is generated using different fluorochromes excited by different laser beams and transmitted by different filters, can be detected in a comprehensive way.

A typical filter configuration of the 488nm argon laser in a BD LSR II cytometer which was used in this study is shown in Figure 4.

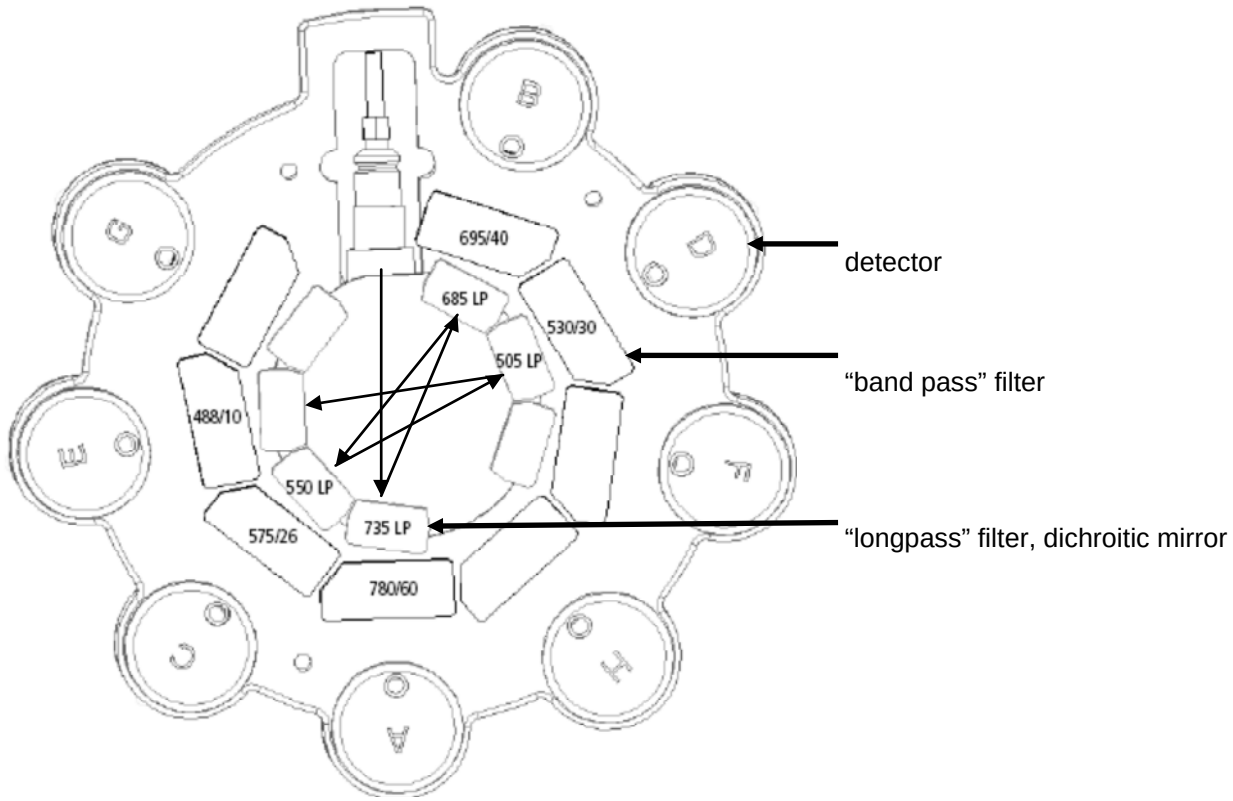

Figure 4: Filter configuration of the 488 nm argon laser reproduced from the BD LSRII Benutzerhandbuch, 2003

The four laser flow cytometer LSR II was used for all experimental settings. The filter combination of the different fluorochromes used are summarized in Table 5. All acquired data sets were later on analyzed using the FlowJo software.

Table 5: Different filter configurations for the antibody fluorochromes used in this study

Fluorochrome	Laser	Detector	Longpass-filter	Bandpass-filter
FITC	488-nm blue laser	D	505	530/30
PE	488-nm blue laser	C	550	575/26
PerCP; PE-Cy5	488-nm blue laser	B	635	670/14
PerCP Cy5.5	488-nm blue laser	B	685	695/40
PE-Cy7	488-nm blue laser	A	735	780/60
Alexa 405; DAPI; Pacific Blue	405-nm violet laser	A	-	440/40
AmCyan; Pacific Orange	405-nm violet laser	D	505	525/50
APC-Cy7	633-nm red laser	A	735	780/60
APC; Cy5	633-nm red laser	B	-	660/20
Alexa 700	633-nm red laser	B	685	720/30

4.8 Detection of the Virus Load by RT-PCR

The detection of the viral load and quantification of an antibody and neutralizing antibody development, respectively, have been generated in cooperation with Matthias Böthe, PhD student at the Robert Koch institute working in the group of Prof. Dr. Niedrig. With permission the data was used in this study to compare the immunological cellular parameters with the viral determinates.

Detection of virus load was essentially performed as previously described (Bae, Nitsche et al. 2003). In brief, RNA was extracted from 140µl of serum using a QIAamp Viral RNA Mini Kit according to the manufacturer's instructions. 10 µL RNA was heated to 65°C for 10 min and subsequently chilled on ice for 5 min. Then First-Strand buffer, 1 mM DTT, 0.625 mM dNTP, 1.5 µg of random hexamer primer, 100 U of reverse transcriptase and 40 U of ribonuclease inhibitor were added to the RNA and reverse transcription was performed at 42 °C for 1 h. Enzyme activity was terminated by heating the sample to 93 °C for 5 min.

Quantitative real-time PCR was performed in a MX3000P QPCR Cycler with minor modifications (5 µL cDNA and 0.2 µM of each primer were used). A serial dilution of pYFV-NS3amp plasmid was used for generating reference values.

Table 6: Sequences for primer pair and fluorescent probe for NS3

NS3	Sequence
Forward Primer (NS3 s)	AGGTCCAGTTGATCGCGGC
Reverse Primer (NS3 as)	GAGCGACAGCCCCGATTTCT
Probe (NS3 TM)	6FAM-TGGTCAACGTCCAGACAAAACCGAGCXTTG-X-TAMRA

4.9 Indirect Immune Fluorescence Assay

YFV specific IgM and IgG antibodies were detected and quantified with EUROIMMUN-IIFA YFV according to the manufacturer's instructions. For improved detection of IgM, the IgM sample buffer was supplemented with 2% (v/v) Tween 20.

4.10 Plaque Reduction Neutralization Test (PRNT)

PS-cells were cultivated in Leibovitz medium supplemented with 5% FCS and 1% glutamine. All sera were assayed in quadruplicates in serial dilutions from 1:10 to 1:320. Serum was mixed with 100 plaque-forming units of the reference 17D virus preparation (lot number: 354/1) and incubated for 1h at 37 °C. The mixture was added to an equal volume of PS-cells at a concentration of 6 x 10^5 cells/ mL in 24-well plates. After 4h incubation, a carboxymethylcellulose (CMC)/ L-15 solution was added to obtain a final concentration of 0.8 % CMC. Cells were then cultured for 4 days at 37 °C, fixed with 3.7% formaldehyde and stained with Naphthalene black for 30 min. Plaques were counted and the 90% neutralization titres were calculated according to Reed and Münch (Reed 1938).

4.11 Data Analysis and Statistics

Table 7: Software used for data analysis and statistics

Software	Company
FlowJo Macintosh 8.6 – 8.8.6	TreeStar Inc. (Ashland, OR, USA)
Prism Software 4.03	GraphPad Inc.(La Jolla, CA, USA)
SPSS for Windows XP 16.0	SPSS Inc. (Chicago, IL, USA)
Microsoft Office	Microsoft (Redmond, WA,USA)

The graphs displayed in this work were generated using the Prism GraphPad Software 4.03. All statistical analyses were performed with the SPSS Software 16.0. For statistical differences between antigen specific T cells and lymphocyte subsets induced by vaccination the nonparametric Wilcoxon-test, a two-sided testing of values at the individual time points against values at day 0 was used. The testing of different subsets in correlation to $PCR^{positive}$ and $PCR^{negative}$ donors and NT^{high} and NT^{low} donors, respectively, was analysed by the two-sided Mann Whitney U-test for independent samples. Values with $p<0,05$ were considered to be statistically significant.

5 Results

5.1 Induction of Antibodies Directed Against YFV 17D

In order to evaluate the successful induction of a protective immunity against YFV 17D, the generation of YFV 17D-specific IgM, IgG and neutralizing antibodies was analyzed. As expected, in all donors an induction of IgM and IgG could be observed (data not shown). Neutralizing antibodies were induced in all vaccinees at day 14 (Figure 5a): that was the first time-point at which all vaccinees developed neutralizing antibody titer.

a) **b)**

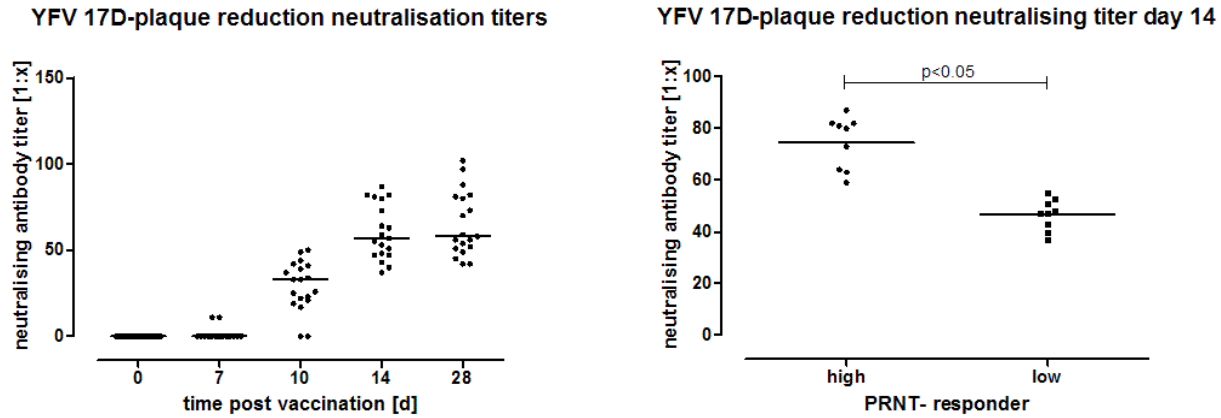

Figure 5: Neutralizing antibody titers in serum after vaccination with YFV 17D
Induction of neutralizing antibody responses detected by plaque reduction neutralizing test at indicated time points after vaccination with YFV 17D (**a**). These neutralizing antibody titers were grouped into high and low responders according to the median response of all vaccinees at day 14 (**b**).

Additionally, a clear difference in neutralizing antibody titers could be detected that was used to group the vaccines into high and low antibody responders on day 14 and day 28 (data not shown). As all vaccinees had measurable antibody titers on day 14, this day was chosen to group the vaccinees into high (NT^{high}) and low responders (NT^{low}) (Figure 5b) in order to correlate immune parameters with magnitude of antibody induction (see Figure 24 and Figure 25).

5.2 Detection of YFV 17D Viremia

In order to characterize the initial strength of the immune response against the live virus challenge, the YFV 17D viremia in peripheral blood after vaccination was analyzed. For this purpose, serum was sampled at all time-points throughout the study and subjected to YFV 17D-specific RT-PCR.

In 8 of 18 vaccinees, the YFV 17D could be detected in patient's serum at least at one time-point. Most of the participants were tested positive at day 4 after vaccination. These participants will therefore be referred to as $PCR^{positive}$ in contrast to $PCR^{negative}$ participants (Table 8). These two groups were later on used to correlate immune parameters with viremia (see Figure 23).

Vaccinee	day 2	day 3	day 4	day 7	day 10
1	**343**	neg	neg	neg	neg
2	neg	**701**	neg	neg	neg
3	neg	neg	**252**	neg	neg
4	neg	neg	**2113**	neg	neg
5	neg	neg	**5233**	neg	neg
6	neg	neg	**5167**	neg	neg
7	neg	neg	**339**	**1803**	neg
8	neg	neg	neg	**420**	neg
9	neg	neg	neg	neg	neg
10	neg	neg	neg	neg	neg
11	neg	neg	neg	neg	neg
12	neg	neg	neg	neg	neg
13	neg	neg	neg	neg	neg
14	neg	neg	neg	neg	neg
15	neg	neg	neg	neg	neg
16	neg	neg	neg	neg	neg
17	neg	neg	neg	neg	neg
18	neg	neg	neg	neg	neg

Table 8: Detected YFV 17D viremia in a fraction of vaccinees between Day2 and Day7 after vaccination.
Shown are the results of a YFV 17D-specific RT-PCR in serum at the indicated time points. Values represent the genome equivalents per ml calculated according to standard. (neg = negative)

5.3 Activation of Innate Immune Cells by YFV 17D Vaccination

5.3.1 Dendritic Cell Subsets and Monocytes

Dendritic cells are major players of the innate immunity, but may also serve as a bridge to adaptive immunity by presentation of antigens to $CD4^+$ and $CD8^+$ T cells. In humans the conventional dendritic cells (DCs) are divided into distinct subsets in which the terminology is based on different phenotypical and functional characteristics of these subsets. Phenotypical analysis includes myeloid DC (mDC) expressing $CD11c^{high}$ BDCA-1^+ ($CD1c^+$) BDCA-3^+ and plasmacytoid DC (pDC) expressing $CD11c^{low}$ BDCA-2^+ ($CD303^+$) $CD123^+$ BDCA-4^+ (MacDonald, Munster et al. 2002). In particular, plasmacytoid dendritic cells are the natural interferon (IFN) type I -producing cells that secrete high amounts of lFNα in response to viruses and thus play an important role in anti-viral immunity (Asselin-Paturel and Trinchieri 2005). Myeloid DCs in turn are characterized by a strong expression of co-stimulatory molecules and the production of pro-inflammatory cytokines like IL-12 and TNFα.

In the course of YFV 17D vaccination, both pDCs and mDCs showed an elevated frequency in peripheral blood at day 7 after vaccination (Figure 6b and Figure 7b).

With respect to recent publications showing infection and maturation of DC subsets by YFV 17D the activation status of the DC subsets were analyzed by comparing MHC class II expression at all time points after vaccination to time-points prior to vaccination (day0). Paralleling their rising numbers, the mean fluorescent intensity of HLA-DR on mDCs increased constantly reaching a maximum at day 7 and a sharp drop at day 14 (Figure 6c). In contrast to mDCs, pDCs did not show a significant regulation of MHC class II expression after vaccination (Figure 7c).

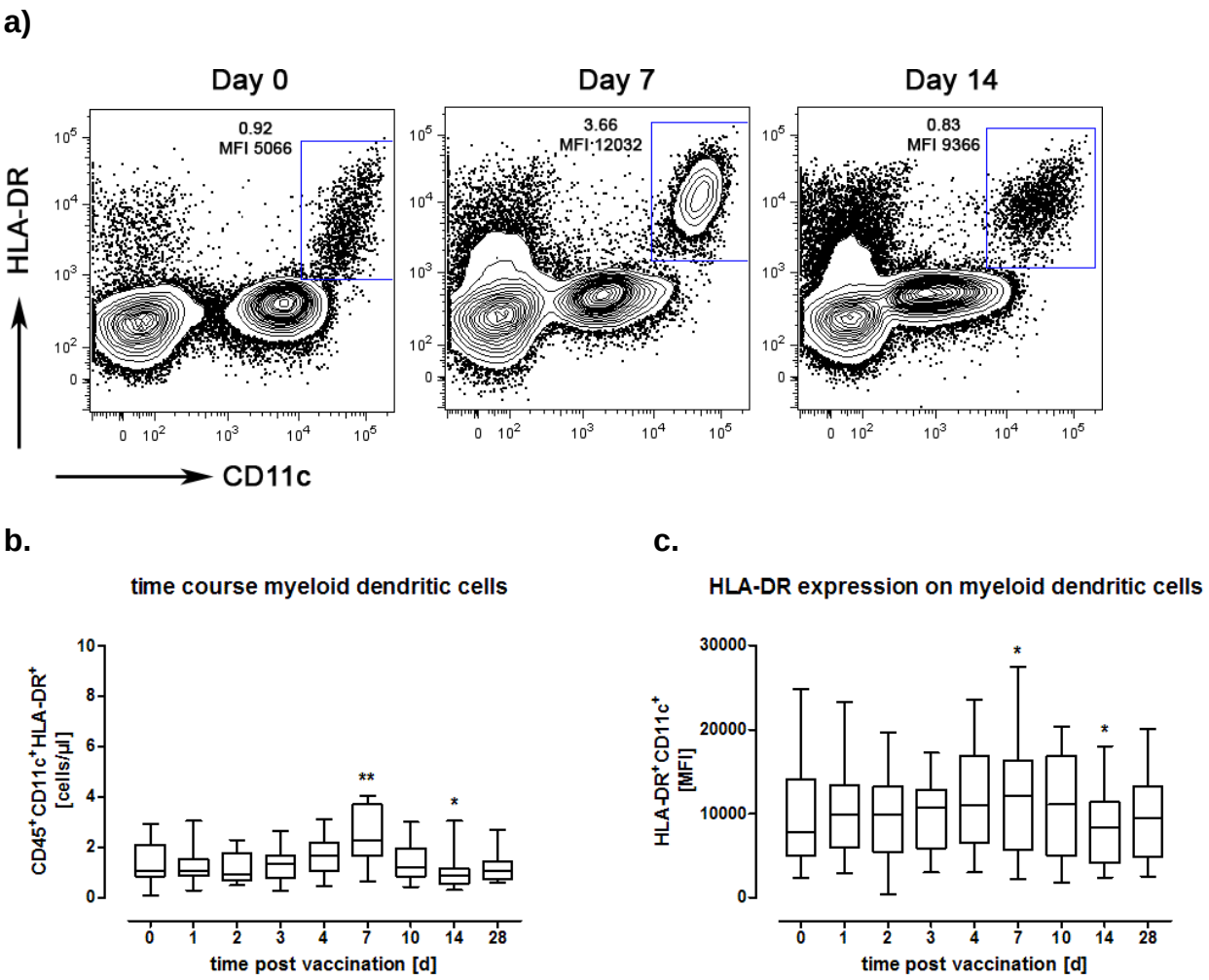

Figure 6: Time course of activated myeloid DCs after vaccination
Elevated frequencies of peripheral blood mDC numbers among $CD45^+$ leucocytes expressing the HLA-DR molecule at individual time points after vaccination in one representative donor (frequency of $CD11c^+$/ $HLA\text{-}DR^+$ and the MFI of $HLA\text{-}DR^+$ are shown above the gate) **(a)**. After exclusion of dead cells by DAPI staining, peripheral blood mDCs were gated on $CD45^+$ leucocytes and defined by $CD11c^+$ and $HLA\text{-}DR^+$ expression in the absence of $CD19^-$ $CD14^-$ $CD56^-$ $BDCA\text{-}2^-$. Increase in MFI as a sign of activation of peripheral blood $CD11c^+$ $HLA\text{-}DR^+$ $CD19^-$ $CD14^-$ $CD56^-$ $BDCA\text{-}2^-$ mDC cell numbers among total $CD45^+$ leucocytes at indicated time points after YFV 17D vaccination in all vaccinees **(b)** (boxes represent the median, 25^{th} and 75^{th} percentile and whiskers indicate the minimum and maximum of absolute values for all donors; "$*$" indicates statistical significance with $p< 0.05$, "$**$" $p< 0.01$). Time course of the mean fluorescence intensity of HLA-DR expression on peripheral blood mDCs in all vaccinees at indicated time points **(c)** (boxes represent the median, 25^{th} and 75^{th} percentile and whiskers indicate the minimum and maximum of absolute values"$*$" indicates statistical significance with $p< 0.05$, "$**$" $p< 0.01$).

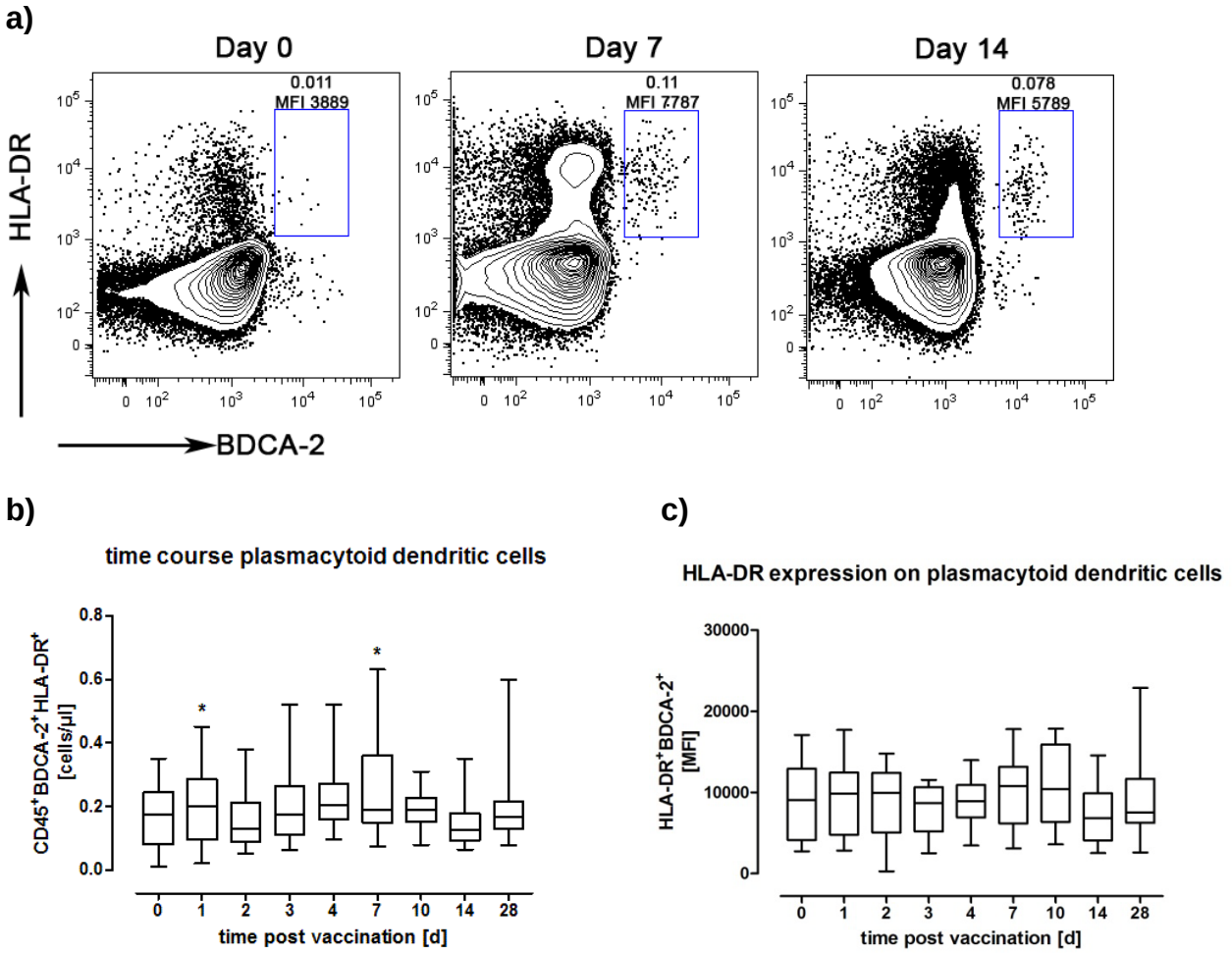

Figure 7: Time course of plasmacytoid DCs after vaccination
Elevated frequencies of peripheral blood pDC numbers among $CD45^+$ leucocytes expressing the HLA-DR molecule at individual time points after vaccination in one representative donor (frequency of $BDCA\text{-}2^+$/ $HLA\text{-}DR^+$ and the MFI of $HLA\text{-}DR^+$ are shown above the gate) **(a)**. After exclusion of dead cells by DAPI staining peripheral blood pDCs were gated on $CD45^+$ leucocytes and defined by $BDCA\text{-}2^+$ and $HLA\text{-}DR^+$ expression in the absence of $CD19^-$ $CD14^-$ $CD56^-$ $CD11c^-$. Time course of peripheral blood $BDCA\text{-}2^+$ $HLA\text{-}DR^+$ $CD19^-$ $CD14^-$ $CD56^-$ $CD11c^-$ pDC cell numbers among total $CD45^+$ leucocytes at indicated time points after YFV 17D vaccination in all vaccinees **(b)** (boxes represent the median, 25^{th} and 75^{th} percentile and whiskers indicate the minimum and maximum of absolute values for all donors; "*" indicates statistical significance with $p< 0.05$, "**" $p< 0.01$). Time course of the mean fluorescence intensity of HLA-DR expression on peripheral blood pDCs in all vaccinees at indicated time points **(c)** (boxes represent the median, 25^{th} and 75^{th} percentile and whiskers indicate the minimum and maximum of absolute values, "*" indicates statistical significance with $p< 0.05$, "**" $p< 0.01$).

However, mDC cell numbers expressing HLA-DR showed a steady increase from day 0 to day 7, followed by a significant drop of frequency at day 14 and a later return to pre-vaccination levels (Figure 6a and b). The increase in pDC cell numbers expressing HLA-DR was rather small, but biphasic with a short significant peak already at day 1 (Figure 7a and b).

Monocytes are known to migrate through the endothelial barrier to become sessile in peripheral tissue. These cells that are a replenishing source for either the pool of macrophages or dendritic cells showed a short but distinct drop in absolute numbers at day 14 in peripheral blood as indicated in Figure 8.

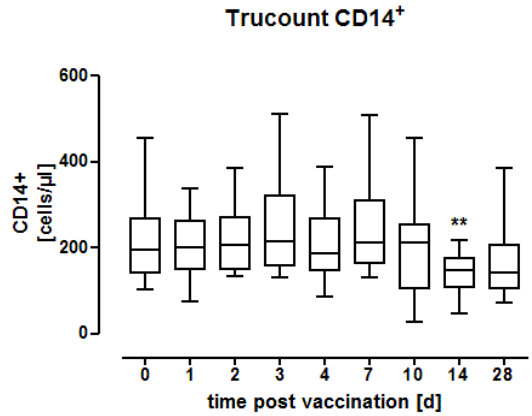

Figure 8: Time course of monocytes after vaccination with YFV 17D
Decrease of absolute cell numbers for $CD14^+$ monocytes showing a sharp drop at day 14 in all donors (boxes represent the median, 25^{th} and 75^{th} percentile and whiskers indicate the minimum and maximum of absolute values. "**" indicates statistical significance with a $p< 0.01$)

Taken together, professional APCs are apparently mobilized into the periphery within a week after vaccination with monocytes serving as a possible replenishing source.

5.3.2 Natural Killer Cells

Human natural killer (NK) cells, capable of killing virus infected cells apart from $CD8^+$ T cells, can be generally subdivided into $CD56^{bright}CD16^-$ cytokine producing and $CD56^{dim}CD16^+$ more cytolytic NK cell subsets. Besides this natural cytotoxicity, another effector mechanism is related to an antibody-dependent cell mediated cytotoxicity that NK cells use to destroy an antibody-coated target without having any antigen specificity themselves. This is facilitated by the expression of the stimulatory high-affinity Fc receptor (CD16) on the surface of NK cells that recognizes an antigen-bound antibody with specificity for antibody subclasses IgG_1 and IgG_3. After binding with this receptor, cytoplasmic granules containing granzyme and perforin that destroy the target cell are released (Perussia 1998; Perussia 2000).

Interestingly, these two different subsets showed quite different kinetics. The cytokine producing $CD56^{bright}$ significantly dropped in cell numbers in peripheral blood at day7 normalizing at later time points. In contrast, already early on day 3 $CD56^{dim}$ cytolytic NK

cells showed a continuous decrease in absolute numbers in peripheral blood, which was most pronounced at day 28, the latest time point examined in this study (Figure 9).

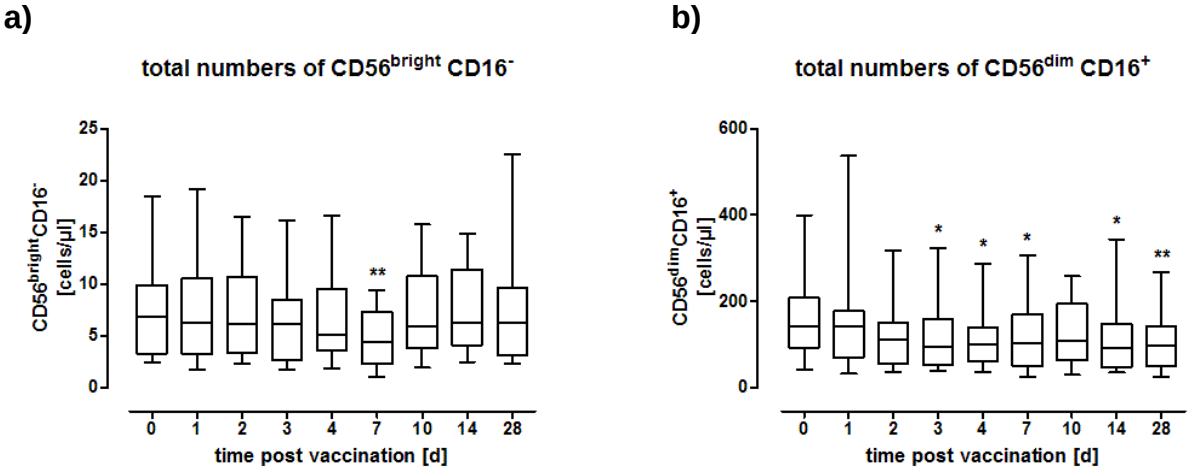

Figure 9: Time course of CD56^{bright} and CD56^{dim} NK cells after vaccination
Short-term decrease in peripheral blood CD56^{bright} NK cells **(a)** and prolonged decrease in CD56^{dim} NK cells **(b)** among CD56^{+} CD3^{-} cells at indicated time points after YFV 17D vaccination in all vaccinees (boxes represent the median, 25th and 75th percentile and whiskers indicate the minimum and maximum of absolute values for all donors, "$*$" indicates statistical significance with a $p< 0.05$, "$**$" $p< 0.01$).

A further subdivision of NK cells by staining for CD62L and a panel of killer inhibitory receptors (KIR) among CD56^{dim} NK cells revealed that the frequency of CD62L^{+} cells was significantly increased at day 10 and day 28 after vaccination shown in Figure 10. In CD56^{bright} NK cells, no alterations of these subsets could be detected (data not shown).

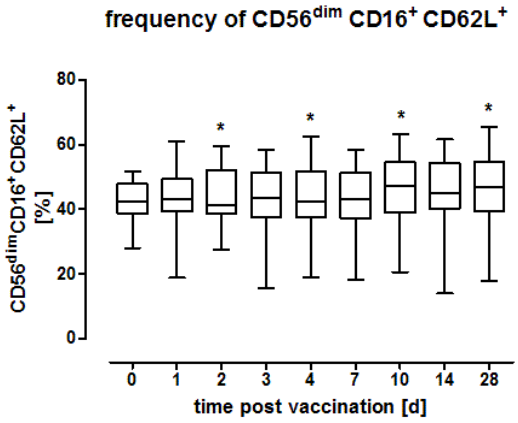

Figure 10: Time course for CD62L expression for the CD56^{dim} NK cell subset
Shown is the increase of peripheral blood CD62L^{+} expression on CD56^{dim} NK cells among CD56^{+} CD3^{-} cells at indicated time points after YFV 17D vaccination in all vaccinees (boxes represent the median, 25th and 75th percentile and whiskers indicate the minimum and maximum of absolute values for all donors, "$*$" indicates statistical significance with a $p< 0.05$).

In conclusion an activation of different arms of the innate immune system that was represented by DC subsets, monocytes and NK cells could be detected. There was no uniform behaviour, but rather different patterns were measurable. Especially at day 7, the results show the strongest modulation of innate immune responses across different cell types.

5.4 Adaptive Immunity

5.4.1 $CD8^+$ T Cells

Adaptive immunity in response to a viral challenge is, represented on the one hand, by $CD8^+$ T cells that are able to detect and kill infected cells expressing viral antigens in a MHC class I context. On the other hand, the interaction of activated $CD4^+$ T cells with B cells is essential to induce high affinity neutralizing antibodies that confer long-term immunity against rechallenge in most vaccination schemes.

In order to analyze the activation of $CD8^+$ T cells in response to YFV 17D vaccination, the expression of CD38 on $CD8^+$ T cells was studied. This activation marker has recently been shown to be expressed on all YFV specific $CD8^+$ T cells in the primary vaccination phase and changes in the percentage of $CD8^+CD38^+$ T cells closely reflect the extent of induction of YFV specific $CD8^+$ T cells (Miller, van der Most et al. 2008).

Similar to CD4 T cells (see below), there was a small though here non-significant peak of absolute numbers of $CD8^+CD38^+$ T cells in peripheral blood at day 2, followed by a boost of $CD8^+CD38^+$ T cells with a maximum at day 14, remaining still above background levels at day 28 (Figure 11).

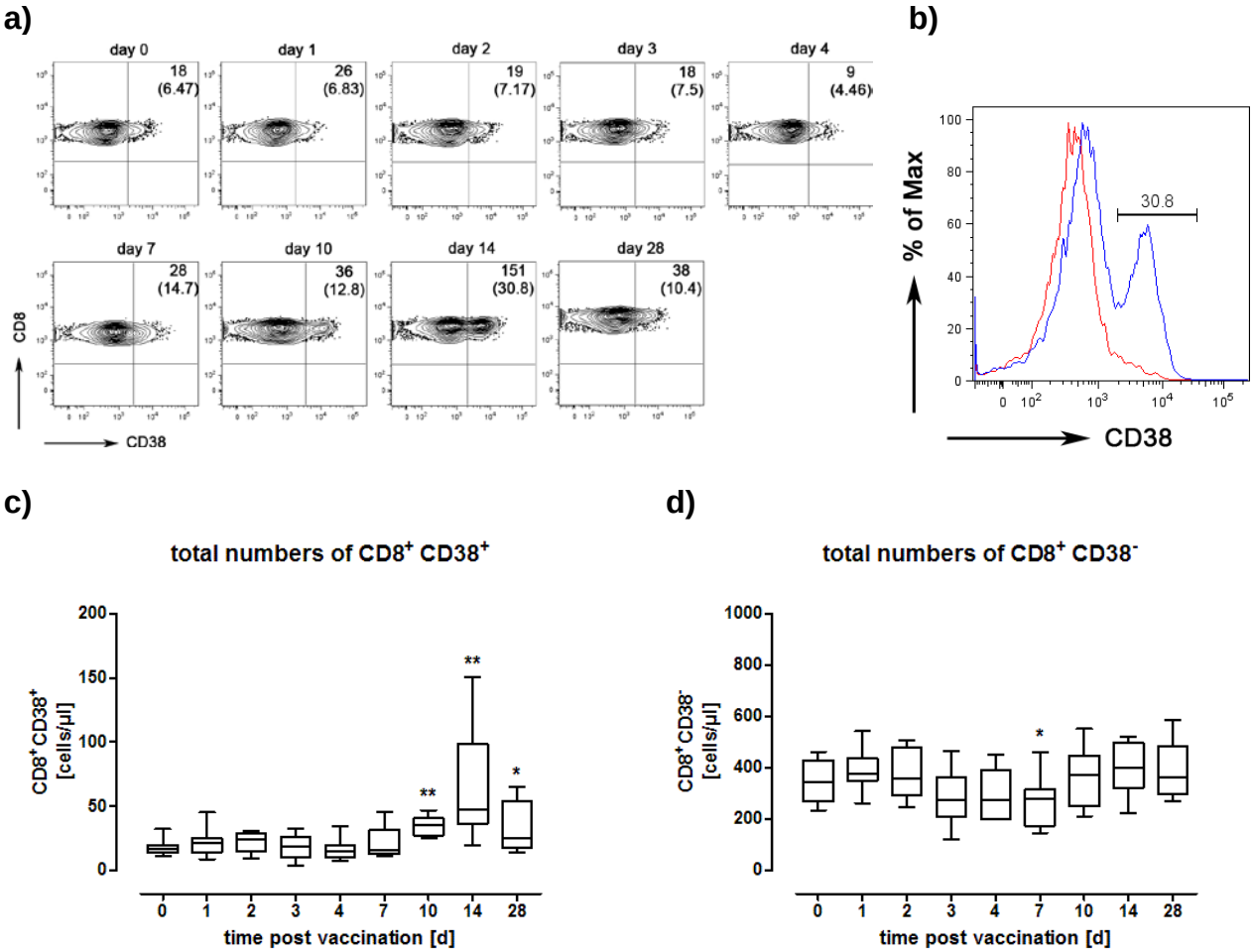

Figure 11: Time course of CD8$^+$CD38$^+$ T cells following YFV 17D vaccination
Boost of CD8$^+$CD38$^+$ numbers at all time points after vaccination in one representative donor (**a**). Numbers indicate absolute cell numbers and relative population frequencies (in brackets). Contour plots were gated on CD3$^+$ CD8$^+$ CD4$^-$ T cells. The histogram plot (**b**) demonstrates the increase of CD8$^+$ CD38$^+$ T cells between day 0 and day 14 in one representative donor.
Increase in absolute CD8$^+$CD38$^+$ T cell numbers with maximum at day 14 for all donors (**c**). Decrease in absolute cell numbers for CD8$^+$CD38$^-$ T cells of all donors present at day 7 (**d**). Individual subsets were gated on CD3$^+$ CD8$^+$ CD4$^-$ T cells (boxes represent the median, 25th and 75th percentile and whiskers indicate the minimum and maximum of absolute values for all donors, "$*$" indicates statistical significance with a $p< 0.05$, "$**$" $p< 0.01$).

Notably, as shown in Figure 12 this increase in CD8$^+$CD38$^+$ T cells activated by YFV 17D was preceded by a drastic drop in the numbers of total CD8$^+$ T cells at day 7 in the peripheral blood of vaccinees.

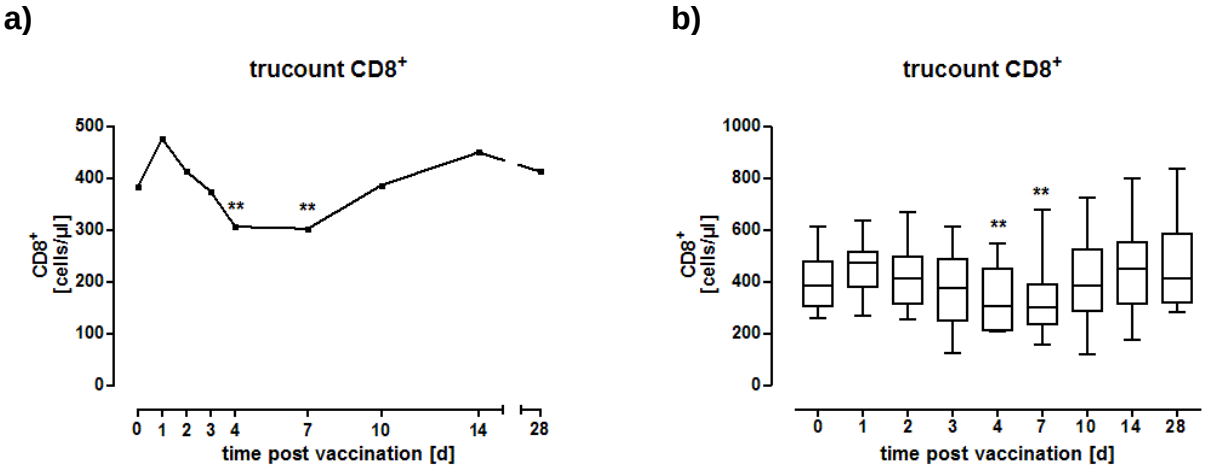

Figure 12: Time course of total CD8$^+$ T cells following vaccination with YFV 17D in all donors
Median for absolute numbers of total CD8$^+$ T cells among total CD45$^+$ leucocytes in peripheral blood of all donors (**a**). Prolonged drop of total CD8$^+$ T cells among total CD45$^+$ leucocytes (**b**) in peripheral blood of all donors (boxes represent the median, 25th and 75th percentile and whiskers indicate the minimum and maximum of absolute values for all donors, "**" indicates statistical significance with p< 0.01).

The analysis of activated CD38$^+$CD8$^+$ T cells also revealed characteristic changes during immunization shown in Figure 13. At day 7, day 10 and day 14 there were significant decreases in the frequency of CD45RA$^+$ and CD45RA$^+$CD127$^+$ subsets among CD8$^+$CD38$^+$ T cells indicating differentiation at the peak of the CD8 T cell response against YFV 17D. These changes returned to near baseline levels at day 28.

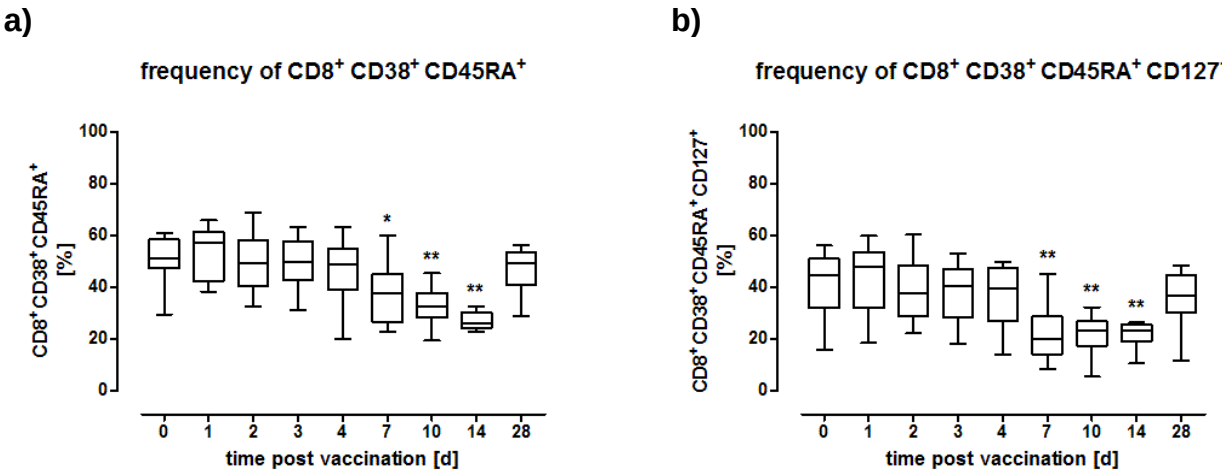

Figure 13: Phenotypical characteristics of activated CD8$^+$CD38$^+$ T cells following vaccination with YFV 17D
Significant decrease of peripheral blood CD45RA$^+$ (**a**) and CD45RA$^+$CD127$^+$ (**b**) among CD8$^+$CD38$^+$ at indicated time points after YFV 17D vaccination in all vaccinees (boxes represent the median, 25th and 75th percentile and whiskers indicate the minimum and maximum of absolute values for all donors, "*" indicates statistical significance with a p< 0.05, "**" p< 0.01).

5.4.2 B Cell Subsets

In parallel to the measurement of anti-YFV 17D-specific antibodies, total numbers and kinetic changes of B cell subsets in peripheral blood of the vaccinees were analyzed at all time points. These B cells can differentiate into two different cell types: antibody secreting plasma cells and memory B cells. Antibody secreting B cells develop from proliferating B cells that differentiate into plasma cell precursors, also known as plasmablasts, expressing surface molecules like $CD19^{low}$ $CD27^{high}$ that are able to secrete affinity matured antibodies. Following this, these cells differentiate further into short-lived plasma cells, which continue to secrete antibodies in the absence of antigenic stimulation. Memory B cells develop with the additional help of helper T cells. These long-lived cells, usually present in a quiescent state, are characterized by surface molecules CD19 and CD27 and they too express affinity matured membrane-bound antibodies. In the case of an antigen re-exposure, memory B cells are able to undergo rapid expansion and become plasmablasts. These plasmablasts have the competence to develop into long-lived plasma cells that maintain affinity selected antibodies which are reactivated during a secondary immune response (Radbruch, Muehlinghaus et al. 2006). Plasma cells differ from plasmablasts in that they lose their expression of MHC class II and therefore lose their ability for antigen presentation. The isotype of secreted antibody in plasma cells is already determined and no longer inducible by class switching. A very crucial step for differentiation of plasmablasts into long-lived plasma cells is the migration of plasmablasts to so called “survival niches” like e.g. the bone marrow.

Naive $CD19^{+}$ $CD27^{-}$ IgD^{+} and memory $CD19^{+}$ $CD27^{+}$ B cell subsets showed changes similar to those of other lymphocyte subsets e.g. CD4+ and CD8+ T cells (Figure 14). An initial small rise at day 2 and a subsequent drop with a minimum at day 7 with further normalization of absolute cell numbers around day 14 could be detected.

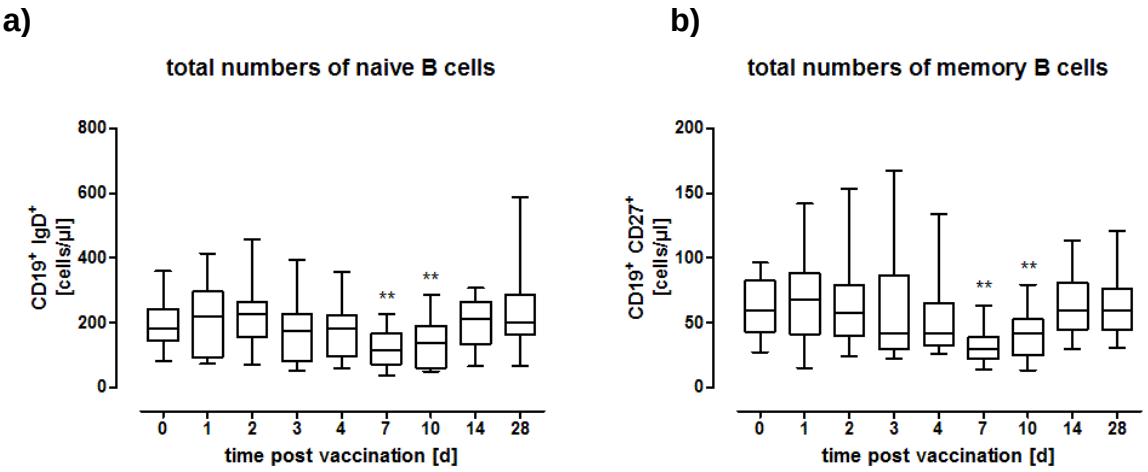

Figure 14: Time course of B cell subsets in peripheral blood after YFV 17D vaccination
Different regulation of B cell subsets in peripheral blood showing a decrease in absolute cell numbers for naïve $CD19^+$ $CD27^-$ IgD^+ (**a**) and memory $CD19^+$ $CD27^+$ (**b**) B cells at indicated time points after YFV 17D vaccination in all vaccinees (boxes represent the median, 25th and 75th percentile and whiskers indicate the minimum and maximum of absolute values for all donors, "**" indicates statistical significance with a $p< 0.01$).

A different picture could be observed for absolute numbers of plasmablasts in peripheral blood characterized by the $CD19^{low}$ $CD27^{high}$ expression. This population initially remained rather constant and then significantly declined in absolute cell numbers at day 7 in a manner comparable to that of naïve and memory B cell subsets. In contrast to the other B cell subsets, there was no further drop of this population but rather a subsequent rise in numbers reaching a detectable maximum at day 14 (Figure 15). This in turn converged with the appearance of YFV 17D-specific antibodies in blood already shown in Figure 5.

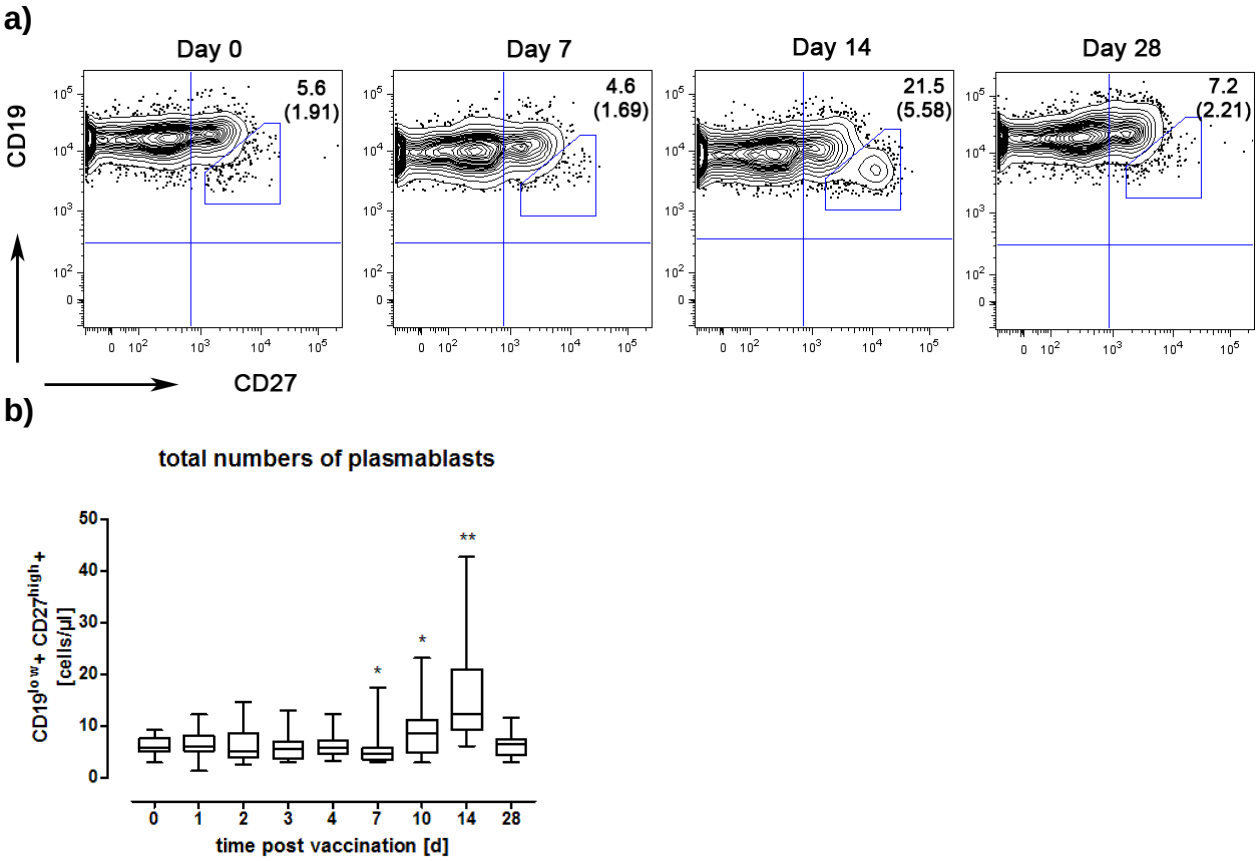

Figure 15: Time course of plasmablasts in peripheral blood after vaccination with YFV 17D

Generation of plasmablasts defined by the surface $CD19^{low}$ $CD27^{high}$ expression at individual time points after vaccination in one representative donor (**a**). Contour plots were gated on $CD19^{+}$ SSC. Numbers indicate absolute cell numbers and relative population frequencies (in brackets). Initial drop followed by a significant increase of absolute plasmablast cell numbers defined by the surface markers $CD19^{low}$ $CD27^{high}$ for all donors (**b**). Individual subsets were gated on SSC $CD19^{+}$ B cells (boxes represent the median, 25^{th} and 75^{th} percentile and whiskers indicate the minimum and maximum of absolute values for all donors, "⋆"indicates statistical significance with a $p< 0.05$, "⋆⋆" $p< 0.01$).

In summary, the number of naïve and memory B cell subsets dropped at day 7 as a result of being presumably recruited from the peripheral blood into the lymph nodes, whilst the number of $CD19^{low}CD27^{high}$ plasmablasts subsequently increased in blood reaching a maximum at day 14. The occurrence of plasmablasts was functionally paralleled by the appearance of YFV 17D-specific antibodies.

5.4.3 Antigen-specific $CD4^+$ T Cells

Pathogen specific $CD4^+$ T cells are not only essential for the production of virus-neutralizing antibodies by B cells that differentiate into plasma cells, but also for the generation of a $CD8^+$ T cell memory. Furthermore, it has been shown that the protective effect of YFV vaccination in a murine encephalitis model is dependent on $CD4^+$ T and B cells, indicating a fundamental role for their interaction in protection mediated by YFV immunization (Chambers and Nickells 2001).

At first, the changes in absolute numbers of $CD4^+$ T cell subsets in the peripheral blood were analyzed in order to study the extent to which they reflect the induction of YFV 17D-specific $CD4^+$ T cell immunity.

To define different human naïve and memory $CD4^+$ T cell subsets, different splice variants of the surface-membrane protein CD45 (CD45RA; CD45RO) were used. Further markers were investigated to describe naïve $CD4^+$ T cells referring to their activation status (CD27) or to their *in vivo* localization (CD62L and CD31). Interestingly, naïve and memory $CD4^+$ T cell subsets showed similar kinetic changes. After an initial non-significant rise, a constant decline of cell numbers until day 7 followed by a return to pre-vaccination levels around day 10 could be observed after vaccination (Figure 16a and Figure 16b). In this study, the two subsets of $CD31^+$ ^{thymic}naive and $CD31^+$ ^{central}naive $CD4^+$ T cells behaved in a way similar to that shown in Figure 16c and Figure 16d. After birth, the development of naïve $CD4^+$ T cells proceeds in the thymus. Interestingly, as it is known that the thymic function after puberty is reduced due to a thymus involution, the absolute numbers of peripheral naïve $CD4^+$ T cells remain stable. This stability can be ensured by the existence of a second peripheral naïve $CD4^+$ T cell subset which cells retain their naïve phenotype due to homeostatic proliferation (Freitas and Rocha 2000). The surface marker CD31 (PECAM-1; Platelet–endothelial-cell-adhesion-molecule-1) allows the discrimination between these two subsets of naïve $CD4^+$ T cells as recent thymic emigrants (RTE) express the CD31 molecule ($CD31^+$ ^{thymic} naïve $CD4^+$ T cells), whereas the $CD4^+$ T cells that have proliferated in the periphery do not ($CD31^-$ ^{central} naïve $CD4^+$ T cells) (Kohler and Thiel 2009).

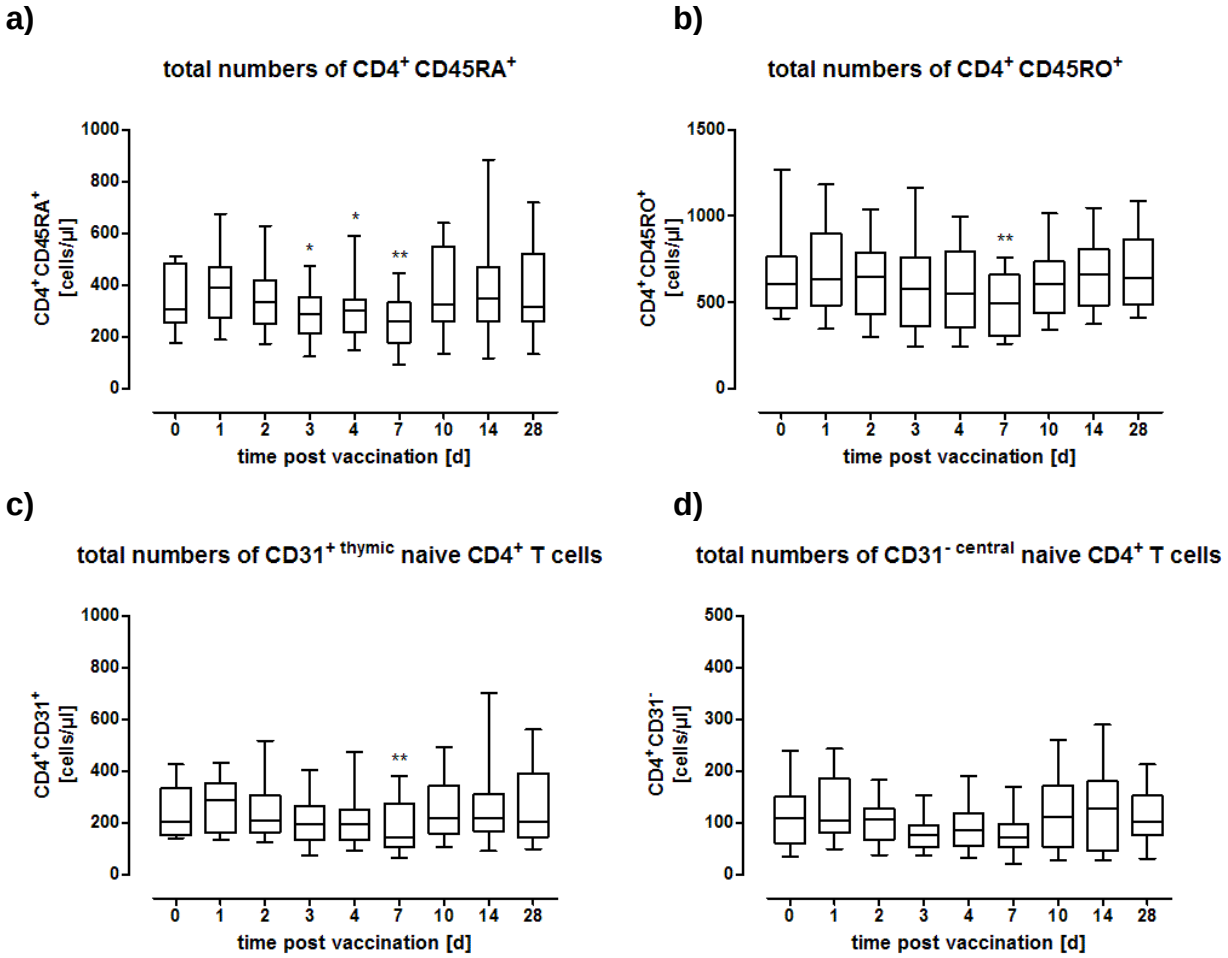

Figure 16: Appearance of absolute cell numbers of different CD4$^+$ T cell subsets in peripheral blood after YFV 17D vaccination

Time course of total peripheral blood naïve (**a**) and memory (**b**) CD4$^+$ T cell numbers after YFV 17D vaccination in all vaccinees showing a constant decline of cell numbers until day 7 followed by a return to pre-vaccination levels around day 10. Gating was performed on CD4$^+$ CD45RA$^+$ CD45RO$^-$ CD27$^+$ CD62L$^+$ (naïve) and CD4$^+$ CD45RO$^+$ CD45RA$^-$ (memory) CD4$^+$ T cells (boxes represent the median, 25th and 75th percentile and whiskers indicate the minimum and maximum of absolute values for all donors, "$*$"indicates statistical significance with a $p< 0.05$, "$**$" $p< 0.01$).

Significant decrease in absolute numbers of peripheral blood CD31$^{+\ thymic}$ naïve CD4$^+$ T cells (**c**), whereas there were no changes detectable in absolute numbers of CD31$^{+\ central}$ naïve CD4$^+$ T cells (**d**) after YFV 17D vaccination in any vaccinees. Gating was performed on CD4$^+$ CD45RA$^+$ CD45RO$^-$ CD27$^+$ CD62L$^+$ CD31$^+$ and CD4$^+$ CD45RA$^-$ CD45RO$^+$ CD27$^-$ CD62L$^-$ CD31$^-$ CD4$^+$ T cells according to the appropriate isotype control (boxes represent the median, 25th and 75th percentile and whiskers indicate the minimum and maximum of absolute values for all donors, "$**$"indicates statistical significance with a $p< 0.01$).

In order to assess in detail the induction of antigen-specific CD4$^+$ T cell immunity during primary vaccination, the expression of CD40L and cytokine production after YFV 17D stimulation were analyzed at different time points in all vaccines (Frentsch, Arbach et al. 2005; Meier, Stark et al. 2008). It was possible to calculate the absolute numbers of antigen-specific CD4$^+$ T cells per µl of blood at all time points by combining the analysis

of frequency of antigen specific $CD4^+$ T cells after *in vitro* antigenic re-stimulation with the absolute number of $CD4^+$ T cells determined in individual donors by TruCount analysis

While the analysis of an up-regulation of CD40L on $CD4^+$ T cells served as a marker of antigen specificity irrespective of the individual cytokine secretion (Frentsch, Arbach et al. 2005), the functional capacity of $CD4^+$ T cells induced by vaccination was determined by discriminating IL-2, IFNγ, TNFα and IL-4 secreting $CD4^+CD40L^+$ T cells.

In line with the induction of neutralizing antibody responses (see Figure 5), an induction of $CD40L^+$ YFV 17D-specific $CD4^+$ T cells could be observed in all donors. The appearance of CD40L on $CD4^+$ T cells after *in vitro* re-stimulation started to increase significantly from day 7 (frequency) and day 10 (absolute numbers) on with a maximum at day 14 (Figure 17 a and Figure 17b).

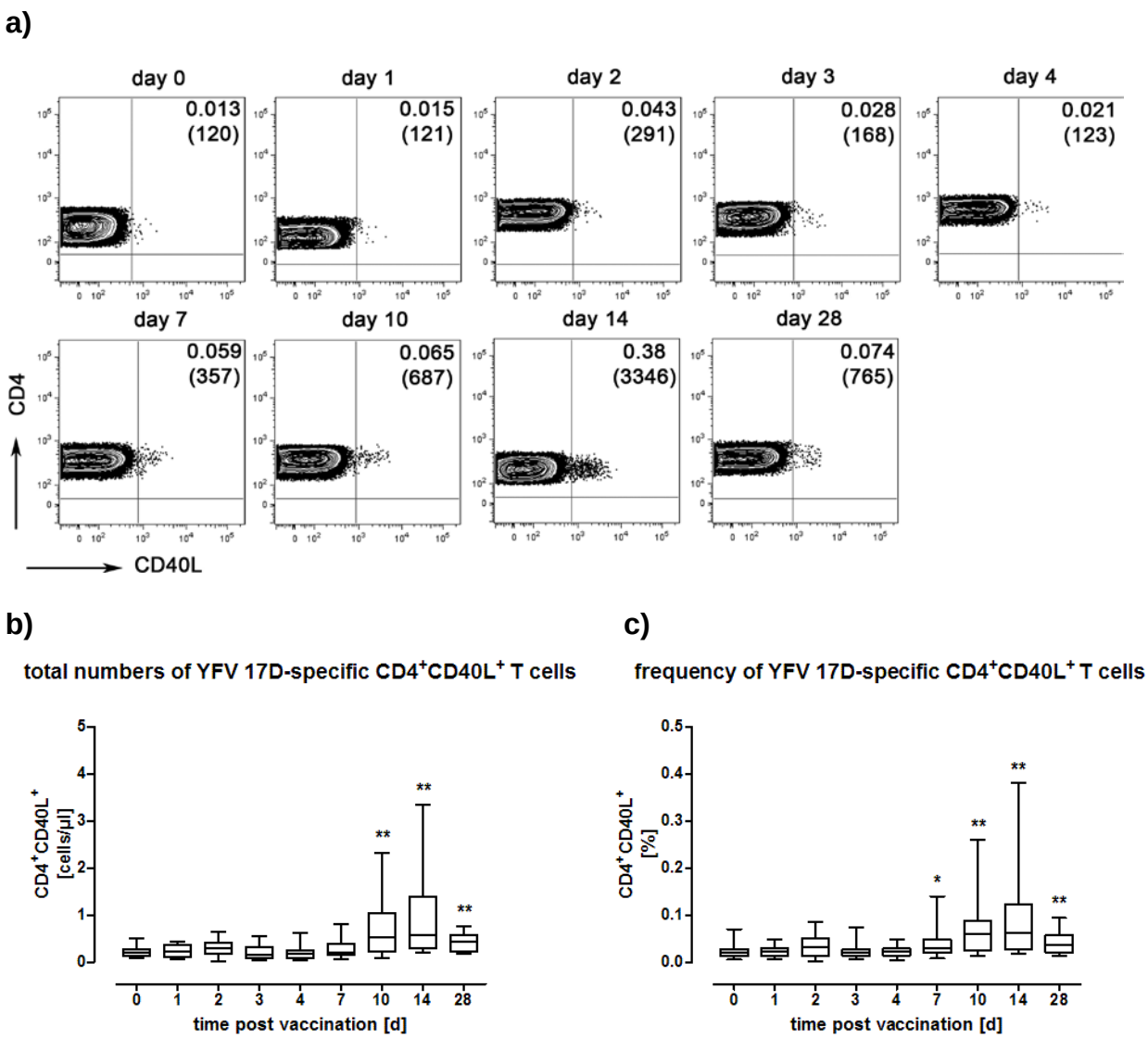

Figure 17: Time course of antigen specific CD4$^+$CD40L$^+$T cells after *in vitro* re-stimulation with YFV 17D

Generation of YFV 17D-specific CD4$^+$CD40L$^+$ T cells (**a**) at individual time points after *in vitro* re-stimulation following vaccination in one representative donor. Contour plots were gated on CD4$^+$ CD14$^-$ lymphocytes. Numbers indicate relative population frequencies and absolute cell numbers (in brackets).

Time course of YFV 17D-specific CD4$^+$CD40L$^+$ T cells for total numbers (**b**) and frequency (**c**) after *in vitro* re-stimulation with YFV 17D in all donors (boxes represent the median, 25th and 75th percentile and whiskers indicate the minimum and maximum of absolute values for all donors, "*"indicates statistical significance with a p< 0.05, "**" p< 0.01).

Interestingly, the analysis of absolute CD40L$^+$ CD4$^+$ cytokine secreting T cells revealed rising numbers from day 2 on, depending on the individual cytokine analyzed. Notably, already at day 2 significant absolute numbers for IL-2, TNFα and IFNγ secreting CD40L$^+$ T cells were observed. Subsequently, on day 3 the cell numbers decreased in peripheral blood and reappeared on day 4 (IL-2 and TNFα) and day 7 (IFNγ), respectively, resulting in a biphasic appearance of these cytokine producing YFV 17D-

specific $CD4^+$ T cells in peripheral blood (Figure 18d-f). In contrast, a significant number of YFV 17D-specific $CD4^+$ $CD40L^+$ $IL\text{-}4^+$ T cells was not detectable in peripheral blood before day 7 (Figure 18g). Nevertheless the maximum number of YFV 17D-specific cells was detected on day 14 in most donors and declined thereafter.

a) Negative Control

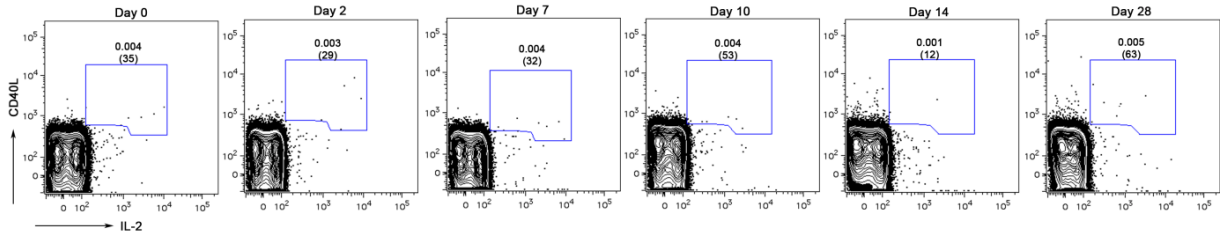

b) YFV 17D antigen specific $CD4^+CD40L^+IL\text{-}2^+$ T cells

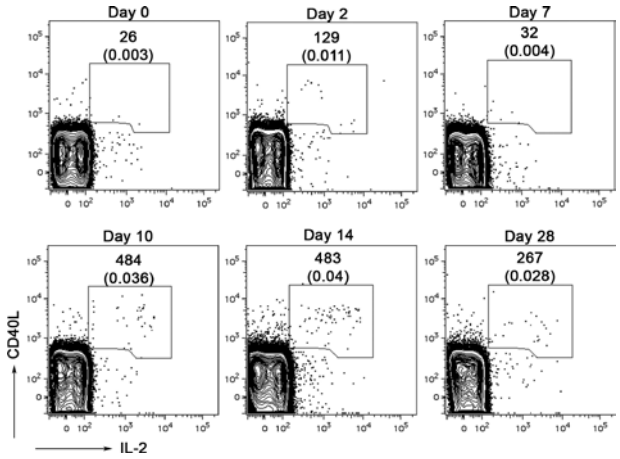

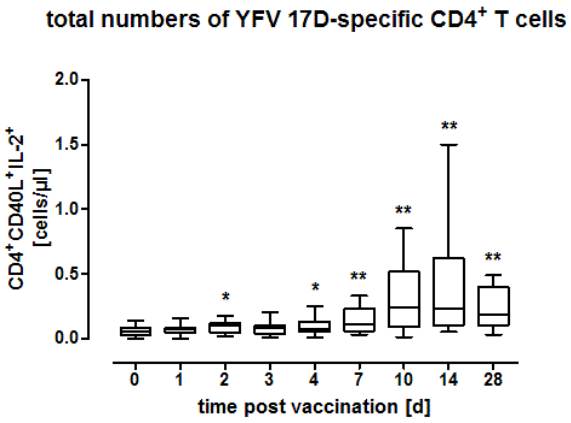

c) YFV 17D antigen specific $CD4^+CD40L^+IFN\gamma^+$ T cells

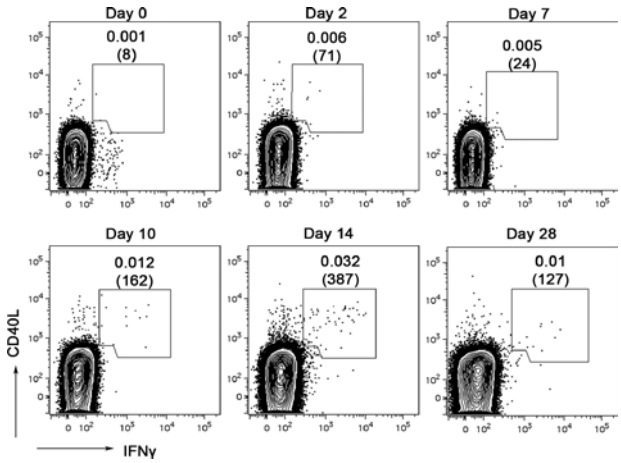

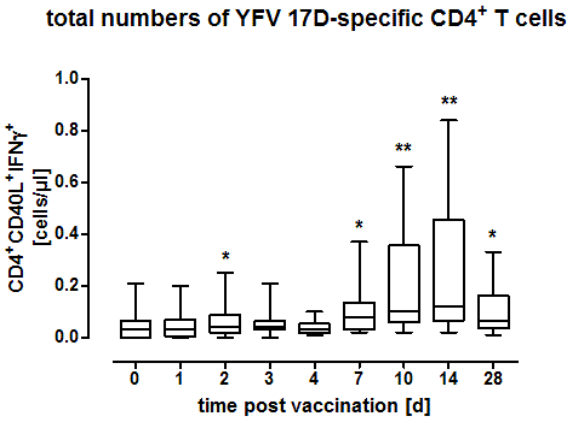

d) YFV 17D antigen specific CD4$^+$CD40L$^+$TNFα$^+$ T cells

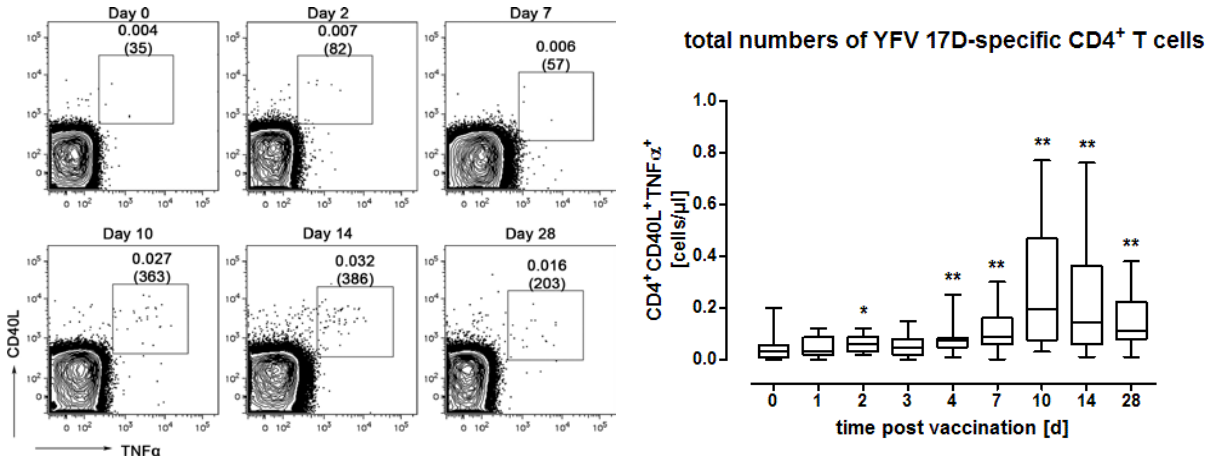

e) YFV 17D antigen specific CD4$^+$CD40L$^+$IL-4$^+$ T cells

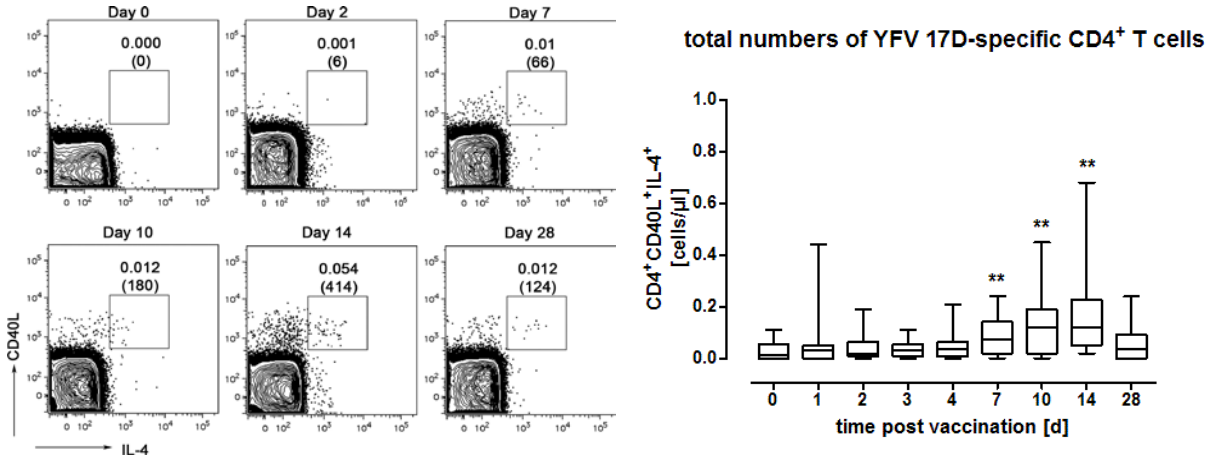

Figure 18: Time course of YFV 17D-specific cells CD40L$^+$CD4$^+$ T cells in peripheral blood after vaccination

One representative analysis of a negative control for IL-2$^+$ secreting CD4$^+$CD40L$^+$ T cells (**a**) after *in vitro* re-stimulation with α CD28 in one donor. Representative dot plot analyses for IL-2$^+$ (**b**), IFNγ$^+$ (**c**), TNFα$^+$ (**d**) and IL-4$^+$ (**e**) secreting YFV 17D-specific CD4$^+$CD40L$^+$ T cells after *in-vitro* whole blood re-stimulation with α CD28 and YFV 17D in one donor. For every sample lymphocytes were gated on CD4$^+$ CD14$^-$ T cells at individual time points. Numbers indicate relative population frequencies and absolute cell numbers (in brackets). Corresponding box and whisker plots showing increases in absolute numbers of IL-2$^+$ (**b**), IFNγ$^+$ (**c**), TNFα$^+$ (**d**) and IL-4$^+$ (**e**) secreting YFV 17D-specific CD4$^+$CD40L$^+$ T cells for all donors at indicated time points (boxes represent the median, 25th and 75th percentile and whiskers indicate the minimum and maximum of absolute values for all donors, "*"indicates statistical significance with a p< 0.05, "**" p< 0.01). Interestingly, for IL-2$^+$ (**b**), IFNγ$^+$ (**c**) and TNFα$^+$ (**d**) secreting YFV 17D-specific CD4$^+$CD40L$^+$ T cells a significant peak already appears at day two.

In summary, in parallel to an early decline of total CD4$^+$ T cells, there were two waves of YFV 17D-specific CD4$^+$ T cells in peripheral blood of vaccines. YFV 17D-specific T cells producing IL-2, IFNγ and TNFα T cells first peaked at day 2, declined briefly and reappeared at day 4 and day 7, respectively. In contrast, YFV 17D-specific CD4$^+$ CD40L$^+$ IL-4$^+$ T cells started to show a significant increase from day 7 on.

5.4.4 Polyfunctional YFV 17D-specific CD4$^+$ T Cells

Recent studies could show that the induction of polyfunctional T cells, i.e. of cells with a broad spectrum of effector cytokines and functions, is an important predictor for the successful induction of protective immunity in mice and men (De Rosa, Lu et al. 2004; Darrah, Patel et al. 2007).

Referring to this it was shown that YFV immunization induces CD4$^+$ T cells with a broad functional capability (Gaucher, Therrien et al. 2008; Guy, Nougarede et al. 2008). However these analyses were performed only at rather late time points at which the virus is already cleared (Niedrig, Lademann et al. 1999; Miller, van der Most et al. 2008) and a protective antibody titer was present. To what extent this polyfunctional pattern is already present at earlier time points or whether it develops gradually over the course of immune reaction is not known yet. Therefore, the kinetic of the functional composition of YFV 17D-specific T cells at earlier time points was analysed, focussing on the two peaks before (day 2) and after (day 10/14) viral clearance.

At all time points, YFV 17D-specific TNFα, IL-2, IFNγ and IL-4 expressing T cells could be detected. The comparison of the functional composition of cytokine secreting CD4$^+$ CD40L$^+$ T cells at different time points after immunization revealed significant differences in the percentage of cytokine distribution with maximum numbers of quatriple and triple cytokine producers at day 10 (Figure 19). Nevertheless a distinct composition of a cytokine fraction comprised of 3, any 2, or any 1 cytokine in response to *in vitro* stimulation was already present at day 2.

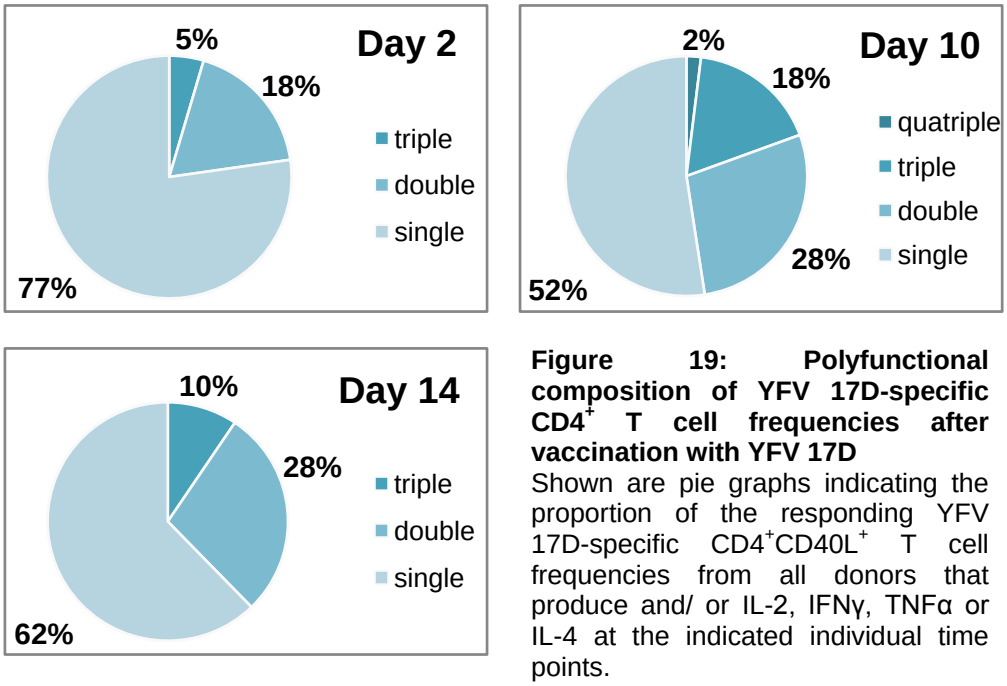

Figure 19: Polyfunctional composition of YFV 17D-specific CD4$^+$ T cell frequencies after vaccination with YFV 17D
Shown are pie graphs indicating the proportion of the responding YFV 17D-specific CD4$^+$CD40L$^+$ T cell frequencies from all donors that produce and/ or IL-2, IFNγ, TNFα or IL-4 at the indicated individual time points.

5.4.5 Bystander Mobilization of CD4$^+$ T Cells Specific for Non-Vaccine Related Antigens

The results described above indicate a strong activation of different arms of the immune system in the course of YFV vaccination. But it is uncertain whether under these conditions an activation of CD4$^+$ T cells harbouring a TCR specificity not directed against YFV antigens can be observed, though recently bystander activation of CD8$^+$ T cells measured by tetramer staining could not be observed during primary YFV and VV vaccination (Miller, van der Most et al. 2008).

In order to access bystander activation, the amounts of tetanus toxoid (TT) and cytomegalovirus (CMV) specific CD4$^+$ T cells in all vaccinees at different time points after vaccination were quantified.

In the case of CMV-specific CD4$^+$ T cells secreting IL-2 or IFNγ, no significant changes of the absolute numbers of specific cells could be detected in peripheral blood after vaccination. However, there was an increase in the number of CMV-specific CD4$^+$ CD40L$^+$ TNFα$^+$ T cells at day 4 (Figure 20a), but more pronounced for CMV-specific CD4$^+$ CD40L$^+$ IL-4$^+$ T cells that showed a significantly higher frequency at day 10 and day 14 (Figure 20b).

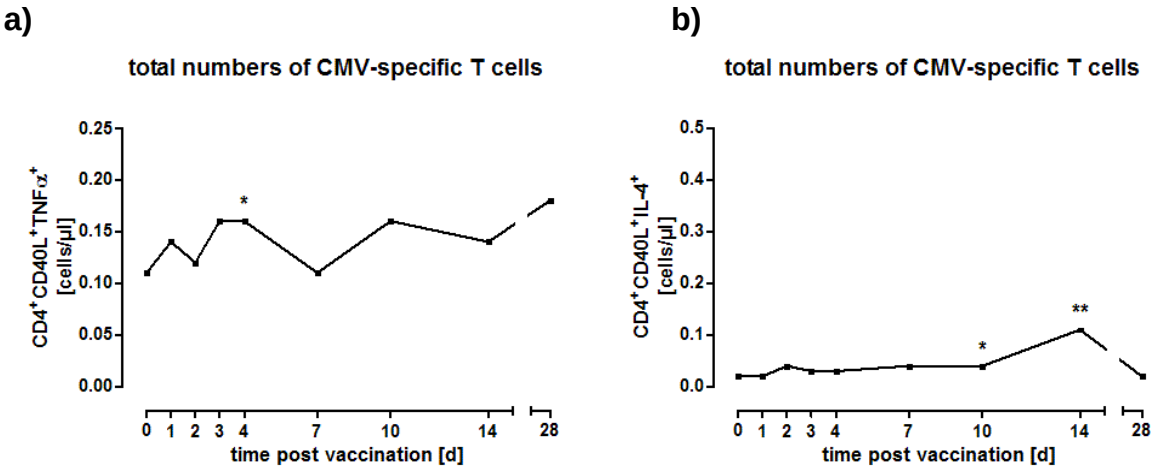

Figure 20: Bystander activation towards non-vaccine related antigens for CMV during the course of vaccination with YFV 17D

Median values for absolute numbers of CMV-reactive CD4$^+$ CD40L$^+$ TNFα$^+$ **(a)** and CD4$^+$ CD40L$^+$ IL-4$^+$ **(b)** T cells at indicated time points for all vaccinees.

Furthermore, an increased number of TT reactive CD4$^+$ CD40L$^+$ T cells could be detected displaying a pattern strikingly similar to YFV 17D-specific cells. Specifically, a short early wave of IL-2$^+$ (Figure 21a and b) and IL-4$^+$ (Figure 21e and f) secreting TT-specific CD4$^+$ CD40L$^+$ T cells in the peripheral blood of vaccinees at day 2/3 could be

observed. At day 14 the highest activation of TT-specific IL-4$^+$ T cells was detected, preceding an increased count of IL-2$^+$, IL-4$^+$ and TNFα$^+$ TT-specific T cells at day 28 (Figure 21c and d).

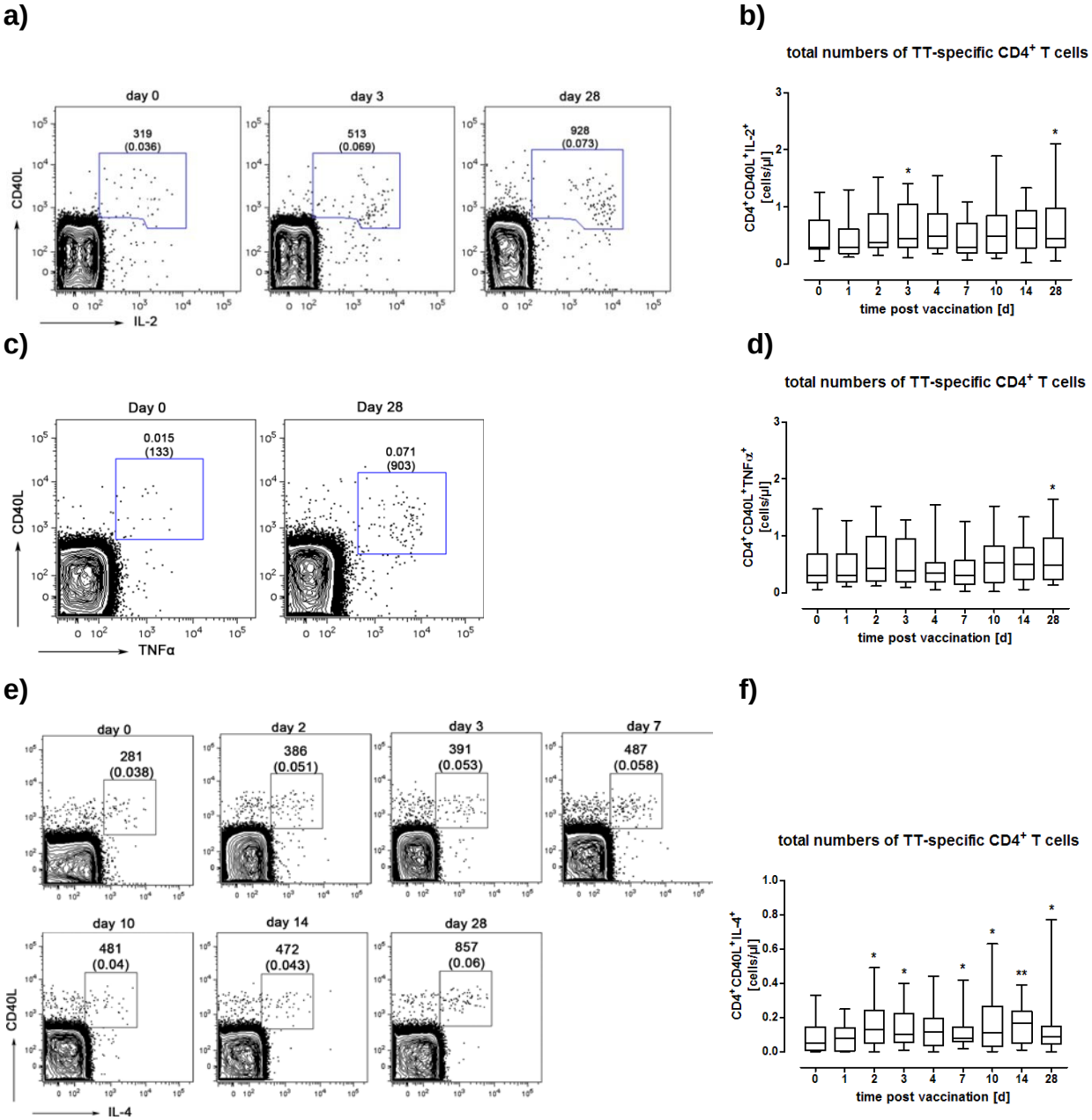

Figure 21: Bystander activation towards non-vaccine related antigens for TT in the course of vaccination with YFV 17D

Increased T cell reactivity after *in vitro* re-stimulation of whole blood with TT in one representative donor. Numbers indicate relative population frequencies and absolute cell numbers (in brackets) of CD4$^+$ CD40L$^+$ IL-2$^+$ **(a)** respectively CD4$^+$ CD40L$^+$ TNFα$^+$ **(c)** and CD4$^+$ CD40L$^+$ IL-4$^+$ **(e)** T cells. Dot plots are gated on CD4$^+$, CD14$^-$ lymphocytes. Gates were set according to negative (αCD28) and positive (SEB) controls. Time courses are shown for absolute numbers of TT-specific CD4$^+$ CD40L$^+$ IL-2$^+$ (**b**) TNFα$^+$ (**d**) and IL-4$^+$ (**f**) T cells in the course of YFV vaccination with 17D in all donors (boxes represent the median, 25th and 75th percentile and whiskers indicate the minimum and maximum of absolute values for all donors, "*"indicates statistical significance with a p< 0.05, "**" p< 0.01).

Comparing the composition of cytokine expression among TT- and CMV-specific $CD4^+$ $CD40L^+$ T cells at different time points after vaccination, no significant changes, determined by the distribution of cytokine frequencies, could be detected. In contrast, there was a significantly higher frequency of IL-2 producers among TT-specific T cells in general compared to CMV- and YFV 17D-specific T cells. Concerning TNFα production again TT-specific T cells revealed maximum frequencies, however, here too TNFα production was higher among CMV-specific cells as compared to YFV 17D-specific T cells.

In summary, though distinguishable by different kinetics, an increased number of both TT- and CMV-reactive $CD4^+$ T cells could be detected in the course of primary vaccination with YFV 17D.

Possible mechanisms that explain this increased *in vitro* reactivity against stimulation with CMV and TT is bystander activation or the mobilization of these antigen specific $CD4^+$ T cells from survival niches like e.g. the bone marrow in the course of vaccination. In order to rule out this possibility, in some of the vaccinees (n=10) the expression of Ki-67, a nuclear antigen which is up-regulated in cells in the G_1,G_2 and S phase of cell cycle and therefore indicates ongoing cell proliferation, was analyzed.

This analysis revealed clearly an induction of proliferation in IL-2^+ and TNFα^+ expressing YFV 17D-specific T cells indicating a recent activation of these cells. On day 2, the first time point at which significant numbers of cytokine secreting YFV 17D-specific T cells could be detected (Figure 18), a low level of Ki-67 expression was detectable in a minority of vaccinees. An significant increase of Ki-67 expression in the majority of vaccines started for both cytokines on day 7, reaching a maximum on day 10 followed by a decline, though to still detectable levels, at day 28 (Figure 22).

In contrast, the analysis of Ki-67 expression in TT- and CMV-specific T cells showed that before the vaccination with live virus (day 0), no significant steady state proliferation of TT- and CMV-specific cells was present. At all later time points analyzed, no significant expression of Ki-67 was measurable in TT- and CMV-specific TNFα^+ or IL-2^+ secreting $CD4^+$ T cells in any of the vaccinees. For technical reasons, the Ki-67 expression could not be analyzed in IFNγ^+ and IL-4^+ producing $CD4^+CD40L^+$ T cells.

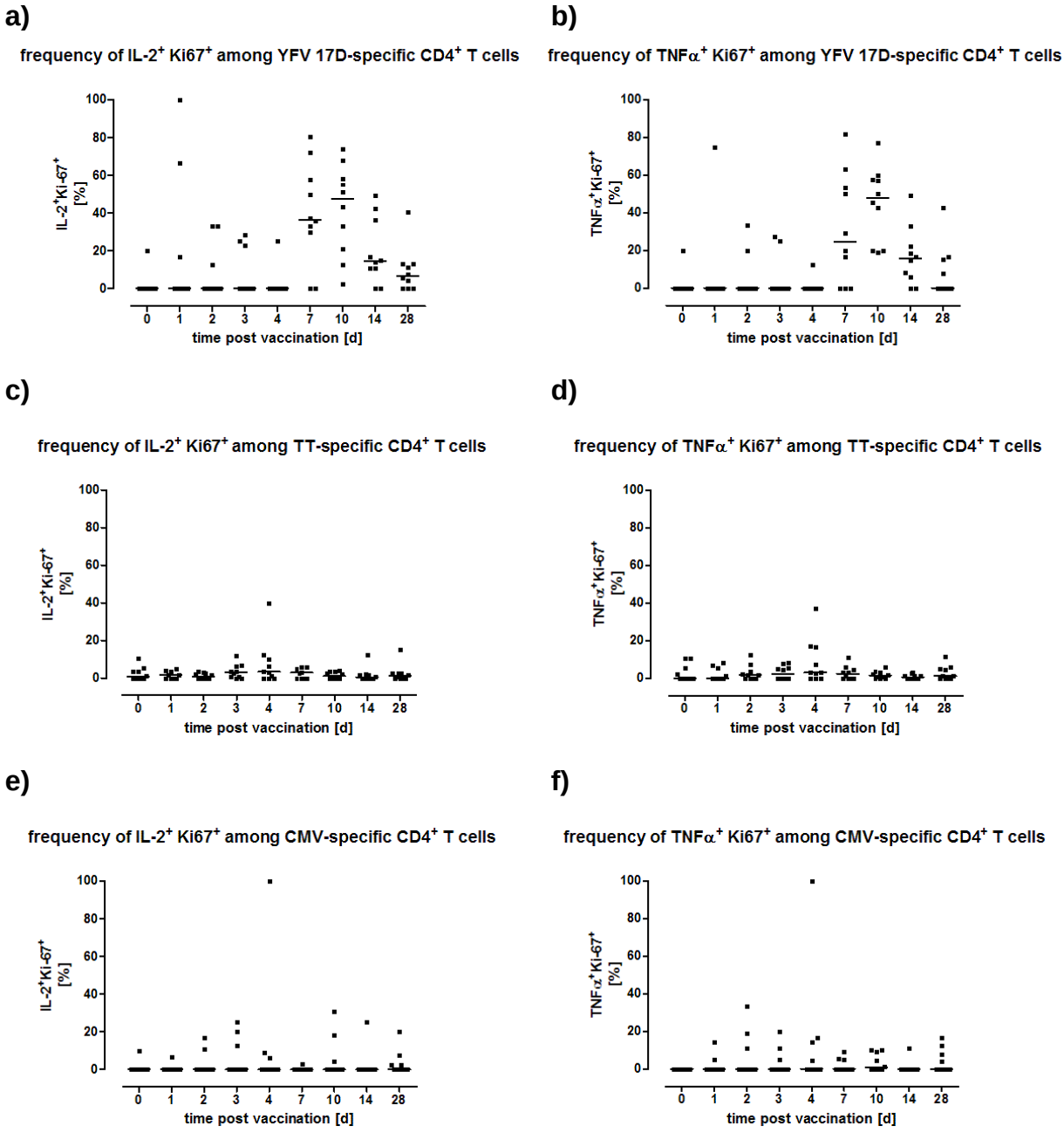

Figure 22: Expression of Ki-67 among antigen specific CD4$^+$ T cells during the course of vaccination with YFV 17D

Frequencies of Ki-67 expression indicating proliferation of IL-2$^+$ (**a,c,e**) and TNFα$^+$ (**b,d,f**) secreting CD4$^+$ CD40L$^+$ T cells after *in vitro* re-stimulation with YFV 17D (**a and b**), TT (**c and d**) and CMV pp65 (**e and f**) in 10 vacinees.

5.5 Correlation of Immune Parameters with YFV 17D Viremia

In cooperation with the group of Prof. Niedrig at the Robert-Koch Institute, specific immune responses were used to correlate them to viral parameters and the induction of neutralizing antibody titers following YFV 17D vaccination.

The fact that YFV 17D RNA is detectable in nearly half of the vaccines at early time points between day 3 and day 7 could be indicative of differences in the innate immune response in the group of viremic versus non-viremic vaccinees. To confirm this, some of the innate immune parameters in these two groups of donors were compared.

Surprisingly, the viremic donors had significantly more CD56^{dim} cells at day 4, day 7 and day 14 as compared to non-viremic donors. Interestingly, also a correlation of HLA-DR expression on myeloid DCs could be observed already early at day 1 and rather late at day 14. Strikingly, for both subsets this difference could already be detected on day 0 before vaccination (Figure 23).

For other parameters like CD56^{bright} NK cells, pDC and their up-regulation of mean fluorescence intensity of HLA-DR no significant differences could be detected.

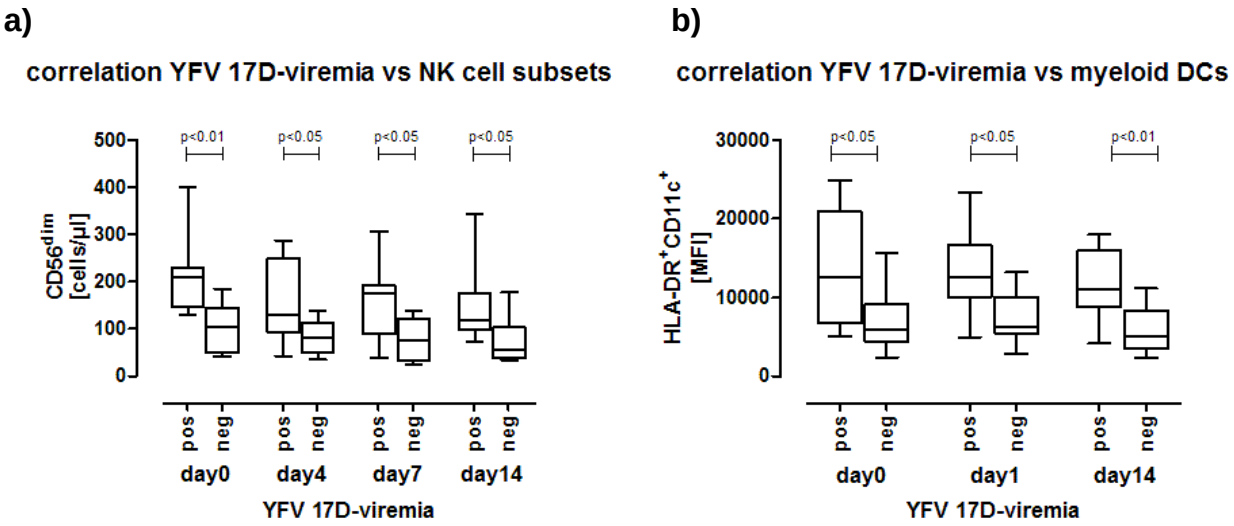

Figure 23: Correlation of innate immune parameters with YFV 17D detected RNA in peripheral blood after vaccination

Correlation of the CD56^{dim} NK cell subset (**a**) and the MFI of HLA-DR expression on mDCs (**b**) with positive (pos) versus negative (neg) detected YFV 17D viremia at indicated time points (boxes represent the median, 25th and 75th percentile and whiskers indicate the minimum and maximum of absolute values for all donors).

Thus, a lower frequency of NK cells and a lower HLA-DR expression on mDCs before vaccination did predict the prevention of viral dissemination as measured by virus-specific PCR.

5.6 Correlation of Immune Parameters with Neutralizing Antibodies Against YFV 17D

Analogous to the viremia indicating the strength of the innate arm of the immune system, the height of the anti-YFV 17D neutralizing antibody titer indicates the magnitude of protection against the viral challenge, basically based upon the cooperation between T and B cells.

Concerning this, two groups of NT^{high} and NT^{low} responders defined by their differences in the immune response at day 14 (Figure 5b) were analyzed.

There was no difference in the number of YFV 17D-specific $CD4^+$ $CD40L^+$ $IL\text{-}4^+$ or $TNF\alpha^+$ T cells after vaccination between the two groups. In contrast, a significantly increased number of $CD4^+$ $CD40L^+$ $IL\text{-}2^+$ (day 1 and day 2) and $IFN\gamma^+$ cells (day 2) in the NT^{high} responders was detectable (Figure 24). In contrast to the antigen specific $CD4^+$ $CD40L^+$ T cells, no correlation of total numbers of $CD4^+$ T cells with the antibody titer could be detected.

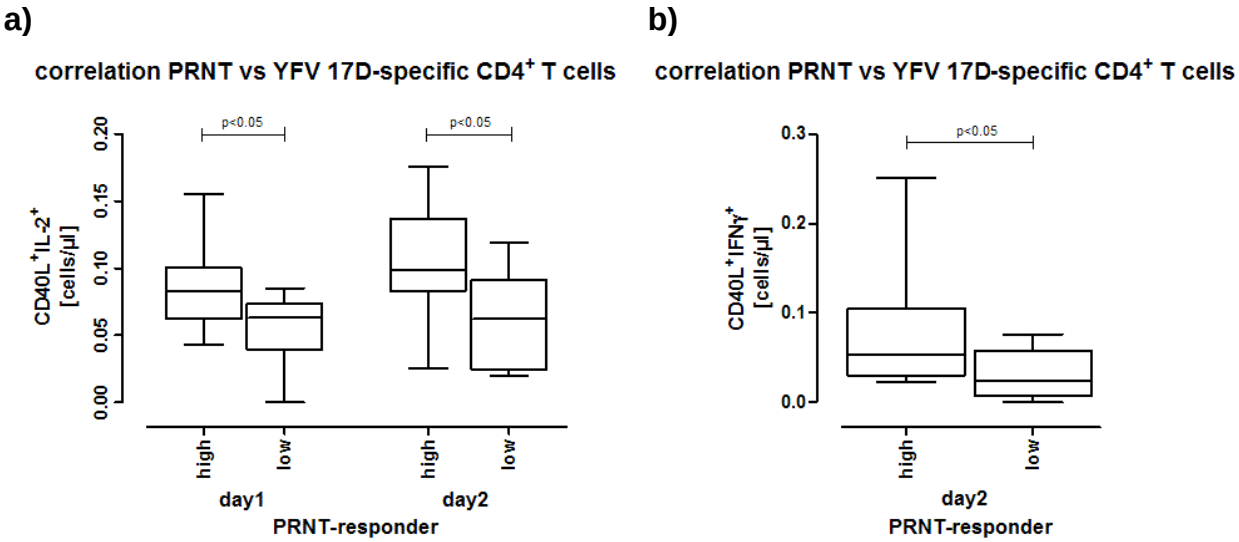

Figure 24: Correlation of YFV 17D-specific $CD4^+$ $CD40L^+$ T cells with neutralizing antibodies directed against YFV 17D in peripheral blood

Correlation of YFV 17D-specific $CD4^+$ $CD40L^+$ T cells secreting IL-2 (**a**) and IFNγ (**b**) with high and low neutralizing antibody titers grouped at day 14 for indicated time points (boxes represent the median, 25^{th} and 75^{th} percentile and whiskers indicate the minimum and maximum of absolute values for all donors).

Interestingly, here, too, there was a difference in the distribution of the number of NK cells between the two groups. The correlation revealed a significantly lower number of

CD56^{dim} and CD56^{bright} NK cells at early time points after vaccination in the NT^{high} group (Figure 25).

For total CD8^{+} T cells, B cells, DC subsets and HLA-DR expression, no significant differences could be detected. But there was a tendency (p 0.077) detectable in the NT^{high} group of vaccinees to have a higher number of CD19^{low}CD27^{high} plasmablasts at day 10.

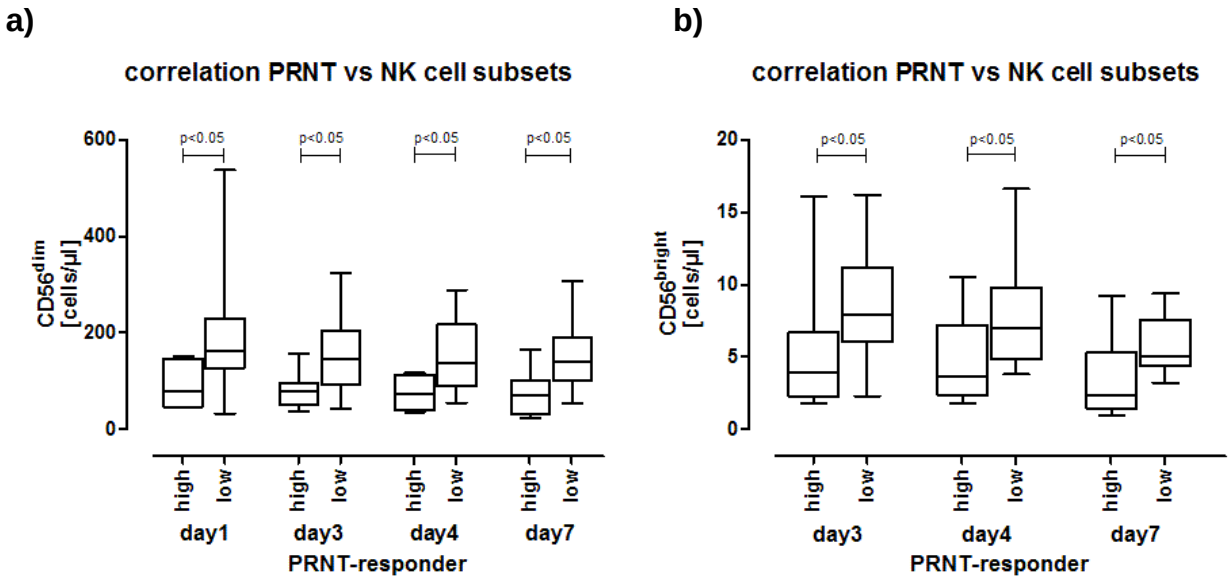

Figure 25: Correlation of NK cell subsets with neutralizing antibody titers directed against YFV 17D in peripheral blood

Correlation of CD56^{dim} (**a**) and CD56^{bright} (**b**) NK cell subsets with high and low neutralizing antibody titers grouped at day 14 for indicated time points (boxes represent the median, 25th and 75th percentile and whiskers indicate the minimum and maximum of absolute values for all donors).

In summary, a strong early peak of CD4^{+} T cell immunity and rather lower numbers of innate NK cell subsets were associated with a strong antibody response in healthy vaccinees.

6 Discussion

Recently different approaches have lead to important insights into YFV-induced immune response and the definition of YFV 17D-induced gene expression signatures (Gaucher, Therrien et al. 2008; Querec, Akondy et al. 2009). However, on the cellular level a comprehensive picture of the cellular signature after YFV immunization has not yet been reported.

With respect to this, this study was performed to gain a detailed analysis of the impact of the vaccination with YFV 17D on the healthy immune system. The induction of YFV 17D-specific T- and B cell immunity, bystander activation, turnover of a variety of cell types and viremia in the peripheral blood of vaccinees were characterized. Furthermore, the vaccination with YFV 17D is an excellent model for challenging the immune system with a live virus and the subsequent induction of a protective immunity in general. This model might be used to improve the efficiency of already tested chimeric vaccines against dengue fever or to develop new vaccines. Nevertheless, despite the safety and efficiency of the vaccination, though small, a number of cases of yellow fever associated viscerotropic disease after YFV 17D vaccination have been reported. Until now, the mechanisms underlying these events are largely unknown, but it seems like the immune system loses the fight against the virus. A comparison of immune parameters after normal vaccination as compared to these cases might give important insights into the underlying processes.

The generation of a sufficient titer of neutralizing antibodies is a hallmark of protective antiviral immunity against YFV 17D (Schlesinger, Brandriss et al. 1990). The development of neutralizing anti-YFV 17D antibody titers is generally used in order to determine the efficiency of the vaccination (Pulendran and Ahmed 2006). As expected, the development of anti-YFV 17D IgM, IgG and protective levels of neutralizing antibodies could be observed in all vaccinees. However, the neutralizing antibody titers showed a clear variation among the vaccinees. Until now, no specific neutralizing antibody titer is proposed for an effective protection. A recent stoichiometric analysis of flavivirus antibody binding revealed a given threshold required for neutralization. Therefore, the study participants were grouped in neutralizing titer-high (NT^{high}) and neutralizing titer-low (NT^{low}) responders according to the antibody levels at day 14. With respect to the concentration dependence of antibody-mediated protection of YFV 17D (Mason, Tauraso et al. 1972) and other infectious agents (Boettler, Panther et al. 2006;

Peachman, Rao et al. 2006) and the possible paradox infection-enhancing effect of low levels of neutralizing antibodies on Fc gamma bearing cells (Pierson, Xu et al. 2007), the NT^{high} group was used as surrogate marker for the strength of protection. Most prominently, this paradoxical antibody-dependent enhancement might occur in the case of a dengue virus infection, another flavivirus infection, due to preformed antibodies generated against a different serotype of the dengue virus. In the case of a second infection with a different serotype, these antibodies promote a severe (haemorrhagic) reaction in cells bearing the Fc-γ receptor (Morens and Halstead 1990). Furthermore, as antibody production is the net result of complex interaction of a variety of cell types (antigen-presenting cells, T and B cells), it represents the distinct coordination of a variety of players in the immune system. However, as specific neutralizing antibodies were appearing rather late, it might not adequately represent the early phases of the immune response.

Thus, the second parameter that was used as a surrogate marker for the immunogenicity of the vaccine was the absence or presence of viral RNA in peripheral blood. Interestingly, viremia could only be detected in 8 of 18 vaccinees and only between day 3 and day 7, which is consistent with other findings where transient viremia could be observed from day 2 until day 6 after vaccination (Reinhardt, Jaspert et al. 1998). The absence before day 3 clearly indicates that the observed viremia is dependent on active viral replication, which can be assumed to be equal in all participants. Thus the presence of viral RNA in the blood of only some of the donors points to differences in the extent of early antiviral immunity, which is orchestrated mainly by the innate immune system.

6.1 Innate Immune Mechanisms Following Yellow Fever Virus Vaccination with YFV 17D

One of the key players are dendritic cells that on the one hand produce cytokines like IL-12 or type I IFN and present antigens to $CD4^+$ and $CD8^+$ T cells, thereby initiating the adaptive immune response. With respect to this, myeloid dendritic cells (mDCs) as well as plasmacytoid dendritic cells (pDCs) have been shown to be infected and activated by the yellow fever virus vaccine (Barba-Spaeth, Longman et al. 2005; Querec, Bennouna et al. 2006; Palmer, Fernandez et al. 2007) and therefore could serve on the one hand as disseminator of the virus and secondly as the afore- mentioned initiator of the adaptive immune response. To contact T cells, maturing dendritic cells exit the site of

pathogen entry and migrate to the secondary lymphoid tissues, thereby down-regulating their antigen sampling and transit to a rather immune-stimulatory state.

A clear increase in the frequency of mDC in the peripheral blood of vaccinees peaking at day 7 could be observed. Interestingly, these cells also showed signs of recent activation/ maturation, as they showed an increased expression of MHC class II on their surface. Following activation and consecutive maturation, these mDCs are sufficient to initiate an adoptive immune response. Also pDC numbers were increased in the peripheral blood at day 1 and day 7, however to a lesser extent and here the expression of MHC class II was not altered. Interestingly, the early rise in pDCs complements previous reports generated in rhesus monkeys, where after occulation of dengue virus, a yellow fever related flavivirus, an increased frequency of pDCs has been detected. Furthermore, in humans a rise in pDC number could be observed in less severe dengue fever, whereas in haemorrhagic dengue fever, a life threatening form, this rise in pDC frequency was absent (Pichyangkul, Endy et al. 2003). In contrast to pDCs, mDC have been shown to be rather reduced during acute dengue infection, yet also for them a correlation between low cell numbers and worse clinical outcome with detected virus replication has been described in the case of an HIV infection (Donaghy, Pozniak et al. 2001). In contrast to the low cell numbers of mDCs described during dengue fever infection, the number of mDCs following YFV 17D vaccination rather increases. This might be explained by the fact that, although the YFV 17D successfully infects DCs, this infection does not support viral replication that would then lead to cell death and reduced cell numbers (Barba-Spaeth, Longman et al. 2005).

The general mobilisation of dendritic cell subsets might indicate the activation of DCs in the peripheral tissue by cytokines, which initially leads to their migration through lymphatic vessels towards the secondary lymph nodes or through the blood stream to the spleen and bone marrow. Interestingly, the final destination for pDCs might preferentially be the lymph nodes (Diacovo, Blasius et al. 2005), whereas activated peripheral blood mDCs have been shown to migrate preferentially into the spleen and bone marrow (Cavanagh, Bonasio et al. 2005). This mechanism could also explain why lower pDC and mDC cell numbers have been shown to be correlated with a worse clinical outcome, as insufficient DC mobilisation might result in an insufficient further activation of the immune system. The detected up-regulation of MHC class II in mDCs, but not in pDCs, following vaccination with YFV 17D most probably reflects their distinctive characteristic with different susceptibility of infection with the live-attenuated

virus. In monocyte derived DCs, YFV 17D could be monitored by intracellular FACS staining 24 h after infection (Barba-Spaeth, Longman et al. 2005) whereas, although not divided into distinct DC subsets, the work of Palmer et al. could not detect intracellular replicative RNA of the YFV vaccine after infection of DCs (Palmer, Fernandez et al. 2007). Nevertheless, after infection with YFV 17D activation and maturation only of mDCs, but not pDCs, was shown to lead to an up-regulation of MHC class II and CD86 (Querec, Bennouna et al. 2006). In contrast, pDCs were the main cytokine producers especially of IFNα (Querec, Bennouna et al. 2006). This distinct difference between m- and pDCs has also been shown following dengue virus infection. There, only in mDCs an infection detected by an anti-viral monoclonal antibody was observed. Furthermore, only mDCs, but not pDCs, obtained additional up-regulation of activation as well as maturation markers like e.g. CD40 and CD86. Nevertheless, pDCs were able to produce cytokines like e.g. IFNα with titers 10 times higher than that of mDC (Sun, Fernandez et al. 2009). Taken together, this might suggest a disparity between DC subsets, with mDCs functioning as antigen-presenting cells, while pDCs are the principal Type-I IFN producing cells.
The drop in monocytes at day 14 could indicate refreshment of the mDC/ pDC pool, as monocytes have been shown to have the ability to differentiate into macrophages or dendritic cells depending on the cytokine milieu (Randolph, Beaulieu et al. 1998; Randolph, Inaba et al. 1999; Chomarat, Banchereau et al. 2000).

Other direct effectors of the innate immunity in an antiviral response are NK cells that can detect and lyse virus-infected cells. In humans, these can be subdivided into rather cytotoxic $CD56^{dim}$ $CD16^{+}$ and $CD56^{bright}$ $CD16^{-}$ NK cells with a rather high potential for the production of cytokines. Interestingly, $CD56^{bright}$ and $cd56^{dim}$ NK cells behaved quite differently during vaccination.
$CD56^{bright}$ NK cells showed an unchanged pattern of absolute cell counts in peripheral blood despite a short decrease at day 7 with normalization at later time-points. The significant drop of $CD56^{bright}$ NK cells observed at day 7 could be due to a possible homing of these cells into the lymph node, as it is known that $CD56^{bright}$ NK cells do have the capability to enter secondary lymphoid organs by the expression of CD62L, CXCR3 and CCR7 (Frey, Packianathan et al. 1998; Campbell, Qin et al. 2001), enabling them to get into close contact with DCs (Fehniger, Cooper et al. 2003). In an *in vitro* cross-talk between NK cells and DC subsets, it has been shown by several authors

that their interaction leads to an activation and cytokine production of both cell types. Mature myeloid DCs are the major source of the secretion of IL-12, which is known to enhance NK cell activation and IFNγ secretion (Trinchieri 2003). In contrast, as it is known that $CD56^{bright}$ cells have the ability to respond to low doses of IL-2 by the expression of their high affinity interleukin-2 receptor (IL-2R) (Frey, Packianathan et al. 1998; Campbell, Qin et al. 2001), these IL-2 activated NK cells have the reciprocal ability to induce maturation of DCs and to activate IFNα secretion from pDCs (Gerosa, Gobbi et al. 2005). Plasmacytoid DCs, on the other hand are also known to be early producers of IL-2 (Granucci, Vizzardelli et al. 2001), which enables them to provide further activating and survival signals for NK cell populations. Furthermore, as $CD56^{bright}$ NK cells could be found in the T-cell-rich area of lymph nodes, they are also known to interact with T cells (Fehniger, Cooper et al. 2003). As $CD56^{bright}$ NK cells produce large amounts of IFNγ, these cells could promote a Th_1 polarization of helper $CD4^+$ T cells. Nevertheless, $CD56^{bright}$ NK cells are also capable of producing Th_2 polarizing cytokines like IL-10 (Cooper, Fehniger et al. 2001).

In contrast to the $CD56^{bright}$ NK cell subset, there was a constant drop of $CD56^{dim}$ NK cells detectable during the course of vaccination, with lowest levels at day 28, the latest time-point of the analysis. Though difficult to compare, these observations are also at least partially in line with previous reports about a drop of NK cell subsets at day 15 during vaccination with YFV 17D, however this analysis was solely based on frequencies in peripheral blood and NK cell subset definitions were different (Martins, Silva et al. 2008). Nevertheless, a decreased frequency of $CD56^{dim}CD16^+$ NK cells in some donors at time points similar to those used in the present study has been reported after influenza vaccination (Long, Michaelsson et al. 2008). As DCs are one of the first targets for an YFV 17D infection, their cytokine production might be a potent stimulus to recruit NK cells from blood to the site of infection. Recently, da Costa Neves et al. have confirmed the activation of NK cells, as measured by the increase of surface activation markers like CD69, CD25 and MHC class II, soon after YFV vaccination. This activation seemed to be dependent on viral recognition by NK cells at the site of infection provoking their engagement of TLR 3 and 9. Thereby also the cytotoxicity of NK cells, as measured by the up-regulation of the activation marker CD38 and the stimulatory high-affinity Fc receptor CD16, is increased (Neves, Matos et al. 2009).

This notwithstanding, not only the recruitment of NK cells to the site of infection but also the consumption of NK cells during the fight against the pathogen could be interpreted

as an explanation for the constant drop in the number of $CD56^{dim}$ NK cells. As the $CD56^{dim}$ subset appears to be nearly unsusceptible to IL-2-mediated proliferative signals (Baume, Robertson et al. 1992), the proliferative capacity of these cells is believed to be low. Therefore, these cells have to be recovered from other sources, but until now it is not clear what pre-cursor cells are used for the $CD56^{dim}$ and $CD56^{bright}$ subsets, to what extent this occurs and how time-consuming this is (Parrish-Novak, Dillon et al. 2000). Nevertheless, as the reduction of $CD56^{dim}$ NK cells is rather prolonged, this could point to a substantially longer persistence of the virus than measured by serum PCR. As previously assumed, also the subset of $CD56^{dim}$ cells could have preferentially migrated to tissues like for example the liver with further ongoing, although not detectable, YFV 17D replication (Monath 2001; Lefeuvre, Contamin et al. 2006).

6.2 Adaptive Immune Mechanisms Following Yellow Fever Virus Vaccination with YFV 17D

In contrast to the innate immune system that provides an early defence with no memory function upon re-exposure, adaptive immunity takes longer to provide effective effector functions during the primary pathogen contact. However, by providing a virus-specific cellular and humoral immune mechanism, it is essential for the response to the virus, as it encrypts the virus into its memory and thereby confers protection for future challenges.

Following the admission of YFV 17D, serious adverse events, including the yellow fever vaccine associated viscerotropic disease (YFV-AVD), have been reported. The analysis of the pre-existing conditions for the development of an YFV-AVD has identified different risk factors. Besides the age of the vaccinees, a history of thymic pathologies leading to thymectomy in about 25% could be defined (Barwick 2004). Therefore, a reduced thymic function due to the age-dependent involution or a thymectomy might point towards a connection between YFV-YVD and the T cells involved. Recently it has been shown that the subset of ^{thymic} naïve $CD31^{+}$ T cells uses the broadest polyclonal TCR repertoire, whereas the $CD31^{-}$ ^{central} naïve $CD4^{+}$ T cells display a restricted TCR repertoire (Kohler, Wagner et al. 2005; Kohler and Thiel 2009). Nevertheless, these two subsets behaved in a similar manner during the course of vaccination with YFV 17D, and the different proliferative history in the periphery and the breadth of TCR repertoires do not correlate with the efficiency of the YFV-17D vaccination.

Besides, there was a clearly distinct response pattern of YFV17D-specific versus non-specific T and B cells. In general, naive and memory T and B cell population behaved in a similar manner, showing a clear reduction in absolute numbers in peripheral blood rather early (day 7) and a subsequent rise to pre-vaccination levels at later time-points (day 14 and 28). These findings are at odds with the data generated by Reinhard et al., who did not find any changes in the $CD4^+$ T cell counts but observed that the $CD8^+$ T cell counts were elevated by about 10% at day 4 after vaccination (Reinhardt, Jaspert et al. 1998). Nevertheless, also in other YFV 17D vaccination studies, reduced frequencies of B cells and a drop in $CD62L^+CD8^+$ T cell frequencies could be observed at day 7 after vaccination, indicating a transmigration of these cells through high endothelial venules entering e.g. the lymph node (Martins, Silva et al. 2007). Corresponding with the fact that the $CD56^{bright}$ NK cell count also dropped at day 7, this might indicate the recruitment of T and B cells to secondary lymphoid organs regardless of their specificity. In the lymph node, this acquisition of naïve and memory lymphocytes can be used for an efficient scan of dendritic cells, which present their processed antigens via the MHC complexes to stimulate the T – and B cell receptor (Westermann, Bode et al. 2005; Batista and Harwood 2009). These receptors are able to bind a variety of antigens with varying strength determining the affinity of the interaction. In the case of a low affinity or absent co-stimulatory signals, the lymphocytes do not get activated, leave the lymph node and reappear in the blood stream. This could be observed for naïve and memory lymphocytes indicated by the subsequent normalization of their absolute cell counts. For the $CD4^+$, $CD8^+$ T and B cells that find their receptor specific antigen and get involved into the immune reaction, the pattern was different, which could be characterized by their cytokine expression, activation or differentiation markers.

6.3 Antigen-Specific $CD4^+$ T Cells Following Yellow Fever Virus Vaccination with YFV 17D

Antigen-specific $CD4^+$ $CD40L^+$ T cells were defined by the expression of CD40L (CD154), which is a marker for antigen specific $CD4^+$ T cells irrespective of their cytokine secretion (Frentsch, Arbach et al. 2005). $CD4^+$ $CD40L^+$ T cells showed a rise in frequencies at day 7 and in absolute numbers at day 10, with maximum profiles at day 14 for frequencies and absolute numbers. Also Gaucher et al. could detect antigen-specific T cells marked by the expression of CD154 at day 28 after yellow fever vaccination (Gaucher, Therrien et al. 2008).

To evaluate the quality of helper $CD4^+$ T cell immunity based on the nature of different cytokine secretion, antigen-specific $CD4^+CD40L^+$ T cells were assessed by flow cytometry analysis. Interestingly, already very early at day 2, a significant peak of $CD4^+$ $CD40L^+$ T cells producing IL-2, IFNγ and TNFα in response to YFV 17D could be detected in the peripheral blood of the vaccinees. The fact that a significant proportion of $CD4^+$ $CD40L^+$ cytokine producing T cells was detected on day 2, whereas there was no significant increase in the $CD4^+$ $CD40L^+$ T cell count might be attributed to technical reasons, with a relatively dim $CD40L^+$ staining and a background level also seen in the negative control. Therefore, as only the $CD40L^{bright}$ stained cells could be gated, this leads to a false negative CD40L population. The exclusion of this population results in lower absolute numbers in $CD4^+$ $CD40L^+$ T cells that only tend to be up-regulated (p-value 0.076). The gating strategy on functionally active $CD40L^+$ cytokine producing $CD4^+$ T cells seems to more precisely and sensibly depict the antigen-specific $CD4^+$ T cells.

The same tendency, although not statistically significant at day 2, could also be observed for $CD8^+$ T cells expressing $CD38^+$, a surface molecule that has recently been described to be up-regulated on antigen-specific $CD8^+$ T cells during YFV 17D immunization. $CD8^+$ T cells with other specificities like CMV, EBV and influenza do not regulate the expression of this molecule during YFV 17D vaccination (Miller, van der Most et al. 2008). With respect to the increase measured in $CD38^+$ on $CD8^+$ T cells, indicating not only an activation but indirectly also an antigenic specificity, already genomic signatures have been shown that predict the development of a large amount of antigen specific $CD8^+$ T cells by using the DAMIP method, a computational classification approach in predicting various biomedical phenomena. A positive correlation with the magnitude of the CD8+ T cell response could be identified for the expression of the glucose transporter regulating protein SLC2A6 (Solute carrier family 2, facilitated glucose transporter, member 6) and the stress response regulating protein EIF2AK4 (eukaryotic translation initiation factor 2 alpha kinase 4) (Querec, Akondy et al. 2009).

This early peak at the second day post vaccination seems to be the result of a local priming e.g. in the draining lymph node at the site of vaccine administration involving early recruited $CD4^+$ and $CD8^+$ T cells which react with antigen specificity. The early acquisition of CD40L on cytokine producing $CD4^+$ T cells may also be functionally important, as the CD40L/ CD40 interaction is known to result in activation of the MAPK

and NF-κB pathways in DCs, thereby also inducing their maturation with up-regulation of MHC class II, longevity and pro-inflammatory cytokine secretion of e.g. IL-12p40 (Miga, Masters et al. 2001; Morel, Truneh et al. 2001; Quezada, Jarvinen et al. 2004). In return, the secreted pro-inflammatory cytokine IL-12 is able to further induce CD40L up-regulation on $CD4^+$ T cells that promotes a further activation of antigen specific T cells (Peng, Remacle et al. 1998). Nevertheless, as the viral replication continues and viral RNA can be found in the sera of some vaccinees, the immune system seems to intensify its response. The massive recruitment of T and B cells presumably to the secondary lymphatic organs, which can be detected by a drop in total $CD4^+$ and $CD8^+$ T cell numbers at day 7, might lead to a strong increase in YFV 17D-specific $CD4^+$ and $CD8^+$ T cells peaking at day 14.

This is paralleled by elevated numbers of peripheral blood plasmablasts, defined by $CD19^{low}$ and $CD27^{high}$ expression, that also peak at day 14, indicating a parallel regulation. One aspect might be explained by the fact that the early CD40L expression by antigen specific $CD4^+$ T cells leads to the CD40L/ CD40 interaction that is essential for the clonal expansion, germinal center formation, isotype class switching or affinity maturation of B cells (Bishop and Hostager 2003). On the other hand by the technique that was used in this work it is not possible to differentiate between newly generated, YFV 17D-specific plasmablasts and antibody secreting long-term plasma cells for other specificities that might be mobilized from the bone-marrow due to competition for survival niches. Therefore one should use a more precise panel of markers including HLA-DR^{high} $CD38^{high}$ versus HLA-DR^{low} $CD38^+$ for newly generated plasmablasts respectively long-lived plasma cells emerging from the bone marrow. Using this panel, Odendahl et al. found a significant part of $CD19^+$ $CD27^{high}$ intracellular IgG^{high} $CD20^-$ $CD95^+$ HLA-DR^{high} $CD38^{high}$ antibody secreting cells to be specific for the tetanus toxoid (TT) vaccine following TT booster vaccination (Odendahl, Mei et al. 2005). Accordingly, one also might assume that during the vaccination with YFV 17D an antigen specific population of plasmablasts appears in peripheral blood. This is further supported by the fact, that day 14 is the first time-point at which anti- YFV 17D neutralizing antibodies could be detected in all donors and the plateau of the antibody titers seemed to be reached. Yet, it should be mentioned, that while in a secondary immunization the peak of plasmablasts in peripheral blood can be detected between day 6 and day 8 (Odendahl, Mei et al. 2005; Clutterbuck, Salt et al. 2006) in this approach, like in other

primary immunizations the generation of plasma cells takes place later (Davis, Hersh et al. 1972; Brinkman, Jol-van der Zijde et al. 2003; Miller, van der Most et al. 2008).

In summary, the results complement previous reports about the generation of vaccine-specific T and B cell immunity. It could be shown that following a general decrease in absolute T and B cell numbers, the often described peak of immunity at day 14 after primary immunization (Miller, van der Most et al. 2008) is preceded by the early appearance of YFV 17D-specific T cells in the blood already at day 2. Interestingly, the observed drop in total naïve and memory B and T cell numbers at day 7 coincides with increased pDC and mDC numbers in the blood, which presumably have been already activated in the periphery and now migrate through the blood to the spleen and bone marrow to engage in the immune reaction. This could indicate a common regulation, although at first glance it might seem counterproductive that while T cells seem to enter the lymphoid tissues, DCs with their high antigen-presenting and thus T cell activating capacity are in the blood stream instead and presumably enter the spleen and the bone marrow (Cavanagh, Bonasio et al. 2005). Nevertheless, it has been reported that especially for blood-borne antigens, the bone marrow is well-suited for the generation of efficient $CD8^+$ T cell immunity and memory responses (Feuerer, Beckhove et al. 2003).

Furthermore, the analysis of YFV 17D-specific $CD4^+$ T cells revealed their polyfunctional effector properties as represented by the production of various cytokines already at early time points after vaccination. Previously, polyfunctional $CD4^+$ T cells that simultaneously produce different effector cytokines were defined as a protective immune correlate following vaccination (Darrah, Patel et al. 2007; Kannanganat, Ibegbu et al. 2007). Notably, the polyfunctional expression of cytokines in YFV 17D-specific $CD4^+$ T cells is qualitatively already developed at day 2 and only increases significantly when comparing *ex vivo* YFV 17D stimulated $CD4^+$ T cells from day 2 and day 10/day 14, the two peaks of the $CD4^+$ T cell response.

In addition, the question as to whether or not the choreography of the developing immune response is also reflected by phenotypic changes within the $CD8^+$ T cell responses was resolved. There was a continuous decrease of CD45RA and IL-7 receptor (CD127) expression on $CD8^+CD38^+$ T cells with maximal down-regulation on day 14, indicating a predominant effector population involved at the height of the immune response. This phenotype is similar to what has been reported for Vaccinia virus (VV) vaccination and acute hepatitis B in humans (Boettler, Panther et al. 2006; Miller, van der Most et al. 2008). Nevertheless, the down regulation of CD127 on

$CD8^+CD38^+$ T cells might also be a control mechanism for IL-7 sensitive T cells expressing the IL-7R to limit their rapid expansion and uncontrolled proliferation as it has been shown by Kaech et al. that a population of full functional cytotoxic effector $CD8^+$ T cells appeared to have a high IL-7R expression (Kaech, Tan et al. 2003). The later shift towards higher expression of CD127 again indicates resolution of the infection and transition into the memory phase, as it could be observed that memory precursor T cells expressing CD127 have the ability to become T_{CM} or T_{EM} (Huster, Busch et al. 2004). Moreover, in a model of an acute hepatitis B infection it has been shown that the up-regulation of CD127 phenotypically correlates with a consecutive loss of the activation marker CD38 and acquisition of CCR7 expression (Boettler, Panther et al. 2006).

Altogether, the results indicate that the early evolution of the immune response, which is detectable by changes in the numbers of peripheral blood T and B cell subsets, is also reflected by a phenotypic differentiation of $CD8^+$ T cells. Furthermore, also the functional capacity of $CD4^+$ T cells increases following vaccination when comparing the first and the second peak of the anti-viral adaptive immunity in peripheral blood.

6.4 Activation of $CD4^+$ T Cells with Non-Vaccine Related Specificity Following Vaccination with YFV 17D

By analyzing the *in vitro* $CD4^+$ T cell response to antigens with specificities most likely not related to YFV 17D, an increased number of CMV and TT-specific cells, secreting TNFα , IL-2 and in a most pronounced manner IL-4 could be observed. At first sight this seems to be in contrast to a recent study (Miller, van der Most et al. 2008) which has excluded an important role for bystander activation in $CD8^+$ T cells during YFV 17D immunization. Yet, apart from the obviously possible general difference between $CD4^+$ and $CD8^+$ T cells, a close examination of the different methods of detection used and further results might prove insightful.

Thus, no signs could be detected of recent proliferation as determined by acquisition of the Ki-67 antigen in TT and CMV-specific cells secreting IL-2 or TNFα. Though for technical reasons the Ki-67 status of IL-4 producing cells could not be analyzed, this argues against proliferation as a reason for the increased number of CMV and TT-specific $CD4^+$ T cells that have been detected.

An alternative explanation might be the expulsion of memory cells from niches like the bone marrow due to competition with cells newly generated in the course of the immune

reaction (Tokoyoda, Zehentmeier et al. 2009). But as the recruitment for the generation and possible displacement of memory $CD4^+$ T cells from the bone marrow has been reported to occur 3-4 weeks after the first encounter of a new antigen, the time points of a detected increased number of CMV and TT-specific cells are rather too early. Furthermore, if this was the case, also an increased absolute number of memory $CD4^+$ $CD45RO^+$ T cells would be expected in peripheral blood, but the opposite was the case.
Thus, with respect to the generalized activation of the immune system that could be observed, it could be concluded that bystander activation has not increased the absolute number of antigen-specific T cells in peripheral blood. It might be rather the case that the sensitivity of $CD4^+$ T cells towards TCR stimulation with non-vaccine related antigens in an *in-vitro* re-stimulation assay is augmented by soluble factors (Ehl, Hombach et al. 1997; Bangs, Baban et al. 2009). Presumably, this is a local effect, as it is known that T cells of heterologous specificities are recruited towards the site of infection (Ostler, Pircher et al. 2003; Chapman, Castrucci et al. 2005). There, cells like dendritic cells or NK cells might also contribute to bystander activation by their cytokine secretion (Kamath, Sheasby et al. 2005). This in turn results in the activation of the Jak-STAT pathway with initiation of bystander functional effects further downstream like e.g. cytokine production (Horvath 2004; Horvath 2004). In addition, a low-level of cross-reactivity of the TCR specific for CMV and TT with peptides sharing no sequence homology, like the YFV-peptides, might also contribute to the increased sensitivity towards TCR stimulation and resulting cytokine production (Hemmer, Vergelli et al. 1998). Nevertheless, the fact that lower absolute numbers of cytokine secreting CMV- as compared to TT-specific T cells could be analyzed, might be explained due to a repetitive re-activation of the CMV virus. This endogenous re-activation of effector T cells can influence the interaction between DCs and T cells, as it has been shown that DC treatment with IFNγ inhibited DC maturation and generated hyporesponsive $CD4^+$ T cells (Rojas and Krishnan).
Taken together, this scenario could equally explain the increased absolute numbers of CMV and TT reactive cytokine producing cells that were detected in the functional *ex vivo* analysis, as well as the unchanged number of EBV tetramer positive $CD8^+$ T cells that has recently been observed (Miller, van der Most et al. 2008). It is also compatible with other studies, that have shown bystander activation of $CD4^+$ T cells during TT immunization, as also there the readout has involved T cell function and might have

been influenced by an increased sensitivity of T cells after encounter of (pro-) inflammatory cytokines in an immune reaction (Di Genova, Roddick et al. 2006).

6.5 Correlation of Immune Parameters with Viremia

In agreement with an earlier study (Reinhardt, Jaspert et al. 1998) transient viremia could be only observed by virus specific PCR in the serum of about half of the vaccinees. As on day 1 and day 2 the virus was detectable in none of the participants, it is obvious that the viremia is essentially dependent on the interplay between the ability of the virus to efficiently replicate and generalize in the blood and the immune system. A strong anti-viral response clearly should be able to diminish the chances of the virus being detectable peripherally.

To define the ability of the immune system to quickly and strongly react and thereby prevent the generalization of the virus, immune parameters were correlated with the presence or absence of viremia. Interestingly, higher absolute counts of $CD56^{dim}$ NK cells and a higher mean expression of HLA-DR on mDCs pre- and at some time points post vaccination correlated with positive viremia, thus indicating a greater chance of an infection with YFV 17D spreading throughout the whole body. While this result might seem surprising at first, the fact that the increased HLA DR expression and NK cell numbers were already present before vaccination could mean that within the vaccinees a preoccupation with some other pathogens and thereby an activation of the innate immune system had already been present. For DCs, a refractory state towards an additional stimulation has been shown following a strong stimulus that induces IL-12 production (Langenkamp, Messi et al. 2000). Constantly elevated mature dendritic cell numbers have also been reported in a mouse model chronically infected with Salmonella enterica (Johansson, Ingman et al. 2006). Moreover, a state of so called “hyporesponsiveness” might be explained by over-stimulation of NK cells via stimulating NK cell receptors due to repeated activation. Referring to this in the context of chronically elevated NK cell numbers, other authors have reported a decreased NK cell function (Orange, Chehimi et al. 2001). Therefore the immune response against YFV 17D, though certainly successful, might have been somehow distracted and diminished. Thereby the chance of a short term generalization of the virus might also be enhanced. The reported increase in NK cells numbers in children with recurrent infections might support this hypothesis (Wisniewska-Ligier, Wozniakowska-Gesicka et al. 2002; Kendirli, Ikinciogullari et al. 2008).

6.6 Correlation of Immune Parameters with Neutralizing Antibody Titer

The presence of viremia might indicate the host's ability to fight the pathogen early and is probably to a large part dominated by the innate part of the immune system, especially on the first encounter. In contrast as discussed before, the rationale behind vaccination is to induce protection from a subsequent encounter, and in the protective antiviral immunity against YFV 17D the generation of a sufficient titer of neutralizing antibodies is a hallmark of the protective memory response (Brandriss, Schlesinger et al. 1986). Thus, the height of the anti-YFV 17D neutralizing antibody titer indicates the magnitude of protection against viral challenge and is dependent on the successful interaction of a variety of cell types like APCs, B and T cells.

The importance of the early peak of YFV 17D-specific $CD4^+$ T cells at day 2 that could be detected was further confirmed in the analysis of day 14 NT^{high} and NT^{low} responders after vaccination. Here, a significantly higher number of IL-2 and IFNγ expressing $CD4^+$ T cells at day 1/2 and day 2 respectively, could be observed only in the blood of high responders. Interestingly, at later time points the correlation between higher numbers of antigen-specific $CD4^+$ T cells and higher neutralizing antibody titers was not present anymore. This points to the special importance of this early peak of an adaptive immune response. As significant proliferation of naïve T cells at this early time point had presumably not taken place yet, it might simply reflect the number of T cells that have been locally activated already presenting antigen specificities and a fully responsible polyfunctional repertoire. These results are in line with studies determining the correlation of neutralizing hepatitis B titers and *in vitro* anti-HbS antigen reactivity of $CD4^+$ T cells (Suzuki, Yamauchi et al. 2001). Moreover, the results complement findings showing that the expression of the receptor for BLYS-BAFF correlates with the height of the antibody titer after YFV 17D immunization at day 7 (Querec, Akondy et al. 2009). All in all, this strengthens the concept that quantitative differences on both sides of the T- and B cell interaction can influence the final outcome, i.e. the resulting neutralizing antibody titer.

Interestingly, also a strong association of developing high neutralizing antibody titers with the absolute numbers of NK cells could be detected. Early after immunization, there were significantly lower numbers of $CD56^{bright}$ and $CD56^{dim}$ NK cells in neutralizing $antibody^{high}$ responders, a difference that was detectable neither before nor at later time points after immunization. This correlation could be explained in the context of the

regulatory role of the DC-NK cell interaction and the aforementioned reciprocal cytokine interplay between these cells (Cooper, Fehniger et al. 2004). By that, lower NK cell numbers in the peripheral blood after vaccination might indicate a migration towards the site of infection leading to the broader expression of pro-inflammatory cytokines like IFNγ by NK cells. This in turn might enhance the maturation of dendritic cells as well as the direct activation of YFV 17D-specific T cells, reflected by their early peak at day 2, thereby inducing a higher antibody production by B cell stimulation/ interaction.

Taken together, a broad activation of different cell types following YFV 17D vaccination is mandatory for the development of sufficient protection represented by the generation of neutralizing antibodies and polyfunctional antigen specific helper $CD4^+$ T cells. In particular, the early peak of these antigen specific helper $CD4^+$ T cells at day 2 after vaccination correlated with the induction of a high neutralizing antibody titer. Regarding the innate immune response, a broad commitment of NK cells migrating from peripheral blood to the side of antigen entry is essential in providing not only cytotoxic features but also polarizing capabilities by cytokine production and also correlating with a high neutralizing antibody response.

7 Summary

Until now, most studies on the induction of a protective immune response following vaccination focused on rather later time points after vaccination and concentrated on certain cell types like e.g. B cells. But an immunological challenge with a “neo”-antigen also involves other cell types like T cells, NK cells and APCs.

In this study, the primary vaccination with the attenuated yellow fever virus YFV 17D was used to examine, especially at early post vaccination time points, the complex interplay of different cell types during an efficient vaccination. In line with other studies it could be confirmed that the live-attenuated YFV 17D vaccine still replicates *in vivo* leading to viremia in about half of the healthy donors. Thus, the YFV 17D vaccination serves also as an excellent model not only for studying the interaction of different cell types during the induction of a highly protective immune response but also for defining immunological components that correlate with an acute viral challenge.

Phenotypical analyses of different elements of the innate immunity, the induction of a YFV 17D-specific T- and B cell immunity, bystander activation and absolute cell counts in peripheral blood were performed at short-term intervals following vaccination using flow cytometry. The generation of neutralizing antibody titers was evaluated using the plaque-reduction neutralizing assay, whereas viral detection in peripheral blood was determined using the quantitative RT-PCR.

The results showed an increase in dendritic cell subset numbers and an up-regulation of their MHC class II molecules, serving as a hint of increased antigen presentation. A drop in the number of NK cell subsets in peripheral blood might indicate a migration of NK cells from the blood stream towards the site of infection and secondary lymphoid tissues. Nevertheless, distinct changes in an adoptive immune response were also evident, indicating a significant activation of components involved in antiviral immunity. Apart from the activation of cytotoxic $CD8^+$ T cells, determined by the up-regulation of CD38, the generation of $CD19^{low}CD27^{high}$ plasmablasts could be detected, reaching a maximum at day 14 following vaccination with YFV 17D. This was paralleled by the induction of neutralizing antibodies in all donors at that time point. Also the generation of antigen specific polyfunctional helper $CD4^+$ T cells, producing not only one but a variety of cytokines, were observed appearing in a biphasic manner, with an early and a later peak of YFV 17D-specific $CD4^+$ T cells appearing in the peripheral blood. By that the first early peak correlated with the later appearance of higher neutralizing antibody

titers. Regarding the activation of other non-vaccine related specificities, increased cytokine production for tetanus toxoid- and cytomegalovirus-specific $CD4^+$ T cells could be shown. As this bystander activation was not accompanied by a significant proliferation of these antigen specific $CD4^+$ T cells, the activation could have been caused by an increased sensitivity of the corresponding T cell receptor towards its definite protein.

In summary, the analysis of the impact of an attenuated live viral vaccination with YFV 17D on a healthy immune system is a suitable model to get a better insight into an acute viral infection. By that a confirmed cell infection with increased antigen presentation, an active viral replication and a robust activation of the immune system, resulting also in a sensitization of other non-vaccine related helper $CD4^+$ T cells were detectable. The immunization provides not only effective long-term protection thanks to the development of neutralizing antibodies, but also indicates the innate and adoptive immune signatures that define an effective early immune response, prevent a viral replication and lead to the generation of highly neutralizing antibody titers.

The results of this study can contribute to the understanding of the induction of a robust and persistent protective immune response and could be used for designing new vaccines.

8 Zusammenfassung

Viele der bisherigen Studien der Induktion einer schützenden Immunantwort durch eine Impfung konzentrieren sich überwiegend auf die Untersuchung relativ später Zeitpunkte nach Impfung sowie die Betrachtung bestimmter Zellpopulationen wie z.B. B-Zellen. Die immunologische Auseinandersetzung mit einem unbekannten Antigen involviert jedoch die Rekrutierung und das Zusammenspiel vieler verschiedener Zelltypen wie T-, NK- oder Antigen-Präsentierender Zellen.

In dieser Studie wurden daher anhand des Modells einer Erstimmunisierung mit dem abgeschwächten Gelbfieber-Lebendimpfstoffvirus YFV 17D insbesondere die in der frühen Phase der Immunantwort auftretenden, komplexen Interaktionsmechanismen verschiedener Zellpopulationen, die zur erfolgreichen Impfantwort führen, untersucht. Wie schon in anderen Arbeiten beschrieben, konnte auch in dieser Studie beobachtet werden, dass es nach Impfung zu einer Replikation des Impfviruses kommt, welche in der Hälfte der gesunden Probanden als Virämie nachweisbar war. Deshalb stellt die Impfung mit YFV 17D ebenfalls ein exzellentes Modell für die Untersuchung immunologischer Komponenten, welche mit einer akuten viralen Infektion korrelieren, dar.

In kurzen zeitlichen Intervallen nach Vakzinierung wurden phänotypische Untersuchungen der Komponenten der angeborenen Immunität, das Auftreten einer YFV 17D spezifischen T- und B-Zell-Immunität, „Bystander“-Aktivierung sowie absolute Zellzahlverläufe im peripheren Blut mittels der Methode der Durchflusszytometrie analysiert. Des Weiteren wurden mittels Plaquereduktionstest die Produktion neutralisierender Antikörper analysiert und mittels quantitativer RT-PCR das Auftreten einer Virämie im peripheren Blut untersucht.

Mit Hilfe dieser Methoden konnten eindeutige Veränderungen der Komponenten der angeborenen Immunität nach Impfung mit dem Gelbfieber-Impfstoff YFV 17D nachgewiesen werden. Neben einer Zunahme dendritischer Zellgruppen sowie einer Hochregulation ihrer Oberflächen-MHC Klasse II Moleküle, welche als ein Ausdruck der erhöhten Antigenpräsentation interpretiert werden können, konnte eine Reduktion der NK-Zellpopulationen im peripheren Blut nachgewiesen werden. Diese wiederum deutet auf eine Migration der NK-Zellen aus dem Blutstrom zur viralen Eintrittsstelle respektive den sekundären lymphoiden Organen hin. Des Weiteren waren auch deutliche Veränderungen der Komponenten einer adaptiven Immunantwort nachweisbar, die eine

signifikante Aktivierung wichtiger Komponenten der antiviralen Immunität anzeigen. Neben der Aktivierung von zytotoxischen $CD8^+$ T-Zellen stellte sich die Generation von $CD19^{low}CD27^{high}$ Plasmablasten kontinuierlich mit einem Maximum an Tag14 nach Vakzinierung mit YFV 17D dar. Bis zu diesem Tag kam es im Blut aller Probanden auch zu einer Induktion von neutralisierenden Antikörpern.

Zusätzlich konnte die Bildung von antigenspezifischen, multifunktionalen $CD4^+$ Helfer-T-Zellen nachgewiesen werden. Interessanterweise traten diese antigenspezifischen $CD4^+$ Helfer-T-Zellen in einem biphasischen Verlauf im peripheren Blut auf. Dabei korrelierte ein frühes Auftreten YFV 17D-spezifischer $CD4^+$ T-Zellen mit einem späteren hohen Titer neutralisierender Antikörper. Bezogen auf die Aktivierung anderer Nicht-Vakzin abhängiger Spezifitäten zeigen die Ergebnisse eine im Verlauf nach Impfung erhöhte Zytokinproduktion Tetanus-Toxoid- und Zytomegalievirus-spezifischer $CD4^+$ T-Zellen. Da diese Bystander-Aktivierung mit keiner signifikanten Proliferation der $CD4^+$ T-Zellen einherging, könnte diese aus einer erhöhten Sensitivität der antigenspezifischen T-Zell-Rezeptoren gegenüber ihren jeweiligen Proteinen resultieren.

Zusammenfassend stellt die Vakzinierung mit dem abgeschwächten viralen Gelbfieber-Lebendimpfstoff YFV 17D ein hervorragendes Modell der Auseinandersetzung des gesunden Immunsystems mit einer viralen Infektion dar. Dabei kommt es zu einer nachweisbaren Zellinfektion mit vermehrter Antigenpräsentation, einer aktiven Replikation sowie einer robusten Aktivierung des Immunsystems, die gleichfalls zur Sensibilisierung anderer antigenspezifischer $CD4^+$ Helfer-T-Zellen im Sinne einer Bystander Aktivierung führt. Die Immunisierung induziert nicht nur einen effektiven Langzeitschutz mittels neutralisierender Antikörper, sondern beschreibt gleichfalls effiziente angeborene und erworbene Immunsignaturen. Diese korrelieren mit einer effektiven frühen Immunantwort, verhindern eine Replikation des Impfviruses und führen zur Generierung hoher neutralisierender Antikörpertiter.

Die Erkenntnisse dieser Studie können zum besseren Verständnis der Auseinandersetzung des Immunsystems mit einer akuten viralen Infektion beitragen sowie bei der Herstellung neuer Impfstoffe dienen.

9 References

Akondy, R. S., N. D. Monson, et al. (2009). "The yellow fever virus vaccine induces a broad and polyfunctional human memory CD8+ T cell response." J Immunol **183**(12): 7919-30.

Appay, V., P. R. Dunbar, et al. (2002). "Memory CD8+ T cells vary in differentiation phenotype in different persistent virus infections." Nat Med **8**(4): 379-85.

Asselin-Paturel, C. and G. Trinchieri (2005). "Production of type I interferons: plasmacytoid dendritic cells and beyond." J Exp Med **202**(4): 461-5.

Badovinac, V. P. and J. T. Harty (2003). "Memory lanes." Nat Immunol **4**(3): 212-3.

Bae, H. G., A. Nitsche, et al. (2003). "Detection of yellow fever virus: a comparison of quantitative real-time PCR and plaque assay." J Virol Methods **110**(2): 185-91.

Bangs, S. C., D. Baban, et al. (2009). "Human CD4+ memory T cells are preferential targets for bystander activation and apoptosis." J Immunol **182**(4): 1962-71.

Barba-Spaeth, G., R. S. Longman, et al. (2005). "Live attenuated yellow fever 17D infects human DCs and allows for presentation of endogenous and recombinant T cell epitopes." J Exp Med **202**(9): 1179-84.

Barouch, D. H., A. Craiu, et al. (2000). "Augmentation of immune responses to HIV-1 and simian immunodeficiency virus DNA vaccines by IL-2/Ig plasmid administration in rhesus monkeys." Proc Natl Acad Sci U S A **97**(8): 4192-7.

Barrett, A. D. and T. P. Monath (2003). "Epidemiology and ecology of yellow fever virus." Adv Virus Res **61**: 291-315.

Barrett, A. D. and D. E. Teuwen (2009). "Yellow fever vaccine - how does it work and why do rare cases of serious adverse events take place?" Curr Opin Immunol **21**(3): 308-13.

Barros, V. E., J. A. Thomazini, et al. (2004). "Cytopathological changes induced by selected Brazilian flaviviruses in mouse macrophages." J Microsc **216**(Pt 1): 5-14.

Barwick, R. (2004). "History of thymoma and yellow fever vaccination." Lancet **364**(9438): 936.

Batista, F. D. and N. E. Harwood (2009). "The who, how and where of antigen presentation to B cells." Nat Rev Immunol **9**(1): 15-27.

Baume, D. M., M. J. Robertson, et al. (1992). "Differential responses to interleukin 2 define functionally distinct subsets of human natural killer cells." Eur J Immunol **22**(1): 1-6.

Bishop, G. A. and B. S. Hostager (2003). "The CD40-CD154 interaction in B cell-T cell liaisons." Cytokine Growth Factor Rev **14**(3-4): 297-309.

Boettler, T., E. Panther, et al. (2006). "Expression of the interleukin-7 receptor alpha chain (CD127) on virus-specific CD8+ T cells identifies functionally and phenotypically defined memory T cells during acute resolving hepatitis B virus infection." J Virol **80**(7): 3532-40.

Brandriss, M. W., J. J. Schlesinger, et al. (1986). "Lethal 17D yellow fever encephalitis in mice. I. Passive protection by monoclonal antibodies to the envelope proteins of 17D yellow fever and dengue 2 viruses." J Gen Virol **67 (Pt 2)**: 229-34.

Brightbill, H. D., D. H. Libraty, et al. (1999). "Host defense mechanisms triggered by microbial lipoproteins through toll-like receptors." Science **285**(5428): 732-6.

Brinkman, D. M., C. M. Jol-van der Zijde, et al. (2003). "Vaccination with rabies to study the humoral and cellular immune response to a T-cell dependent neoantigen in man." J Clin Immunol **23**(6): 528-38.

Campbell, J. J., S. Qin, et al. (2001). "Unique subpopulations of CD56+ NK and NK-T peripheral blood lymphocytes identified by chemokine receptor expression repertoire." J Immunol **166**(11): 6477-82.

Cavanagh, L. L., R. Bonasio, et al. (2005). "Activation of bone marrow-resident memory T cells by circulating, antigen-bearing dendritic cells." Nat Immunol **6**(10): 1029-37.

Chambers, T. J. and M. Nickells (2001). "Neuroadapted yellow fever virus 17D: genetic and biological characterization of a highly mouse-neurovirulent virus and its infectious molecular clone." J Virol **75**(22): 10912-22.

Chapman, T. J., M. R. Castrucci, et al. (2005). "Antigen-specific and non-specific CD4+ T cell recruitment and proliferation during influenza infection." Virology **340**(2): 296-306.

Charles A. Janeway, P. T., Mark Walport (2004). Immunobiology: The Immune System in Health and Disease, B&T.

Chomarat, P., J. Banchereau, et al. (2000). "IL-6 switches the differentiation of monocytes from dendritic cells to macrophages." Nat Immunol **1**(6): 510-4.

Clarke, S. R. (2000). "The critical role of CD40/CD40L in the CD4-dependent generation of CD8+ T cell immunity." J Leukoc Biol **67**(5): 607-14.

Clutterbuck, E. A., P. Salt, et al. (2006). "The kinetics and phenotype of the human B-cell response following immunization with a heptavalent pneumococcal-CRM conjugate vaccine." Immunology **119**(3): 328-37.

Co, M. D., E. D. Kilpatrick, et al. (2009). "Dynamics of the CD8 T-cell response following yellow fever virus 17D immunization." Immunology **128**(1 Suppl): e718-27.

Co, M. D., M. Terajima, et al. (2002). "Human cytotoxic T lymphocyte responses to live attenuated 17D yellow fever vaccine: identification of HLA-B35-restricted CTL epitopes on nonstructural proteins NS1, NS2b, NS3, and the structural protein E." Virology **293**(1): 151-63.

Cooper, M. A., T. A. Fehniger, et al. (2001). "The biology of human natural killer-cell subsets." Trends Immunol **22**(11): 633-40.

Cooper, M. A., T. A. Fehniger, et al. (2004). "NK cell and DC interactions." Trends Immunol **25**(1): 47-52.

Cooper, M. A., T. A. Fehniger, et al. (2001). "Human natural killer cells: a unique innate immunoregulatory role for the CD56(bright) subset." Blood **97**(10): 3146-51.

Daffis, S., R. E. Kontermann, et al. (2005). "Antibody responses against wild-type yellow fever virus and the 17D vaccine strain: characterization with human monoclonal antibody fragments and neutralization escape variants." Virology **337**(2): 262-72.

Darrah, P. A., D. T. Patel, et al. (2007). "Multifunctional TH1 cells define a correlate of vaccine-mediated protection against Leishmania major." Nat Med **13**(7): 843-50.

David M. Knipe, P. M. H. (2007). *Fields' Virology*, Lippincott Williams & Wilkins.

Davis, L. E., E. M. Hersh, et al. (1972). "Immune status of patients with multiple sclerosis. Analysis of primary and established immune responses in 24 patients." Neurology **22**(10): 989-97.

De Rosa, S. C., F. X. Lu, et al. (2004). "Vaccination in humans generates broad T cell cytokine responses." J Immunol **173**(9): 5372-80.

Di Genova, G., J. Roddick, et al. (2006). "Vaccination of human subjects expands both specific and bystander memory T cells but antibody production remains vaccine specific." Blood **107**(7): 2806-13.

Diacovo, T. G., A. L. Blasius, et al. (2005). "Adhesive mechanisms governing interferon-producing cell recruitment into lymph nodes." J Exp Med **202**(5): 687-96.

Diebold, S. S., T. Kaisho, et al. (2004). "Innate antiviral responses by means of TLR7-mediated recognition of single-stranded RNA." Science **303**(5663): 1529-31.

Donaghy, H., A. Pozniak, et al. (2001). "Loss of blood CD11c(+) myeloid and CD11c(-) plasmacytoid dendritic cells in patients with HIV-1 infection correlates with HIV-1 RNA virus load." Blood **98**(8): 2574-6.

Duiker, E. W., C. H. Mom, et al. (2006). "The clinical trail of TRAIL." Eur J Cancer **42**(14): 2233-40.

Ehl, S., J. Hombach, et al. (1997). "Bystander activation of cytotoxic T cells: studies on the mechanism and evaluation of in vivo significance in a transgenic mouse model." J Exp Med **185**(7): 1241-51.

Fehniger, T. A., M. A. Cooper, et al. (2003). "CD56bright natural killer cells are present in human lymph nodes and are activated by T cell-derived IL-2: a potential new link between adaptive and innate immunity." Blood **101**(8): 3052-7.

Feuerer, M., P. Beckhove, et al. (2003). "Bone marrow as a priming site for T-cell responses to blood-borne antigen." Nat Med **9**(9): 1151-7.

Finlay, C. J. (2001). "The mosquito hypothetically considered as the agent of transmission of yellow fever. 1881." Mil Med **166**(9 Suppl): 5, 6-10.

Freitas, A. A. and B. Rocha (2000). "Population biology of lymphocytes: the flight for survival." Annu Rev Immunol **18**: 83-111.

Frentsch, M., O. Arbach, et al. (2005). "Direct access to CD4+ T cells specific for defined antigens according to CD154 expression." Nat Med **11**(10): 1118-24.

Frey, M., N. B. Packianathan, et al. (1998). "Differential expression and function of L-selectin on CD56bright and CD56dim natural killer cell subsets." J Immunol **161**(1): 400-8.

Gasser, S. and D. H. Raulet (2006). "Activation and self-tolerance of natural killer cells." Immunol Rev **214**: 130-42.

Gaucher, D., R. Therrien, et al. (2008). "Yellow fever vaccine induces integrated multilineage and polyfunctional immune responses." J Exp Med **205**(13): 3119-31.

Gerdes, J., H. Lemke, et al. (1984). "Cell cycle analysis of a cell proliferation-associated human nuclear antigen defined by the monoclonal antibody Ki-67." J Immunol **133**(4): 1710-5.

Gerosa, F., A. Gobbi, et al. (2005). "The reciprocal interaction of NK cells with plasmacytoid or myeloid dendritic cells profoundly affects innate resistance functions." J Immunol **174**(2): 727-34.

Givan, A. L. (2001). Flow Cytometry: First Principles, John Wiley & Sons.

Granucci, F., C. Vizzardelli, et al. (2001). "Inducible IL-2 production by dendritic cells revealed by global gene expression analysis." Nat Immunol **2**(9): 882-8.

Guy, B., N. Nougarede, et al. (2008). "Cell-mediated immunity induced by chimeric tetravalent dengue vaccine in naive or flavivirus-primed subjects." Vaccine **26**(45): 5712-21.

Heil, F., H. Hemmi, et al. (2004). "Species-specific recognition of single-stranded RNA via toll-like receptor 7 and 8." Science **303**(5663): 1526-9.

Hemmer, B., M. Vergelli, et al. (1998). "Predictable TCR antigen recognition based on peptide scans leads to the identification of agonist ligands with no sequence homology." J Immunol **160**(8): 3631-6.

Homann, D., L. Teyton, et al. (2001). "Differential regulation of antiviral T-cell immunity results in stable CD8+ but declining CD4+ T-cell memory." Nat Med **7**(8): 913-9.

Horvath, C. M. (2004). "The Jak-STAT pathway stimulated by interferon alpha or interferon beta." Sci STKE **2004**(260): tr10.

Horvath, C. M. (2004). "The Jak-STAT pathway stimulated by interferon gamma." Sci STKE **2004**(260): tr8.

Huster, K. M., V. Busch, et al. (2004). "Selective expression of IL-7 receptor on memory T cells identifies early CD40L-dependent generation of distinct CD8+ memory T cell subsets." Proc Natl Acad Sci U S A **101**(15): 5610-5.

Janeway Charles A., T. P., Walport Mark (2004). Immunobiology: The Immune System in Health and Disease, B&T.

Johansson, C., M. Ingman, et al. (2006). "Elevated neutrophil, macrophage and dendritic cell numbers characterize immune cell populations in mice chronically infected with Salmonella." Microb Pathog **41**(2-3): 49-58.

Kaech, S. M. and R. Ahmed (2001). "Memory CD8+ T cell differentiation: initial antigen encounter triggers a developmental program in naive cells." Nat Immunol **2**(5): 415-22.

Kaech, S. M., J. T. Tan, et al. (2003). "Selective expression of the interleukin 7 receptor identifies effector CD8 T cells that give rise to long-lived memory cells." Nat Immunol **4**(12): 1191-8.

Kamath, A. T., C. E. Sheasby, et al. (2005). "Dendritic cells and NK cells stimulate bystander T cell activation in response to TLR agonists through secretion of IFN-alpha beta and IFN-gamma." J Immunol **174**(2): 767-76.

Kannanganat, S., C. Ibegbu, et al. (2007). "Multiple-cytokine-producing antiviral CD4 T cells are functionally superior to single-cytokine-producing cells." J Virol **81**(16): 8468-76.

Kapsenberg, M. L. (2003). "Dendritic-cell control of pathogen-driven T-cell polarization." Nat Rev Immunol **3**(12): 984-93.

Kendirli, T., A. Ikinciogullari, et al. (2008). "Peripheral blood lymphocyte subsets in children with frequent upper respiratory tract infections." Turk J Pediatr **50**(1): 63-6.

Kiepiela, P., K. Ngumbela, et al. (2007). "CD8+ T-cell responses to different HIV proteins have discordant associations with viral load." Nat Med **13**(1): 46-53.

Koch-Institut, S. I. S. a. R. (2008). "Epidemiologisches Bulletin." **30**.

Kohler, S. and A. Thiel (2009). "Life after the thymus: CD31+ and CD31- human naive CD4+ T-cell subsets." Blood **113**(4): 769-74.

Kohler, S., U. Wagner, et al. (2005). "Post-thymic in vivo proliferation of naive CD4+ T cells constrains the TCR repertoire in healthy human adults." Eur J Immunol **35**(6): 1987-94.

Koup, R. A., J. T. Safrit, et al. (1994). "Temporal association of cellular immune responses with the initial control of viremia in primary human immunodeficiency virus type 1 syndrome." J Virol **68**(7): 4650-5.

Krammer, P. H., R. Arnold, et al. (2007). "Life and death in peripheral T cells." Nat Rev Immunol **7**(7): 532-42.

Kuppers, R. (2003). "B cells under influence: transformation of B cells by Epstein-Barr virus." Nat Rev Immunol **3**(10): 801-12.

Lalezari, J. P., J. A. Beal, et al. (2000). "Low-dose daily subcutaneous interleukin-2 in combination with highly active antiretroviral therapy in HIV+ patients: a randomized controlled trial." HIV Clin Trials **1**(3): 1-15.

Langenkamp, A., M. Messi, et al. (2000). "Kinetics of dendritic cell activation: impact on priming of TH1, TH2 and nonpolarized T cells." Nat Immunol **1**(4): 311-6.

Lechner, F., D. K. Wong, et al. (2000). "Analysis of successful immune responses in persons infected with hepatitis C virus." J Exp Med **191**(9): 1499-512.

Lefeuvre, A., H. Contamin, et al. (2006). "Host-cell interaction of attenuated and wild-type strains of yellow fever virus can be differentiated at early stages of hepatocyte infection." Microbes Infect **8**(6): 1530-8.

Liu, Y. J. (2005). "IPC: professional type 1 interferon-producing cells and plasmacytoid dendritic cell precursors." Annu Rev Immunol **23**: 275-306.

Long, B. R., J. Michaelsson, et al. (2008). "Elevated frequency of gamma interferon-producing NK cells in healthy adults vaccinated against influenza virus." Clin Vaccine Immunol **15**(1): 120-30.

Macatonia, S. E., N. A. Hosken, et al. (1995). "Dendritic cells produce IL-12 and direct the development of Th1 cells from naive CD4+ T cells." J Immunol **154**(10): 5071-9.

MacDonald, K. P., D. J. Munster, et al. (2002). "Characterization of human blood dendritic cell subsets." Blood **100**(13): 4512-20.

Marianneau, P., M. Georges-Courbot, et al. (2001). "Rarity of adverse effects after 17D yellow-fever vaccination." Lancet **358**(9276): 84-5.

Martin-Fontecha, A., L. L. Thomsen, et al. (2004). "Induced recruitment of NK cells to lymph nodes provides IFN-gamma for T(H)1 priming." Nat Immunol **5**(12): 1260-5.

Martins, M. A., M. L. Silva, et al. (2008). "Innate immunity phenotypic features point toward simultaneous raise of activation and modulation events following 17DD live attenuated yellow fever first-time vaccination." Vaccine **26**(9): 1173-84.

Martins, M. A., M. L. Silva, et al. (2007). "Activation/modulation of adaptive immunity emerges simultaneously after 17DD yellow fever first-time vaccination: is this the key to prevent severe adverse reactions following immunization?" Clin Exp Immunol **148**(1): 90-100.

Mason, R. A., N. M. Tauraso, et al. (1972). "Yellow fever vaccine. V. Antibody response in maonkeys inoculated with graded doses of the 17D vaccine." Appl Microbiol **23**(5): 908-13.

Meier, S., R. Stark, et al. (2008). "The influence of different stimulation conditions on the assessment of antigen-induced CD154 expression on CD4+ T cells." Cytometry A **73**(11): 1035-42.

Mercado, R., S. Vijh, et al. (2000). "Early programming of T cell populations responding to bacterial infection." J Immunol **165**(12): 6833-9.

Miga, A. J., S. R. Masters, et al. (2001). "Dendritic cell longevity and T cell persistence is controlled by CD154-CD40 interactions." Eur J Immunol **31**(3): 959-65.

Miller, J. D., R. G. van der Most, et al. (2008). "Human effector and memory CD8+ T cell responses to smallpox and yellow fever vaccines." Immunity **28**(5): 710-22.

Monath, T. P. (2001). "Yellow fever: an update." Lancet Infect Dis **1**(1): 11-20.

Morel, Y., A. Truneh, et al. (2001). "The TNF superfamily members LIGHT and CD154 (CD40 ligand) costimulate induction of dendritic cell maturation and elicit specific CTL activity." J Immunol **167**(5): 2479-86.

Morens, D. M. and S. B. Halstead (1990). "Measurement of antibody-dependent infection enhancement of four dengue virus serotypes by monoclonal and polyclonal antibodies." J Gen Virol **71 (Pt 12)**: 2909-14.

Musey, L., J. Hughes, et al. (1997). "Cytotoxic-T-cell responses, viral load, and disease progression in early human immunodeficiency virus type 1 infection." N Engl J Med **337**(18): 1267-74.

Neves, P. C., D. C. Matos, et al. (2009). "TLR expression and NK cell activation after human yellow fever vaccination." Vaccine **27**(41): 5543-9.

Niedrig, M., M. Lademann, et al. (1999). "Assessment of IgG antibodies against yellow fever virus after vaccination with 17D by different assays: neutralization test, haemagglutination inhibition test, immunofluorescence assay and ELISA." Trop Med Int Health **4**(12): 867-71.

Odendahl, M., H. Mei, et al. (2005). "Generation of migratory antigen-specific plasma blasts and mobilization of resident plasma cells in a secondary immune response." Blood **105**(4): 1614-21.

Orange, J. S., J. Chehimi, et al. (2001). "Decreased natural killer (NK) cell function in chronic NK cell lymphocytosis associated with decreased surface expression of CD11b." Clin Immunol **99**(1): 53-64.

Ostler, T., H. Pircher, et al. (2003). ""Bystander" recruitment of systemic memory T cells delays the immune response to respiratory virus infection." Eur J Immunol **33**(7): 1839-48.

Palmer, D. R., S. Fernandez, et al. (2007). "Restricted replication and lysosomal trafficking of yellow fever 17D vaccine virus in human dendritic cells." J Gen Virol **88**(Pt 1): 148-56.

Parrish-Novak, J., S. R. Dillon, et al. (2000). "Interleukin 21 and its receptor are involved in NK cell expansion and regulation of lymphocyte function." Nature **408**(6808): 57-63.

Peachman, K. K., M. Rao, et al. (2006). "Correlation between lethal toxin-neutralizing antibody titers and protection from intranasal challenge with Bacillus anthracis Ames strain spores in mice after transcutaneous immunization with recombinant anthrax protective antigen." Infect Immun **74**(1): 794-7.

Peng, X., J. E. Remacle, et al. (1998). "IL-12 up-regulates CD40 ligand (CD154) expression on human T cells." J Immunol **160**(3): 1166-72.

Perussia, B. (1998). "Fc receptors on natural killer cells." Curr Top Microbiol Immunol **230**: 63-88.

Perussia, B. (2000). "Signaling for cytotoxicity." Nat Immunol **1**(5): 372-4.

Pichyangkul, S., T. P. Endy, et al. (2003). "A blunted blood plasmacytoid dendritic cell response to an acute systemic viral infection is associated with increased disease severity." J Immunol **171**(10): 5571-8.

Pierson, T. C., Q. Xu, et al. (2007). "The stoichiometry of antibody-mediated neutralization and enhancement of West Nile virus infection." Cell Host Microbe **1**(2): 135-45.

Poland, J. D., C. H. Calisher, et al. (1981). "Persistence of neutralizing antibody 30-35 years after immunization with 17D yellow fever vaccine." Bull World Health Organ **59**(6): 895-900.

Pulendran, B. and R. Ahmed (2006). "Translating innate immunity into immunological memory: implications for vaccine development." Cell **124**(4): 849-63.

Querec, T., S. Bennouna, et al. (2006). "Yellow fever vaccine YF-17D activates multiple dendritic cell subsets via TLR2, 7, 8, and 9 to stimulate polyvalent immunity." J Exp Med **203**(2): 413-24.

Querec, T. D., R. S. Akondy, et al. (2009). "Systems biology approach predicts immunogenicity of the yellow fever vaccine in humans." Nat Immunol **10**(1): 116-25.

Quezada, S. A., L. Z. Jarvinen, et al. (2004). "CD40/CD154 interactions at the interface of tolerance and immunity." Annu Rev Immunol **22**: 307-28.

Radbruch, A., G. Muehlinghaus, et al. (2006). "Competence and competition: the challenge of becoming a long-lived plasma cell." Nat Rev Immunol **6**(10): 741-50.

Randolph, G. J., S. Beaulieu, et al. (1998). "Differentiation of monocytes into dendritic cells in a model of transendothelial trafficking." Science **282**(5388): 480-3.

Randolph, G. J., K. Inaba, et al. (1999). "Differentiation of phagocytic monocytes into lymph node dendritic cells in vivo." Immunity **11**(6): 753-61.

Raulet, D. H. and R. E. Vance (2006). "Self-tolerance of natural killer cells." Nat Rev Immunol **6**(7): 520-31.

Reed, L. J., and H. Muench (1938). "A simple method of estimating fifty per cent endpoints." Am. J. Hyg. (27): 493-497.

Reinhardt, B., R. Jaspert, et al. (1998). "Development of viremia and humoral and cellular parameters of immune activation after vaccination with yellow fever virus strain 17D: a model of human flavivirus infection." J Med Virol **56**(2): 159-67.

Reis e Sousa, C. (2006). "Dendritic cells in a mature age." Nat Rev Immunol **6**(6): 476-83.

Robertson, S. E., B. P. Hull, et al. (1996). "Yellow fever: a decade of reemergence." JAMA **276**(14): 1157-62.

Rojas, D. and R. Krishnan "IFN-gamma generates maturation-arrested dendritic cells that induce T cell hyporesponsiveness independent of Foxp3+ T-regulatory cell generation." Immunol Lett **132**(1-2): 31-7.

Romero, P., A. Zippelius, et al. (2007). "Four functionally distinct populations of human effector-memory CD8+ T lymphocytes." J Immunol **178**(7): 4112-9.

Sallusto, F., J. Geginat, et al. (2004). "Central memory and effector memory T cell subsets: function, generation, and maintenance." Annu Rev Immunol **22**: 745-63.

Sallusto, F. and A. Lanzavecchia (2002). "The instructive role of dendritic cells on T-cell responses." Arthritis Res **4 Suppl 3**: S127-32.

Sallusto, F., D. Lenig, et al. (1999). "Two subsets of memory T lymphocytes with distinct homing potentials and effector functions." Nature **401**(6754): 708-12.

Santos, A. P., A. L. Bertho, et al. (2005). "Lymphocyte subset analyses in healthy adults vaccinated with yellow fever 17DD virus." Mem Inst Oswaldo Cruz **100**(3): 331-7.

Sauce, D., J. R. Almeida, et al. (2007). "PD-1 expression on human CD8 T cells depends on both state of differentiation and activation status." AIDS **21**(15): 2005-13.

Schlesinger, J. J., M. W. Brandriss, et al. (1990). "Cell surface expression of yellow fever virus non-structural glycoprotein NS1: consequences of interaction with antibody." J Gen Virol **71 (Pt 3)**: 593-9.

Sun, P., S. Fernandez, et al. (2009). "Functional characterization of ex vivo blood myeloid and plasmacytoid dendritic cells after infection with dengue virus." Virology **383**(2): 207-15.

Surh, C. D. and J. Sprent (2008). "Homeostasis of naive and memory T cells." Immunity **29**(6): 848-62.

Suzuki, T., K. Yamauchi, et al. (2001). "Characterization of hepatitis B virus surface antigen-specific CD4+ T cells in hepatitis B vaccine non-responders." J Gastroenterol Hepatol **16**(8): 898-903.

Theiler, M. and H. H. Smith (2000). "The use of yellow fever virus modified by in vitro cultivation for human immunization. J. Exp. Med. 65, 787-800 (1937)." Rev Med Virol **10**(1): 6-16; discussion 3-5.

Tokoyoda, K., S. Zehentmeier, et al. (2009). "Professional memory CD4+ T lymphocytes preferentially reside and rest in the bone marrow." Immunity **30**(5): 721-30.

Trinchieri, G. (2003). "Interleukin-12 and the regulation of innate resistance and adaptive immunity." Nat Rev Immunol **3**(2): 133-46.

Wan, Y. Y. and R. A. Flavell (2009). "How Diverse--CD4 Effector T Cells and their Functions." J Mol Cell Biol.

Westermann, J., U. Bode, et al. (2005). "Naive, effector, and memory T lymphocytes efficiently scan dendritic cells in vivo: contact frequency in T cell zones of secondary lymphoid organs does not depend on LFA-1 expression and facilitates survival of effector T cells." J Immunol **174**(5): 2517-24.

WHO (2008). "Meeting of Global Advisory Committee on Vaccine Safety, 18-19 June 2008." Wkly Epidemiol Rec **83**(32): 287-92.

Wisniewska-Ligier, M., T. Wozniakowska-Gesicka, et al. (2002). "Evaluation of lymphocyte subsets and NK cells in septic children." Med Sci Monit **8**(2): CR119-24.

Yokoyama, W. M. and S. Kim (2006). "How do natural killer cells find self to achieve tolerance?" Immunity **24**(3): 249-57.

10 Lebenslauf

„Mein Lebenslauf wird aus datenschutzrechtlichen Gründen in der elektronischen Version meiner Arbeit nicht veröffentlicht.“

11 Danksagung

An dieser Stelle möchte ich mich bei all jenen bedanken, die mich bei der Anfertigung dieser Dissertation unterstützt haben.

Mein Dank gilt zunächst meinem Doktorvater Prof. Dr. Andreas Thiel für die Bereitstellung dieser Arbeit, seine Unterstützung, seinen Enthusiasmus und seine Fähigkeit, ein inspirierendes wissenschaftliches Umfeld zu schaffen.

Ein weiterer Dank gilt Prof. Dr. Matthias Niedrig, der jederzeit Ansprechpartner für jegliche virologische Fragestellung war und mit der Möglichkeit der wissenschaftlichen Kooperation viel zum Gelingen dieser Arbeit beigetragen hat.

Mein besonderer Dank gebührt außerdem Herrn Dr. Siegfried Kohler, meinem direkten Ansprechpartner und Betreuer, der mir bei der täglichen Arbeit inhaltlich wie praktisch zur Seite stand. Danke für die großartige, geduldsame, diskussionsfreudige und lustige Unterstützung bei der Verwirklichung der Arbeit.

Matthias „Matze“ Böthe – danke dir für die vielen gemeinsamen Planungs- und Organisationsstunden, Blutabnahme- und Laborstunden, Auswertungs- und Interpretationsstunden – alles in allem – vielen Dank für deine große Hilfe und deine immerwährende gute Laune.

Zudem möchte ich allen übrigen Mitgliedern der Arbeitsgruppe Thiel für die gegenseitige Hilfsbereitschaft, die angenehme Atmosphäre, die geballte Lebensfreude und all die lange Kurzweil zusammen danken. Insbesondere Sophie danke ich hier für die unkomplizierte Einarbeitung.

Sarah, Johannes, Shokufeh – auch ein kleiner Dank an euch für die Zeit des ersten Kapitels…und ihr wisst – was lange währt, wird gut…

Besonders meinen Eltern danke ich für ihre stetige Unterstützung und Liebe, ihren nicht endenden Motivationsgeist und ihr Vertrauen in mich, ohne die dieses gesamte Vorhaben wohl nicht realisierbar geworden wäre.

Zuletzt möchte ich mich bei Harald dafür bedanken, der richtige-wichtige Mensch an meiner Seite zu sein – danke dir für die Unterstützung, Diskussionsbereitschaft und Geduld sowie all die schönen Momente der vergangenen Jahre.

12 Selbständigkeitserklärung

„Ich, Nicole Bethke, erkläre, dass ich die vorgelegte Dissertation mit dem Thema: „Characterisation of the immune response after yellow fever vaccination“ selbst verfasst und keine anderen als die angegebenen Quellen und Hilfsmittel benutzt, ohne die (unzulässige) Hilfe Dritter verfasst und auch in Teilen keine Kopien anderer Arbeiten dargestellt habe.“

Datum Unterschrift

13 Veröffentlichungen

Nordmeyer J, Eder S, Mahmoodzadeh S, Martus P, Fielitz J, Bass J, Bethke N, Zurbrügg HR, Pregla R, Hetzer R, Regitz-Zagrosek V. *Upregulation of myocardial estrogen receptors in human aortic stenosis.* Circulation 2004 Nov 16; 110(20): 3270-5

Bethke N, Böthe M, Kohler S, Niedrig M, Thiel A. *Bystander activation of recall antigen-specific CD4$^+$ T-Cells during primary immunization with live attenuated yellow fever virus*. Posterpräsentation auf dem 37. Jahrestreffen der Deutschen Gesellschaft für Immunologie/ Heidelberg, Germany, September 2007

Bethke N, Böthe M, Kohler S, Niedrig M, Thiel A. *Bystander activation of recall antigen-specific CD4$^+$ T-Cells during primary immunization with live attenuated yellow fever virus*. Posterpräsentation auf dem 3.MASIR Kongress Januar 2008

Babel N, Brestrich G, Gondek LP, Sattler A, Wlodarski MW, Poliak N, Bethke N, Thiel A, Hammer MH, Reinke P, Maciejewski JP. *Clonotype analysis of cytomegalovirus-specific cytotoxic T lymphocytes.* J Am Soc Nephrol. 2009 Feb;20(2):344-52. Epub 2008 Sep 17.

Babel N, Fendt J, Karaivanov S, Bold G, Arnold S, Sefrin A, Lieske E, Hoffzimmer M, Dziubianau M, Bethke N, Meisel C, Grütz G, Reinke P. *Sustained BK viruria as an early marker for the development of BKV-associated nephropathy: analysis of 4128 urine and serum samples.* Transplantation. 2009 Jul 15;88(1):89-95.